KA-TP-15-2011, FTUV-11-0730, WUB/11-06, FR-PHENO-2011-012, MZ-TH-11-19, CERN-PH-TH/2011-173, LPN11-40, DESY 11-125, TTK-10-51 MAN/HEP/2014/02

VBFNLO: A parton level Monte Carlo for processes with electroweak bosons – Manual for Version 2.7.1

J. Baglio¹, J. Bellm¹, G. Bozzi², M. Brieg³, F. Campanario⁴, C. Englert⁵, B. Feigl¹,

J. Frank¹, T. Figy⁶, F. Geyer¹, C. Hackstein¹, V. Hankele¹, B. Jäger⁷, M. Kerner¹,

M. Kubocz⁸, L.D. Ninh^{1,9}, C. Oleari¹⁰, S. Palmer¹, S. Plätzer¹¹, M. Rauch¹, R. Roth¹,

H. Rzehak¹², F. Schissler¹, O. Schlimpert¹, M. Spannowsky¹³, M. Worek⁸, D. Zeppenfeld¹

¹ Institute for Theoretical Physics, Karlsruhe Institute of Technology (KIT), 76128 Karlsruhe, Germany

- ² Dipartimento di Fisica Universita di Milano and INFN, Milano 20133 Milano, Italy
- ³ Institute of Nanotechnology (INT), Karlsruhe Institute of Technology (KIT), P.O. Box 3640, 76021 Karlsruhe, Germany
- ⁴ Theory Division, IFIC, University of Valencia-CSIC, E-46980 Paterna, Valencia, Spain

⁵ SUPA, School of Physics and Astronomy, University of Glasgow, Glasgow, G12 8QQ, United Kingdom

- ⁶ School of Physics and Astronomy, The University of Manchester, Manchester, M13 9PL, United Kingdom
- ⁷ Institut für Physik (THEP), Johannes-Gutenberg-Universität, 55099 Mainz, Germany

 8 Institut für Theoretische Teilchenphysik und Kosmologie, RWTH Aachen University, 52056 Aachen, Germany

⁹ Institute of Physics, Vietnam Academy of Science and Technology, 10 Dao Tan, Ba Dinh, Hanoi, Vietnam

- ¹⁰ Università di Milano-Bicocca and INFN, Sezione di Milano-Bicocca, 20126 Milan, Italy
 ¹¹ DESY, Notkestr. 85, 22607 Hamburg, Germany
- ¹² Physikalisches Institut, Albert-Ludwigs-Universität Freiburg, Hermann-Herder-Str. 3, 79104 Freiburg im Breisgau, Germany

¹³ Institute for Particle Physics Phenomenology, University of Durham, Durham, DH1 3LE, United Kingdom

Abstract

VBFNLO is a flexible parton level Monte Carlo program for the simulation of vector boson fusion (VBF), QCD induced single and double vector boson production plus two jets, and double and triple vector boson production (plus jet) in hadronic collisions at next-to-leading order (NLO) in the strong coupling constant, as well as Higgs boson plus two jet production via gluon fusion at the one-loop level. For the new version – VERSION 2.7.1 – several major enhancements have been included into VBFNLO. The following new production processes have been added: $W\gamma jj$, $Z\gamma jj$ and HHjj in VBF, $W, Wj, WH, WHj, pp \rightarrow$ Spin-2jj in VBF (with Spin-2 \rightarrow WW/ZZ \rightarrow leptons) and the QCD induced processes WZjj, $W\gamma jj$, $W^{\pm}W^{\pm}jj$ and Wjj production. The implementation of anomalous gauge boson couplings has been extended to all triboson and VBF VVjj processes, with an enlarged set of operators yielding anomalous couplings. Finally, semileptonic decay modes of the vector bosons are now available for many processes, including VVjj in VBF, VVV and $VV\gamma$ production.

July 29, 2015

Contents

1 INTRODUCTION			4	
2	INST	falling Vbfnlo	6	
	2.1	Prerequisites	6	
	2.2	Compilation and installation	6	
	2.3	Source and installation directory layout	8	
	2.4	Running the program	9	
		2.4.1 Parallel jobs and optimised grids	9	
	2.5	MacOSX	10	
	2.6	Bug reports	10	
	2.7	License	10	
3	Pro	DCESSES	11	
	3.1	VBF Higgs boson production in association with two jets	11	
	3.2	VBF Higgs boson production in association with three jets	12	
	3.3	VBF Higgs boson production with a photon and two jets	12	
	3.4	VBF production of a single vector boson and two jets	13	
	3.5	VBF production of a spin-2 particle	14	
	3.6	VBF production of two vector bosons and two jets	14	
	3.7	VBF production of two Higgs bosons and two jets	16	
	3.8	W production with up to one jet $\ldots \ldots \ldots$	16	
	3.9	Double vector boson production	16	
	3.10	1 1	17	
		Double vector boson production in association with a hadronic jet \ldots	18	
		Triple vector boson production in association with a hadronic jet	20	
		Higgs production in association with a W	20	
		Higgs production in association with a W and a hadronic jet \ldots	20	
		QCD induced production of a vector boson in association with two jets	21	
		QCD induced diboson production in association with two jets	21	
		Higgs boson production in gluon fusion with two jets	23	
	3.18	Gluon-induced diboson production	23	
4	INP	UT FILES AND PARAMETERS	25	
	4.1	vbfnlo.dat	25	
		4.1.1 vbfnlo.dat – general parameters	25	
		4.1.2 vbfnlo.dat – physics parameters	28	
		4.1.3 vbfnlo.dat – parameters for event output	34	
		4.1.4 vbfnlo.dat – PDF parameters	35	
		4.1.5 vbfnlo.dat – parameters for output and histograms	36	
	4.2	cuts.dat – parameters for kinematic cuts	36	
		4.2.1 cuts.dat – jet-specific cuts	36	
		4.2.2 cuts.dat – lepton specific cuts	37	
		4.2.3 cuts.dat – photon specific cuts	37	
		4.2.4 cuts.dat – additional cuts	38	
		4.2.5 cuts.dat – jet veto	38	
		4.2.6 cuts.dat – VBF specific cuts	39	
		4.2.7 cuts.dat – special cuts for semileptonic decays	39	

		4.2.8 Treatment of hadronic decays of low-virtuality photons	41
	4.3	ggflo.dat – general parameters for gluon fusion processes	41
	4.4	susy.dat – parameters in the MSSM	43
	4.5	Parameters for anomalous couplings	
		4.5.1 anom_HVV.dat - anomalous HVV couplings	45
		4.5.2 anomV.dat – anomalous triple and quartic gauge boson couplings .	48
		4.5.3 Using anom_HVV.dat and anomV.dat simultaneously	
	4.6	kk_input.dat – parameters for Higgsless models	
	4.7	spin2coupl.dat – parameters for spin-2 models	
	4.8	histograms.dat – parameters for histogram options	
	4.9	random.dat – parameters for seeds	
	4.10	Calculating the s -channel contributions for the VBF processes $\ldots \ldots$	56
5	Сна	ANGES	57
	5.1	Running scales in NLO calculations	57
	5.2	Jet cuts in VBF/gluon fusion Higgs boson production with $H \rightarrow b\bar{b}$	57
	5.3	NLO calculation of W^+W^-Z production	57
	5.4	LO and NLO calculation of W^+jj / Zjj production in VBF	58
	5.5	Event output	58
	5.6	Previous changes – version 2.6.3	58
		5.6.1 Event output	58
		5.6.2 Calculation of the $H \to gg$ partial width $\ldots \ldots \ldots \ldots \ldots$	
		5.6.3 Electroweak corrections in the VBF Hjj processes	58
	5.7	Previous changes – version 2.6.2	58
		5.7.1 Distributions and cross section for $H \to WW$ in VBF and gluon	
		fusion	58
		5.7.2 Les Houches event output for processes with more than one phase	
		space	59
		5.7.3 ZZZ production	59
		5.7.4 Form factor in $\gamma j j$ production with anomalous couplings	59
	5.8	Previous changes – version 2.6.1	59
		5.8.1 Anomalous Higgs couplings	59
		5.8.2 Symmetry factor $ZZ \to \ell^+ \ell^- \ell^+ \ell^- \dots \dots \dots \dots \dots \dots \dots \dots$	59
	5.9	Previous changes – version 2.6.0	59
		5.9.1 Allowed width of virtuality $\ldots \ldots \ldots \ldots \ldots \ldots \ldots \ldots \ldots \ldots$	
		5.9.2 Matrix element $H \to ZZ \to 4\ell$	60
		5.9.3 Anomalous couplings	60
		5.9.4 VBF Higgs boson production in association with three jets	60
	5.10	Previous changes – version 2.5.0	60
		5.10.1 EWSCHEME	61
		5.10.2 Gluon fusion	61
6	Сне	ECKS	62
7	OUT	Outlook 6	
A	Орб	OPERATORS FOR ANOMALOUS GAUGE BOSON COUPLINGS 6	
-			64
		Conventions for anomalous gauge boson coupling parameters in VBFNLO .	
			-

B Process list

1 INTRODUCTION

The physics potential of the LHC depends heavily on our ability to provide accurate cross section predictions for both signal and background processes. The latter are often generated by parton radiation from processes with weak bosons in the final state. A precise description of such hard QCD production processes is needed, as well as a method for simulating the measurable hadronic final states. Reaching these goals requires next-to-leading order (NLO) QCD calculations presented in the form of parton level Monte Carlo (MC) generators, which are an efficient solution when it comes to final states characterized by a high number of jets and/or identified particles. When kinematic cuts are imposed, as is mandatory for processes involving QCD radiation, analytic phase-space integration becomes impractical and implementation of results in the form of Monte Carlo programs becomes the method of choice.

VBFNLO is a flexible MC program for vector boson fusion (VBF), QCD induced single and double vector boson production plus two jets, and double and triple vector boson (plus jet) production processes at NLO QCD accuracy. Furthermore, the electroweak corrections to Higgs boson production via VBF (which are of the same order of magnitude as the QCD corrections in the experimentally accessible regions of phase-space) have been included. Since real emission processes are part of the NLO cross sections, VBFNLO provides the means to calculate cross sections for the corresponding process with one additional jet at leading order (LO) in the strong coupling. In addition, the simulation of \mathcal{CP} -even and \mathcal{CP} -odd Higgs boson production in gluon fusion, associated with two additional jets, is implemented at LO QCD. The full top- and bottom-quark mass dependence of the one-loop contributions in the Standard Model (SM), in the Minimal Supersymmetric Standard Model (MSSM) and in a generic two-Higgs-doublet model is included. VBFNLO can be run in the MSSM (with real or complex parameters), and anomalous couplings of the Higgs boson and gauge bosons have been implemented for a multitude of processes. Additionally, two Higgsless extra dimension models are included – the Warped Higgsless scenario and a Three-Site Higgsless Model – for selected processes. These models can be used to simulate the production of technicolor-type vector resonances in VBF and triple vector boson production. Diboson plus two jets production via VBF can also be run in a spin-2 model and in a model with two Higgs resonances.

Arbitrary cuts can be specified as well as various scale choices. Any currently available parton distribution function (PDF) set can be used through the LHAPDF library. In addition, CTEQ6L1 for LO and CT10 for NLO calculations, as well as MRST2004qed and MSTW2008, are hard-wired into the code. For most processes implemented at leading order the program is capable of generating event files in the Les Houches Accord (LHA) and the HepMC format. When working in the MSSM, the SUSY parameters can be input via a standard SLHA file.

This manual supersedes the previous versions [1–3] released with VBFNLO VERSION 2.0, VERSION 2.5.0 and VERSION 2.6.0.

The new release, VBFNLO 2.7.1, extends the following parts of VBFNLO VERSION 2.6.3:

- The list of new processes includes the following EW processes: $W\gamma jj$, $Z\gamma jj$ and HHjj in VBF, W, Wj, WH and WHj production
- The following QCD-induced processes have been included: $WZjj, W\gamma jj, W^{\pm}W^{\pm}jj, ZZjj, Z\gamma jj, Wjj$ and Zjj production

- The VBF processes with two massive gauge bosons can now be calculated in a model with two CP-even Higgs resonances with arbitrary couplings to the gauge bosons.
- The production of a spin-2 resonance in VBF processes is now available not only in the diphoton channel, but also for $WW \rightarrow 2l2\nu$, $ZZ \rightarrow 4l$ and $ZZ \rightarrow 2l2\nu$ production.
- For several processes semileptonic decays of the vector bosons have been implemented. This means that one vector boson decays hadronically, while the other(s) decay leptonically. The complete list of processes which is available is $W^+W^- / W^{\pm}Z / ZZ$ production, $W^+W^-/W^{\pm}W^{\pm}/W^{\pm}Z/ZZ$ production + two jets in vector boson fusion, Higgs boson production + two jets in VBF with decays into W^+W^- or ZZ and all triple vector boson production processes with zero or one final state photon.
- Anomalous triple and quartic gauge boson couplings are now included for all VVjj production processes via VBF.
- Anomalous triple and quartic gauge boson couplings are now included for ZZZ production and all triple vector boson production processes containing a final state photon.
- The set of operators leading to anomalous triple gauge boson couplings has been extended for the processes WWZ, ZZW and WWW production.
- VBFNLO can now output results not only for a specific choice of final state leptons, but also results summed over all possible combinations of two or three lepton generations.
- Higgs plus two jets production via gluon fusion, with the Higgs boson decaying into WW or ZZ, can now be run with anomalous HVV couplings in the decay as well as for a mixed CP-even CP-odd Higgs being produced.
- It is now possible to specify a desired number of unweighted events for event output. In case it is not possible to achieve the desired number of unweighted events due to single events with very large weights one can opt for "partially unweighted events", where most of the weights will have weight 1, while a few will have larger weights.
- Linking with LHAPDF v6 has been enabled.

Several bug fixes and smaller improvements have also been included. The complete list can be found in the NEWS file included in the tarball.

The VBFNLO webpage - http://www.itp.kit.edu/vbfnlo/ - contains, in addition to the latest version of the code, extra information such as the explicit implementation of the electroweak parameters and couplings, as well as optimised grid files for all processes for a set of standard cuts. To enable a simple installation test VBFNLO is shipped with a complete set of example results, together with input files, in the **regress** directory. On the webpage, users can subscribe to a low-traffic mailing list, where new versions of VBFNLO are announced.

2 INSTALLING VBFNLO

The source code of the current version of VBFNLO can be downloaded from the VBFNLO webpage

http://www.itp.kit.edu/vbfnlo/

and includes a GNU conforming build system for portability and an easy build and installation procedure.

2.1 Prerequisites

The basic installation requires GNU make, a FORTRAN 95¹ and a C++ compiler. VBFNLO offers the possibility of using the LHAPDF² [4] library (versions 5 and 6) for parton distribution functions. In order to include the electroweak corrections to VBF Higgs production, the program LOOPTOOLS³ [5, 6] is required. Additionally, FEYNHIGGS⁴ [7–10] can be linked to the code in order to calculate the Higgs boson sector of the MSSM, although a SLHA file can be used as an alternative. If the simulation of Kaluza-Klein resonances is enabled, an installation of the GNU Scientific Library (GSL)⁵ is required. VBFNLO can also be linked to ROOT⁶ and HEPMC⁷ to produce histograms and event files in those formats.

2.2 Compilation and installation

After unpacking the source archive and entering the source directory, the configure script can be invoked with several options, a complete list of which are available via ./configure --help. Among these, the most important ones are:

```
• --prefix=[path]
```

Install VBFNLO in the location given by [path]. If not specified, VBFNLO is installed in the root directory.

• --enable-processes=[list]

By default, the code for all available processes except those involving hexagon contributions (i.e. triboson plus jet and QCD-induced Vjj/VVjj processes) is compiled⁸. Optionally, [list] gives a comma-separated list of selected process classes to be compiled. Possible choices are:

¹gfortran and ifort have been tested. Pure FORTRAN77 compilers like g77 are no longer supported. ²http://lhapdf.hepforge.org/

³http://www.feynarts.de/looptools/

⁴http://www.feynhiggs.de/

⁵http://www.gnu.org/software/gsl/

⁶http://root.cern.ch/

⁷http://lcgapp.cern.ch/project/simu/HepMC/

⁸This is simply due to the relatively long time required to compile the hexagon routines.

vbf qcdvj	Vector boson fusion processes QCD-induced vector boson plus two jet production
qcdvvjj	QCD-induced vector boson pair plus two jet production
diboson	Double gauge boson production, including W and WH production
triboson	Triple gauge boson production
dibosonjet	Double gauge boson production with a hadronic jet, includ-
	ing Wj and WHj production
tribosonjet	Triboson production in association with a hadronic jet
hjjj	Higgs boson plus three jet production via vector boson fusion
ggf	Higgs boson plus two jet production via gluon fusion
all_except_hexagons	All the above processes except those with hexagon contri-
	butions (default)
all	All the above processes

• FC=/path/to/fortran/compiler

With the FC option a specific FORTRAN 95 compiler can be requested. Otherwise a default compiler will be used, which will be most probably gfortran.

• --disable-NLO

Disable the next-to-leading order QCD corrections.

• --enable-kk

Enable simulation of Kaluza-Klein resonances. Disabled by default, the Kaluza-Klein option requires the installation of the GNU Scientific Library, which can be specified via --with-gsl.

• --enable-spin2

Enable simulation of spin-2 models. Disabled by default.

• --enable-quad

Enable quadruple precision for difficult phase space points. Enabled by default, if QCD-induced vector boson (pair) plus two jet processes are requested, otherwise disabled by default.

• --with-gsl=[path]

Enable the use of the GNU Scientific Library. [path] specifies the location of the GSL installation. If the GSL is available directly from the system libraries this flag can be omitted.

• --with-LHAPDF=[path]

Enable the use of LHAPDF in addition to the built-in PDF sets. Disabled by default. [path] specifies the location of the LHAPDF installation.

• --with-LOOPTOOLS=[path]

Enable the use of LOOPTOOLS in order to calculate the electroweak corrections. If this option is not specified, the electroweak corrections cannot be included. Disabled by default. [path] specifies the location of the LOOPTOOLS installation.

• --with-FEYNHIGGS=[path]

Enable the use of FEYNHIGGS⁹ to calculate the MSSM Higgs sector parameters. Disabled by default. [path] specifies the location of the FEYNHIGGS installation.

• --with-root=[path]

Enable the use of ROOT for histograms. [path] specifies the location of the ROOT installation.

• --with-hepmc=[path]

Enable the production of HEPMC format event files. [path] specifies the location of the HEPMC installation.

Note that, by default, both LOOPTOOLS and FEYNHIGGS are installed as static libraries. If this is the case, configure must be run with the option --enable-shared=no. Also note that, in order to link to an external program such as LHAPDF, the external program needs to have been compiled using the same compiler (e.g. gfortran) as VBFNLO. If no path is specified, VBFNLO will attempt to find the desired program in the system directories. Once configure has finished successfully, the make and make install commands will compile and install VBFNLO, respectively.

If at any point include files, with a file name suffix .inc, are changed, the command make clean must be run so that the changes are picked up correctly. For normal program usage, this will not be necessary, but two cases where options can be altered in the file global.inc will be mentioned later. When changing only Fortran source code files, running make clean first is not mandatory. In both cases, make all install must be run afterwards in the main directory to recompile and reinstall the altered code.

2.3 Source and installation directory layout

The VBFNLO source tree contains the following subdirectories:

- amplitudes/: Routines to calculate matrix elements for the processes provided.
- doc/: The source of this manual.
- helas/: HELAS [11] subroutines used to calculate helicity amplitudes.
- loops/: One-loop tensor integrals up to six-point functions [12].
- PDFsets/: Built-in parton distributions (CTEQ6L1 [13] for LO and CT10 [14] for NLO calculations, as well as MRST2004qed [15] and MSTW2008 [16]).
- phasespace/: Specialized phase-space generators for the processes provided.
- regress/: Folder containing example results, together with input files, for all processes.
- src/ and lib/: Source code of the main programs and input files.
- utilities/: Routines for administrative tasks, cuts, scale choices and interfaces.

⁹Note that different versions of FEYNHIGGS give slightly different results as more corrections are added to the calculations. VBFNLO has been tested with FEYNHIGGS versions 2.6.x, 2.7.x, 2.8.0 and 2.8.3.

The source does not need to be modified to change the simulation parameters. VBFNLO offers several kinematic cuts and scale choices. This is illustrated in Sec. 4. In addition, it provides a few basic histograms. Cuts, histograms and scale choices not already provided may be added in the utilities/cuts.F, utilities/histograms.F and utilities/scales.F files.

The installation is performed in a standard UNIX-layout, i.e. the directory specified with the --prefix option of the configure script contains the following directories:

- bin/: vbfnlo and ggflo executables.
- include/VBFNLO/: VBFNLO header files.
- lib/VBFNLO/: VBFNLO modules as dynamically loadable libraries. These can also be used independently from one of the main programs.
- share/VBFNLO/: Input files and internal PDF tables.

2.4 Running the program

Both the vbfnlo and ggflo executables contained in the bin directory of the installation path look for input files in the current working directory. An alternative path to input files may be specified explicitly by passing the --input=[path] argument to the programs, with path denoting the full path where input files are located. I.e. in order to run VBFNLO from the installation (prefix) directory, the command is

./bin/vbfnlo --input=[path]

The input files contained in the share/VBFNLO directory are meant to represent default settings and should not be changed. We therefore recommend that the user copies the input files to a separate directory. Here, special settings may be chosen in the input files and the program can be run from that directory without specifying further options.

VBFNLO outputs a running 'log' to the terminal, containing information about the settings used. In addition, a file (named, by default, xsection.out) is produced, which contains only the LO and NLO cross sections, with the associated statistical errors. Histograms and event files, in various forms, can be output as described later.

The version number of VBFNLO can be obtained by appending the argument --version. This will print out the string VBFNLO followed by the release number and then exit the program.

2.4.1 Parallel jobs and optimised grids

Owing to the complexity of the calculations involved, some of the processes implemented in VBFNLO (in particular the spin-2 processes and triboson plus jet processes) require a significant amount of time in order to obtain reasonable results. There are, however, methods which can be used in order to reduce the necessary run time.

By using an optimised grid, the number of iterations needed in order to improve the efficiency of the MC integration can be reduced. Optimised grids are provided on the VBFNLO webpage for all processes using standard cuts and parameter settings. The variables used to set the input grid files and number of iterations are described in Sec. 4.1.1.

Another method of improving the run time is to run several jobs in parallel and then combine the results. In order to do this several input directories need to be set up containing all the necessary .dat input files for the process. The variable SEED in random.dat (Sec. 4.9) needs to be set to a different integer value in each directory. A short example of the results of a parallel run, together with their combination, is provided in the regress directory regress/100_Hjj_parallel. On the VBFNLO website there is a shell script which can be used to combine the cross sections and histograms from parallel runs.

2.5 MacOSX

The current version of VBFNLO has been compiled successfully on the current MacOSX version (10.9.2) as well as on an older one (10.6.8), if only static libraries are used. This can be requested with the configure-option --enable-shared=no. However, linking with the library LOOPTOOLS, which is only needed for the calculation of the electroweak corrections in the Hjj process, was not successful.

2.6 Bug reports

Please report any problems to

vbfnlo@itp.kit.edu

with a short report including the **configure** options used to build VBFNLO, as well as the versions of compilers and external libraries used.

2.7 License

VBFNLO is distributed under the GNU General Public License (GPL) version 2. This ensures that the source code will be available to users, grants them the freedom to use and modify the program and sets out the conditions under which it can be redistributed. However, it was developed as part of an academic research project and is the result of many years of work by the authors, which raises various issues that are not covered by the legal framework of the GPL. It is therefore distributed together with a set of guidelines¹⁰, which were originally formulated and agreed on by the MCnet collaboration for event generator software. In particular, the original literature on which the program is based should be cited along with the reference to VBFNLO.

Some parts of the VBFNLO matrix elements are based on automatically generated code from MADGRAPH [17,18] and FEYNARTS/FORMCALC [5,6,19–24]. The routine which reads in SLHA [25] files is largely based on SLHALIB-2.2 [26]. VBFNLO ships with a copy of FF 2.0 [27] for the evaluation of one-loop integrals.

¹⁰These guidelines are contained in the GUIDELINES file distributed with the release.

3 PROCESSES

In the following sections, we describe all production processes and decay modes implemented in VBFNLO, together with references to more detailed discussions of the underlying calculations.

In the phase-space regions that are accessible at hadron colliders, VBF reactions are dominated by t-channel electroweak gauge boson exchange. In this class of processes in VBFNLO s-channel exchange contributions and kinematically suppressed fermion interference contributions [28–30] are therefore disregarded. "Final state" weak bosons decay into massless leptons or quarks, depending on the process ID set. Numerically small contributions from Pauli-interference effects for identical charged fermions in the final state are neglected. For final-state identified photons we employ the isolation criterion of Ref. [31]. This ensures that divergences from collinear emission of a photon from a final-state massless quark or anti-quark are avoided, while the cancellation of the infrared divergences between the virtual and the real part is kept intact. With the inclusion of semileptonic diboson and triboson production processes the missing s-channel gauge boson exchange contributions of several VBF processes can be calculated within VBFNLO as well. This topic is described briefly in Section 4.10.

Higgs contributions (and interference effects) are included in all appropriate processes, using a fixed Higgs width. The Higgs propagator is given by

$$\frac{1}{s - M_H^2 + iM_H\Gamma_H}.$$
(1)

In VBFNLO external quarks are treated as massless. By default, external bottom quarks are excluded in those processes where their inclusion could lead to the presence of a top quark. I.e. in charged current processes such as WW diboson production, external bottom quarks are not allowed, as this would lead to a (massless) *t*-channel top quark, but in ZZ diboson production external bottom quarks are included. In the VBF processes such as $pp \rightarrow Hjj$ there are both neutral and charged current components (when the external quark lines emit Z and W bosons respectively) – by default, external bottom quarks are excluded from this class of processes. A message is printed in the log file stating whether external bottom quarks are included or excluded. In neutral current processes, bottom quarks in the final state are at present treated no differently from other final state quarks. The number of external quark flavours considered is set in the file utilities/global.inc. By changing the parameter nfl from 5 to 4, bottom quarks will not be included in any processes. By changing the parameter vbfNFLb from false to true, external bottom quarks will be included in the neutral current diagrams in VBF processes if nfl is set to 5^{11} .

3.1 VBF Higgs boson production in association with two jets

Hjj production via VBF mainly proceeds via electroweak quark-quark scattering processes such as $qq' \rightarrow qq'H$ and crossing-related reactions. In VBFNLO, tree level cross sections, NLO QCD corrections and one-loop electroweak corrections (in the Standard Model and the MSSM) to the *t*-channel production process are provided. The subsequent decay of the Higgs boson is simulated in the narrow width approximation (NWA). For the

¹¹Note that, if these parameters are changed, make clean must be run in the folders utilities and amplitudes, and then make all install must be run for the VBFNLO code.

 $H \to W^+W^-$ and the $H \to ZZ$ modes, full off-shell effects and spin correlations of the decay leptons are included. The available production process and decay modes are listed with the corresponding process IDs in Table 1. Anomalous couplings between a Higgs boson and a pair of vector bosons are implemented in the code and can be input via the file anom_HVV.dat. Details of the calculations can be found in Refs. [32–34].

Furthermore, semileptonic decay modes of the vector bosons are implemented for the WW and ZZ decay modes [35].

ProcId	Process	Вѕм
100 101 102 103 104 105 106 107	$\begin{split} p_{p}^{(-)} &\to H jj \\ p_{p}^{(-)} &\to H jj \to \gamma\gamma jj \\ p_{p}^{(-)} &\to H jj \to \mu^{+}\mu^{-} jj \\ p_{p}^{(-)} &\to H jj \to \tau^{+}\tau^{-} jj \\ p_{p}^{(-)} &\to H jj \to b\bar{b} jj \\ p_{p}^{(-)} &\to H jj \to W^{+}W^{-} jj \to \ell_{1}^{+}\nu_{\ell_{1}}\ell_{2}^{-}\bar{\nu}_{\ell_{2}} jj \\ p_{p}^{(-)} &\to H jj \to ZZ jj \to \ell_{1}^{+}\ell_{1}^{-}\ell_{2}^{+}\ell_{2}^{-} jj \\ p_{p}^{(-)} &\to H jj \to ZZ jj \to \ell_{1}^{+}\ell_{1}^{-}\nu_{\ell_{2}}\bar{\nu}_{\ell_{2}} jj \\ p_{p}^{(-)} &\to H jj \to ZZ jj \to \ell_{1}^{+}\ell_{1}^{-}\nu_{\ell_{2}}\bar{\nu}_{\ell_{2}} jj \end{split}$	<pre>anomalous HVV couplings, MSSM</pre>
108 109 1010	$\begin{split} p_{p}^{(-)} &\to H jj \to W^{+}W^{-} jj \to q\bar{q} \ell^{-} \bar{\nu}_{\ell} jj \\ p_{p}^{(-)} &\to H jj \to W^{+}W^{-} jj \to \ell^{+} \nu_{\ell} q\bar{q} jj \\ p_{p}^{(-)} &\to H jj \to ZZ jj \to q\bar{q} \ell^{+} \ell^{-} jj \end{split}$	} anomalous HVV couplings, MSSM

Table 1: Process IDs for $p_{p}^{(-)} \rightarrow Hjj$ production via vector boson fusion at NLO (QCD and electroweak) accuracy in the SM and MSSM. Anomalous couplings between the Higgs boson and vector bosons are implemented for all decay modes.

3.2 VBF Higgs boson production in association with three jets

Adding an extra parton to the Higgs production processes of Sec. 3.1 gives rise to Hjjj final states. The corresponding cross sections are implemented at NLO QCD accuracy (with certain approximations) in VBFNLO. A list of all available modes and corresponding process IDs is given in Table 2. Details of the calculation can be found in Ref. [36].

3.3 VBF Higgs boson production with a photon and two jets

The emission of an additional photon in VBF Higgs boson production (Sec. 3.1) results in $H\gamma jj$ final states. These are implemented at NLO QCD accuracy in VBFNLO, with process IDs as given in Table 3. Details of the calculation can be found in Ref. [37].

ProcId	Process
110 111 112 113 114 115 116 117	$ \begin{array}{c} p_{p}^{(-)} \rightarrow H j j j \\ p_{p}^{(-)} \rightarrow H j j j \rightarrow \gamma \gamma j j j \\ p_{p}^{(-)} \rightarrow H j j j \rightarrow \mu^{+} \mu^{-} j j j \\ p_{p}^{(-)} \rightarrow H j j j \rightarrow \tau^{+} \tau^{-} j j j \\ p_{p}^{(-)} \rightarrow H j j j \rightarrow b \bar{b} j j j \\ p_{p}^{(-)} \rightarrow H j j j \rightarrow W^{+} W^{-} j j j \rightarrow \ell_{1}^{+} \nu_{\ell_{1}} \ell_{2}^{-} \bar{\nu}_{\ell_{2}} j j j \\ p_{p}^{(-)} \rightarrow H j j j \rightarrow Z Z j j j \rightarrow \ell_{1}^{+} \ell_{1}^{-} \ell_{2}^{+} \ell_{2}^{-} j j j \\ p_{p}^{(-)} \rightarrow H j j j \rightarrow Z Z j j j \rightarrow \ell_{1}^{+} \ell_{1}^{-} \nu_{\ell_{2}} \bar{\nu}_{\ell_{2}} j j j \\ p_{p}^{(-)} \rightarrow H j j j \rightarrow Z Z j j j \rightarrow \ell_{1}^{+} \ell_{1}^{-} \nu_{\ell_{2}} \bar{\nu}_{\ell_{2}} j j j \end{array} $

Table 2: Process IDs for $p_{p}^{(-)} \rightarrow H_{jjj}$ production via VBF at NLO QCD accuracy.

ProcId	Process
2100 2101 2102 2103	$ \begin{array}{c} p \stackrel{(-)}{p} \rightarrow H\gamma jj \\ p \stackrel{(-)}{p} \rightarrow H\gamma jj \rightarrow \gamma\gamma\gamma jj \\ p \stackrel{(-)}{p} \rightarrow H\gamma jj \rightarrow \mu^+\mu^-\gamma jj \\ p \stackrel{(-)}{p} \rightarrow H\gamma jj \rightarrow \tau^+\tau^-\gamma jj \end{array} $
2104 2105 2106	$ \begin{array}{c} p_{p}^{(-)} \rightarrow H\gamma jj \rightarrow b\bar{b}\gamma jj \\ p_{p}^{(-)} \rightarrow H\gamma jj \rightarrow W^{+}W^{-}\gamma jj \rightarrow \ell_{1}^{+}\nu_{\ell_{1}}\ell_{2}^{-}\bar{\nu}_{\ell_{2}}\gamma jj \\ p_{p}^{(-)} \rightarrow H\gamma jj \rightarrow ZZ\gamma jj \rightarrow \ell_{1}^{+}\ell_{1}^{-}\ell_{2}^{+}\ell_{2}^{-}\gamma jj \end{array} $
2107	$p \stackrel{(-)}{p} \to H\gamma jj \to ZZ\gamma jj \to \ell_1^+ \ell_1^- \nu_{\ell_2} \bar{\nu}_{\ell_2} \gamma jj$

Table 3: Process IDs for $p_{p}^{(-)} \rightarrow H\gamma jj$ production via VBF at NLO QCD accuracy.

3.4 VBF production of a single vector boson and two jets

Vector boson fusion processes can also produce final states with two leptons plus two jets, which are generically referred to as "VBF Zjj and $W^{\pm}jj$ production". These reactions and the one with a photon plus two jets in the final state are implemented to NLO QCD accuracy in VBFNLO, with the process IDs given in Table 4. Anomalous triboson couplings are input via anomV.dat and can be included in all processes in this class. Details of the calculations can be found in Refs. [38, 39].

ProcId	Process	Вѕм
120 121 130 140 150	$ \begin{array}{c} p_{p}^{(-)} \rightarrow Zjj \rightarrow \ell^{+}\ell^{-}jj \\ p_{p}^{(-)} \rightarrow Zjj \rightarrow \nu_{\ell}\bar{\nu}_{\ell}jj \\ p_{p}^{(-)} \rightarrow W^{+}jj \rightarrow \ell^{+}\nu_{\ell}jj \\ p_{p}^{(-)} \rightarrow W^{-}jj \rightarrow \ell^{-}\bar{\nu}_{\ell}jj \\ p_{p}^{(-)} \rightarrow \gammajj \end{array} $	anomalous couplings

Table 4: Process IDs for vector boson + 2 jet production via vector boson fusion at NLO QCD accuracy.

ProcId	Process	Вѕм
191 195 196 197	$p_{p}^{(-)} \rightarrow S_{2} jj \rightarrow \gamma\gamma jj$ $p_{p}^{(-)} \rightarrow S_{2} jj \rightarrow W^{+}W^{-} jj \rightarrow \ell_{1}^{+}\nu_{\ell_{1}}\ell_{2}^{-}\bar{\nu}_{\ell_{2}} jj$ $p_{p}^{(-)} \rightarrow S_{2} jj \rightarrow ZZ jj \rightarrow \ell_{1}^{+}\ell_{1}^{-}\ell_{2}^{+}\ell_{2}^{-} jj$ $p_{p}^{(-)} \rightarrow S_{2} jj \rightarrow ZZ jj \rightarrow \ell_{1}^{+}\ell_{1}^{-}\nu_{\ell_{2}}\bar{\nu}_{\ell_{2}} jj$	<pre>spin-2 resonant production</pre>

Table 5: Process IDs for a spin-2 particle S_2+2 jet production via vector boson fusion at NLO QCD accuracy.

3.5 VBF production of a spin-2 particle

VBFNLO can simulate the production of a spin-2 particle via VBF, which then decays into two photons, with the process ID 191 (see Table 5). This process is only available if it has been enabled at compilation (using the configure flag --enable-spin2), and will only run if the switch SPIN2 in vbfnlo.dat is set to true. Furthermore, spin-2 production is also available in the WW and ZZ modes given in Table 5 if the switch SPIN2 in vbfnlo.dat is set to true. If SPIN2 is set to false, VBF Higgs production is simulated instead, similarly to the processes 105, 106 or 107 of Table 1 for a SM Higgs. The parameters of the spin-2 model are input via spin2coupl.dat. Details of the calculations can be found in Refs. [40-42].

3.6 VBF production of two vector bosons and two jets

The production of four leptons plus two jets in the final state at order $\mathcal{O}(\alpha^6)$ is dominated by VBF contributions. In VBFNLO, all resonant and non-resonant *t*-channel exchange contributions (including contributions from Higgs bosons) giving rise to a specific leptonic final state are considered. For simplicity, we refer to these reactions as "VBF diboson production". Finite width effects of the weak bosons and spin correlations of the decay leptons are fully retained.

The available processes and corresponding process IDs are listed in Table 6. Anomalous gauge boson couplings, input via anomV.dat, are implemented for all processes in this class, as well as a simplified model with two Higgs resonances. This process class can also be run in the Higgsless and spin-2 models implemented in VBFNLO, with the exception of $W\gamma$ and same-sign WW production. Details of the calculations can be found in Refs. [40, 43–48].

Furthermore, semileptonic decay modes of the vector bosons are implemented for the opposite-sign WW, same-sign WW, WZ and ZZ production processes in VBF [35]. In this case only anomalous couplings are available as BSM options.

ProcId	Process	BSM
200 210 211 220 230 250 260 270 280 290 291	$ \begin{array}{c} p_{p}^{(-)} \rightarrow W^{+}W^{-} jj \rightarrow \ell_{1}^{+}\nu_{\ell 1}\ell_{2}^{-}\bar{\nu}_{\ell 2} jj \\ p_{p}^{(-)} \rightarrow ZZ jj \rightarrow \ell_{1}^{+}\ell_{1}^{-}\ell_{2}^{+}\ell_{2}^{-} jj \\ p_{p}^{(-)} \rightarrow ZZ jj \rightarrow \ell_{1}^{+}\ell_{1}^{-}\nu_{\ell 2}\bar{\nu}_{\ell 2} jj \\ p_{p}^{(-)} \rightarrow W^{+}Z jj \rightarrow \ell_{1}^{+}\nu_{\ell 1}\ell_{2}^{+}\ell_{2}^{-} jj \\ p_{p}^{(-)} \rightarrow W^{-}Z jj \rightarrow \ell_{1}^{-}\bar{\nu}_{\ell 1}\ell_{2}^{+}\ell_{2}^{-} jj \\ p_{p}^{(-)} \rightarrow W^{+}W^{+} jj \rightarrow \ell_{1}^{+}\nu_{\ell 1}\ell_{2}^{+}\nu_{\ell 2} jj \\ p_{p}^{(-)} \rightarrow W^{-}W^{-} jj \rightarrow \ell_{1}^{-}\bar{\nu}_{\ell 1}\ell_{2}^{-}\bar{\nu}_{\ell 2} jj \\ p_{p}^{(-)} \rightarrow W^{+}\gamma jj \rightarrow \ell^{+}\nu_{\ell}\gamma jj \\ p_{p}^{(-)} \rightarrow W^{-}\gamma jj \rightarrow \ell^{-}\bar{\nu}_{\ell}\gamma jj \\ p_{p}^{(-)} \rightarrow Z\gamma jj \rightarrow \ell^{+}\ell^{-}\gamma jj \\ p_{p}^{(-)} \rightarrow Z\gamma jj \rightarrow \nu_{\ell}\bar{\nu}_{\ell}\gamma jj \end{array} $	<pre>anomalous couplings, two-Higgs model, Kaluza-Klein models, spin-2 models anomalous couplings, two-Higgs model anomalous couplings</pre>
201 202 212 221 222 231 232 251 261	$\begin{split} p_{p}^{(-)} &\rightarrow W^{+}W^{-} jj \rightarrow q\bar{q} \ell^{-}\bar{\nu}_{\ell} jj \\ p_{p}^{(-)} &\rightarrow W^{+}W^{-} jj \rightarrow \ell^{+}\nu_{\ell} q\bar{q} jj \\ p_{p}^{(-)} &\rightarrow ZZ jj \rightarrow q\bar{q} \ell^{+}\ell^{-} jj \\ p_{p}^{(-)} &\rightarrow W^{+}Z jj \rightarrow q\bar{q} \ell^{+}\ell^{-} jj \\ p_{p}^{(-)} &\rightarrow W^{+}Z jj \rightarrow \ell^{+}\nu_{\ell} q\bar{q} jj \\ p_{p}^{(-)} &\rightarrow W^{-}Z jj \rightarrow q\bar{q} \ell^{+}\ell^{-} jj \\ p_{p}^{(-)} &\rightarrow W^{-}Z jj \rightarrow \ell^{-}\bar{\nu}_{\ell} q\bar{q} jj \\ p_{p}^{(-)} &\rightarrow W^{+}W^{+} jj \rightarrow q\bar{q} \ell^{+}\nu_{\ell} jj \\ p_{p}^{(-)} &\rightarrow W^{-}W^{-} jj \rightarrow q\bar{q} \ell^{-}\bar{\nu}_{\ell} jj \end{split}$	anomalous couplings, two-Higgs model

Table 6: Process IDs for diboson + 2 jet production via vector boson fusion at NLO QCD accuracy.

3.7 VBF production of two Higgs bosons and two jets

Higgs pair production plus two jets via VBF mainly proceeds via electroweak quark-quark scattering processes such as $qq' \rightarrow qq'HH$ and crossing-related reactions. In VBFNLO, tree level cross sections and NLO QCD corrections to the *t*-channel production process are provided. Two decay modes for the subsequent decays of the Higgs bosons are implemented as well. The processes and corresponding process IDs are listed in Table 7. Details of the calculations can be found in Refs. [49, 50].

ProcId	Process
160 161 162	$ \begin{array}{c} p \stackrel{(-)}{p} \rightarrow HH jj \\ p \stackrel{(-)}{p} \rightarrow HH jj \rightarrow b \bar{b} \tau^+ \tau^- jj \\ p \stackrel{(-)}{p} \rightarrow HH jj \rightarrow b \bar{b} \gamma \gamma jj \end{array} $

Table 7: Process IDs for Higgs pair + 2 jet production via vector boson fusion at NLO QCD accuracy.

3.8 W production with up to one jet

The production of a W boson with up to one jet is implemented in VBFNLO at NLO QCD. The W boson decays leptonically and full off-shell effects and spin correlations of the final state leptons are included. The processes are listed in Table 8. Details of the calculation can be found in Ref. [51].

3.9 Double vector boson production

The production of four-lepton final states mainly proceeds via double vector boson production with subsequent decays. Additionally, there are processes where one or more decaying boson is replaced by an on-shell photon, giving rise to lepton production in association with a photon and double photon production. In VBFNLO, the processes listed in Table 9 are implemented to NLO QCD accuracy, including full off-shell effects and spin correlations of the final state leptons and photons. Anomalous vector boson couplings, input via anomV.dat, are implemented for WW, $W^{\pm}Z$ and $W^{\pm}\gamma$ production. The processes with a neutral final state (WW, ZZ, $Z\gamma$ and $\gamma\gamma$) also include the gluon-induced fermionic loop diagrams by default at NLO – both continuum production via box diagrams and the *s*-channel Higgs boson contributions are included, and anomalous HVV couplings (input via anom_HVV.dat) can be used. Details of the calculations can be found in Ref. [52].

Furthermore, semileptonic decay modes of the vector bosons are implemented for the WW, ZZ and WZ production processes [35]. Both anomalous VVV and HVV couplings are available as BSM options.

ProcId	Process
1330 1340 1630 1640	$ \begin{array}{c} p_{p}^{(-)} \rightarrow W^{+} \rightarrow \ell^{+} \nu_{\ell} \\ p_{p}^{(-)} \rightarrow W^{-} \rightarrow \ell^{-} \bar{\nu}_{\ell} \\ p_{p}^{(-)} \rightarrow W^{+} j \rightarrow \ell^{+} \nu_{\ell} j \\ p_{p}^{(-)} \rightarrow W^{-} j \rightarrow \ell^{-} \bar{\nu}_{\ell} j \end{array} $

Table 8: Process IDs for the W production processes with up to one jet at NLO QCD accuracy.

ProcId	Process	BSM
300 310 320 330 340 350 360 370	$\begin{split} p_{p}^{(-)} &\rightarrow W^{+}W^{-} \rightarrow \ell_{1}^{+}\nu_{\ell_{1}}\ell_{2}^{-}\bar{\nu}_{\ell_{2}} \\ p_{p}^{(-)} &\rightarrow W^{+}Z \rightarrow \ell_{1}^{+}\nu_{\ell_{1}}\ell_{2}^{+}\ell_{2}^{-} \\ p_{p}^{(-)} &\rightarrow W^{-}Z \rightarrow \ell_{1}^{-}\bar{\nu}_{\ell_{1}}\ell_{2}^{+}\ell_{2}^{-} \\ p_{p}^{(-)} &\rightarrow ZZ \rightarrow \ell_{1}^{-}\ell_{1}^{+}\ell_{2}^{-}\ell_{2}^{+} \\ p_{p}^{(-)} &\rightarrow W^{+}\gamma \rightarrow \ell_{1}^{+}\nu_{\ell_{1}}\gamma \\ p_{p}^{(-)} &\rightarrow W^{-}\gamma \rightarrow \ell_{1}^{-}\bar{\nu}_{\ell_{1}}\gamma \\ p_{p}^{(-)} &\rightarrow Z\gamma \rightarrow \ell_{1}^{-}\ell_{1}^{+}\gamma \\ p_{p}^{(-)} &\rightarrow \gamma\gamma \end{split}$	anomalous HVV and VVV couplings anomalous VVV couplings anomalous HVV couplings anomalous VVV couplings anomalous HVV couplings
301 302 312 313 322 323 331	$p \stackrel{(-)}{p} \rightarrow W^+ W^- \rightarrow q \bar{q} \ell^- \bar{\nu}_\ell$ $p \stackrel{(-)}{p} \rightarrow W^+ W^- \rightarrow \ell^+ \nu_\ell q \bar{q}$ $p \stackrel{(-)}{p} \rightarrow W^+ Z \rightarrow q \bar{q} \ell^+ \ell^-$ $p \stackrel{(-)}{p} \rightarrow W^+ Z \rightarrow \ell^+ \nu_\ell q \bar{q}$ $p \stackrel{(-)}{p} \rightarrow W^- Z \rightarrow q \bar{q} \ell^+ \ell^-$ $p \stackrel{(-)}{p} \rightarrow W^- Z \rightarrow \ell^- \bar{\nu}_\ell q \bar{q}$ $p \stackrel{(-)}{p} \rightarrow Z Z \rightarrow q \bar{q} \ell^- \ell^+$	$\left. \begin{array}{l} \text{anomalous } VVV \text{ and } HVV \text{ couplings} \\ \\ \text{anomalous } VVV \text{ couplings} \\ \\ \text{anomalous } HVV \text{ couplings} \end{array} \right.$

Table 9: Process IDs for the diboson production processes at NLO QCD accuracy.

3.10 Triple vector boson production

The production of six-lepton final states mainly proceeds via triple vector boson production with subsequent decays. Additionally, there are processes where one or more decaying boson is replaced by an on-shell photon, giving rise to lepton production in association with photon(s) and triple photon production. In VBFNLO, the processes listed in Tables 10

ProcId	Process	BSM
$\begin{array}{c} 400\\ 410\\ 420\\ 430\\ 430\\ 440\\ 450\\ 460\\ 470\\ 472\\ 480\\ 490\\ 500\\ 510\\ 520\\ 521\\ 530\\ \end{array}$	$\begin{split} p_{p}^{(-)} &\to W^{+}W^{-}Z \to \ell_{1}^{+}\nu_{\ell_{1}}\ell_{2}^{-}\bar{\nu}_{\ell_{2}}\ell_{3}^{+}\ell_{3}^{-} \\ p_{p}^{(-)} \to ZZW^{+} \to \ell_{1}^{+}\ell_{1}^{-}\ell_{2}^{+}\ell_{2}^{-}\ell_{3}^{-}\bar{\nu}_{\ell_{3}} \\ p_{p}^{(-)} \to ZZW^{-} \to \ell_{1}^{+}\ell_{1}^{-}\ell_{2}^{+}\ell_{2}^{-}\ell_{3}^{-}\bar{\nu}_{\ell_{3}} \\ p_{p}^{(-)} \to W^{+}W^{-}W^{+} \to \ell_{1}^{+}\nu_{\ell_{1}}\ell_{2}^{-}\bar{\nu}_{\ell_{2}}\ell_{3}^{+}\nu_{\ell_{2}} \\ p_{p}^{(-)} \to W^{-}W^{+}W^{-} \to \ell_{1}^{-}\bar{\nu}_{\ell_{1}}\ell_{2}^{+}\nu_{\ell_{2}}\ell_{3}^{-}\bar{\nu}_{\ell_{3}} \\ p_{p}^{(-)} \to ZZZ \to \ell_{1}^{-}\ell_{1}^{+}\ell_{2}^{-}\ell_{2}^{+}\ell_{3}^{-}\ell_{3}^{+} \\ p_{p}^{(-)} \to ZZ\gamma \to \ell_{1}^{-}\ell_{1}^{+}\ell_{2}^{-}\ell_{2}^{+}\gamma \\ p_{p}^{(-)} \to ZZ\gamma \to \ell_{1}^{-}\ell_{1}^{+}\ell_{2}^{-}\ell_{2}^{+}\gamma \\ p_{p}^{(-)} \to ZZ\gamma \to \ell_{1}^{-}\ell_{1}^{+}\nu_{\ell_{2}}\bar{\nu}_{\ell_{2}}\gamma \\ p_{p}^{(-)} \to W^{+}Z\gamma \to \ell_{1}^{-}\bar{\nu}_{\ell_{1}}\ell_{2}^{-}\ell_{2}^{+}\gamma \\ p_{p}^{(-)} \to W^{+}Z\gamma \to \ell_{1}^{-}\bar{\nu}_{\ell_{1}}\ell_{2}^{-}\ell_{2}^{+}\gamma \\ p_{p}^{(-)} \to W^{+}\gamma\gamma \to \ell^{-}\bar{\nu}_{\ell}\gamma\gamma \\ p_{p}^{(-)} \to Z\gamma\gamma \to \ell^{-}\bar{\nu}_{\ell}\gamma\gamma \\ p_{p}^{(-)} \to Z\gamma\gamma \to \ell^{-}\ell^{+}\gamma\gamma \\ p_{p}^{(-)} \to Z\gamma\gamma \to \nu_{\ell}\bar{\nu}_{\ell}\gamma\gamma \\ p_{p}^{(-)} \to Z\gamma\gamma \to \gamma \gamma \end{split}$	<pre> anomalous couplings, Kaluza-Klein models anomalous couplings anomalous couplings anomalous couplings</pre>

Table 10: Process IDs for the triboson production processes at NLO QCD accuracy with fully leptonic decays.

and 11 are implemented to NLO QCD accuracy, including full off-shell effects and spin correlations of the final state leptons and photons. For processes with three massive gauge bosons the Higgs boson contributions are included. Anomalous vector boson couplings¹² are implemented for all triboson processes, with the anomalous parameters input via anomV.dat. The processes WWZ, ZZW^{\pm} and $W^{\pm}W^{+}W^{-}$ can also be run in the implemented higgsless Kaluza-Klein models. Details of the calculations can be found in Refs. [53–58].

Furthermore, semileptonic decay modes of the vector bosons are implemented for all triple vector boson production processes with zero or one final state photon [35]. In this case only anomalous couplings are available as BSM options.

3.11 Double vector boson production in association with a hadronic jet

 $W\gamma$ and WZ production in association with a hard hadronic jet are available in VBFNLO at NLO QCD accuracy under the process IDs of Table 12. All off-shell and finite width effects are included. The processes can be run with anomalous WWZ and $WW\gamma$ couplings,

¹²Some anomalous VVV (f_W and f_B or, equivalently, $\Delta \kappa_{\gamma}$ and Δg_1^Z) couplings also imply anomalous HVV couplings – these are automatically taken into account.

ProcId	Process	BSM
$\begin{array}{c} 401\\ 402\\ 403\\ 411\\ 412\\ 421\\ 422\\ 431\\ 432\\ 441\\ 442\\ 451\\ 461\\ 462\\ 471\\ 481\\ 482\\ 491\\ 492\\ \end{array}$	$\begin{array}{c} p_{p}^{(-)} \rightarrow W^{+}W^{-}Z \rightarrow q\bar{q}\ell_{1}^{-}\bar{\nu}_{\ell 1}\ell_{2}^{+}\ell_{2}^{-} \\ p_{p}^{(-)} \rightarrow W^{+}W^{-}Z \rightarrow \ell_{1}^{+}\nu_{\ell 1}q\bar{q}\ell_{2}^{+}\ell_{2}^{-} \\ p_{p}^{(-)} \rightarrow W^{+}W^{-}Z \rightarrow \ell_{1}^{+}\nu_{\ell 1}\ell_{2}^{-}\bar{\nu}_{\ell 2}q\bar{q} \\ p_{p}^{(-)} \rightarrow ZZW^{+} \rightarrow \ell_{1}^{+}\ell_{1}^{-}\ell_{2}^{+}\ell_{2}^{-}q\bar{q} \\ p_{p}^{(-)} \rightarrow ZZW^{-} \rightarrow \ell_{1}^{+}\ell_{1}^{-}\ell_{2}^{+}\ell_{2}^{-}q\bar{q} \\ p_{p}^{(-)} \rightarrow ZZW^{-} \rightarrow q\bar{q}\ell_{1}^{+}\ell_{1}^{-}\ell_{2}^{-}\bar{\nu}_{\ell 2} \\ p_{p}^{(-)} \rightarrow ZZW^{-} \rightarrow q\bar{q}\ell_{1}^{+}\ell_{1}^{-}\ell_{2}^{-}\bar{\nu}_{\ell 2} \\ p_{p}^{(-)} \rightarrow W^{+}W^{-}W^{+} \rightarrow q\bar{q}\ell_{1}^{-}\bar{\nu}_{\ell 1}\ell_{2}^{+}\nu_{\ell 2} \\ p_{p}^{(-)} \rightarrow W^{+}W^{-}W^{+} \rightarrow \ell_{1}^{+}\nu_{\ell 1}q\bar{q}\ell_{2}^{-}\bar{\nu}_{\ell 2} \\ p_{p}^{(-)} \rightarrow W^{+}W^{-}W^{+} \rightarrow \ell_{1}^{-}\bar{\nu}_{\ell 1}q\bar{q}\ell_{2}^{-}\bar{\nu}_{\ell 2} \\ p_{p}^{(-)} \rightarrow W^{-}W^{+}W^{-} \rightarrow q\bar{q}\ell_{1}^{-}\ell_{1}^{+}\ell_{2}^{-}\ell_{2}^{+} \\ p_{p}^{(-)} \rightarrow W^{-}W^{+}W^{-}\gamma \rightarrow q\bar{q}\ell_{1}^{-}\bar{\nu}_{\ell}\gamma \\ p_{p}^{(-)} \rightarrow W^{+}W^{-}\gamma \rightarrow \ell^{+}\nu_{\ell}q\bar{q}\gamma \\ p_{p}^{(-)} \rightarrow W^{+}Z\gamma \rightarrow \ell^{-}\nu_{\ell}q\bar{q}\gamma \\ p_{p}^{(-)} \rightarrow W^{+}Z\gamma \rightarrow \ell^{-}\nu_{\ell}q\bar{q}\gamma \\ p_{p}^{(-)} \rightarrow W^{-}Z\gamma \rightarrow \ell^{-}\bar{\nu}_{\ell}q\bar{q}\gamma \\ p_{$	anomalous couplings

Table 11: Process IDs for the triboson production processes at NLO QCD accuracy with semileptonic decays.

ProcId	Process	Вѕм
610 620 630 640	$ \begin{array}{c} p_{p}^{(-)} \rightarrow W^{-}\gamma j \rightarrow \ell^{-}\bar{\nu}_{\ell}\gamma j \\ p_{p}^{(-)} \rightarrow W^{+}\gamma j \rightarrow \ell^{+}\nu_{\ell}\gamma j \\ p_{p}^{(-)} \rightarrow W^{-}Z j \rightarrow \ell_{1}^{-}\bar{\nu}_{\ell_{1}}\ell_{2}^{-}\ell_{2}^{+}j \\ p_{p}^{(-)} \rightarrow W^{+}Z j \rightarrow \ell_{1}^{+}\nu_{\ell_{1}}\ell_{2}^{-}\ell_{2}^{+}j \end{array} $	anomalous couplings

Table 12: Process IDs for $W\gamma j$ and WZ j production at NLO QCD.

input via anomV.dat. Details can be found in Refs. [59-62].

ProcId	Process	Вѕм
800 810	$p_{p}^{(-)} \to W^{+} \gamma \gamma j \to \ell^{+} \nu_{\ell} \gamma \gamma j$ $p_{p}^{(-)} \to W^{-} \gamma \gamma j \to \ell^{-} \bar{\nu}_{\ell} \gamma \gamma j$	} anomalous couplings

Table 13: Process IDs for triboson production in association with a hadronic jet at NLO QCD.

3.12 Triple vector boson production in association with a hadronic jet

 $W\gamma\gamma$ production in association with a hard hadronic jet is available in VBFNLO at NLO QCD accuracy under the process IDs of Table 13. All off-shell and finite width effects are included. Anomalous vector boson couplings are implemented, with the anomalous parameters input via anomV.dat. Details can be found in Ref. [63]. Note that this class of processes is not enabled by default and so, in order to run these processes, they must be enabled at compilation, using the configure option --enable-processes=all or --enable-processes=tribosonjet.

3.13 Higgs production in association with a W

The production of a Higgs boson in association with a W boson proceeds via the production of a single off-shell W boson which radiates the Higgs boson. The W boson decays leptonically, while the Higgs boson can decay in several channels.

In VBFNLO, the processes listed in Table 14 are implemented to NLO QCD accuracy, including full off-shell effects and spin correlations of the final state leptons. Anomalous couplings can be input via anomV.dat and are used both in the production process as well as the decay of the Higgs boson. Details of the calculation can be found in Ref. [51].

3.14 Higgs production in association with a W and a hadronic jet

WH production in association with a hadronic jet is available at NLO QCD accuracy in VBFNLO under the process IDs of Table 15.

Full off-shell effects and spin correlations of the final state leptons are included. Anomalous couplings can be input via anomV.dat and are used both in the production process as well as the decay of the Higgs boson.

The virtual contributions of the NLO calculation include diagrams where the Higgs is radiated off a top quark loop attached to a gluon. They are calculated including the full top mass dependence. These contributions can be disabled using the flag dotoploops in utilities/global.inc¹³. Details of the calculation can be found in Ref. [51].

¹³Note that, if this parameter is changed, make clean must be run in the folder utilities, and then make all install must be run for the VBFNLO code.

ProcId	Process	BSM
1300 1301 1302 1303 1304 1305 1306 1307	$\begin{split} p_{p}^{(-)} &\rightarrow W^{+}H \rightarrow \ell^{+}\nu_{\ell}H \\ p_{p}^{(-)} \rightarrow W^{+}H \rightarrow \ell^{+}\nu_{\ell}\gamma\gamma \\ p_{p}^{(-)} \rightarrow W^{+}H \rightarrow \ell^{+}\nu_{\ell}\mu^{+}\mu^{-} \\ p_{p}^{(-)} \rightarrow W^{+}H \rightarrow \ell^{+}\nu_{\ell}\tau^{+}\tau^{-} \\ p_{p}^{(-)} \rightarrow W^{+}H \rightarrow \ell^{+}\nu_{\ell}b\bar{b} \\ p_{p}^{(-)} \rightarrow W^{+}H \rightarrow W^{+}W^{+}W^{-} \rightarrow \ell_{1}^{+}\nu_{\ell_{1}}\ell_{2}^{+}\nu_{\ell_{2}}\ell_{3}^{-}\bar{\nu}_{\ell_{3}} \\ p_{p}^{(-)} \rightarrow W^{+}H \rightarrow W^{+}ZZ \rightarrow \ell_{1}^{+}\nu_{\ell_{1}}\ell_{2}^{+}\ell_{2}^{-}\ell_{3}^{+}\ell_{3}^{-} \\ p_{p}^{(-)} \rightarrow W^{+}H \rightarrow W^{+}ZZ \rightarrow \ell_{1}^{+}\nu_{\ell_{1}}\ell_{2}^{+}\ell_{2}^{-}\nu_{\ell_{3}}\bar{\nu}_{\ell_{3}} \end{split}$	<pre>anomalous gauge couplings</pre>
$1310 \\1311 \\1312 \\1313 \\1314 \\1315 \\1316 \\1317$	$\begin{split} p_{p}^{(-)} &\to W^{-}H \to \ell^{-}\bar{\nu}_{\ell}H \\ p_{p}^{(-)} \to W^{-}H \to \ell^{-}\bar{\nu}_{\ell}\gamma\gamma \\ p_{p}^{(-)} \to W^{-}H \to \ell^{-}\bar{\nu}_{\ell}\mu^{+}\mu^{-} \\ p_{p}^{(-)} \to W^{-}H \to \ell^{-}\bar{\nu}_{\ell}\tau^{+}\tau^{-} \\ p_{p}^{(-)} \to W^{-}H \to \ell^{-}\bar{\nu}_{\ell}b\bar{b} \\ p_{p}^{(-)} \to W^{-}H \to W^{-}W^{+}W^{-} \to \ell_{1}^{-}\bar{\nu}_{\ell_{1}}\ell_{2}^{+}\nu_{\ell_{2}}\ell_{3}^{-}\bar{\nu}_{\ell_{3}} \\ p_{p}^{(-)} \to W^{-}H \to W^{-}ZZ \to \ell_{1}^{-}\bar{\nu}_{\ell_{1}}\ell_{2}^{+}\ell_{2}^{-}\ell_{3}^{+}\ell_{3}^{-} \\ p_{p}^{(-)} \to W^{-}H \to W^{-}ZZ \to \ell_{1}^{-}\bar{\nu}_{\ell_{1}}\ell_{2}^{+}\ell_{2}^{-}\nu_{\ell_{3}}\bar{\nu}_{\ell_{3}} \end{split}$	<pre>anomalous gauge couplings</pre>

Table 14: Process IDs for the WH production processes at NLO QCD accuracy.

3.15 QCD induced production of a vector boson in association with two jets

A vector boson in association with two jets can be produced at order $\mathcal{O}(\alpha_s^2 \alpha^2)$. This QCD induced process is available in VBFNLO for the production of a W boson in association with two jets at NLO QCD accuracy, including leptonic decays of the vector boson. The process IDs can be found in Table 16. These processes are not included by default and they have to be enabled at compilation, using the configure option --enable-processes=X where X is one of qcdvjj,qcdvvjj,all. These processes use quadruple precision to handle instabilities in the virtual amplitudes. If quadruple precision is not supported by the compiler it can be disabled by adding the configure option --disable-quad. An estimate of the error due to unstable points is printed out at the end of program execution.

3.16 QCD induced diboson production in association with two jets

The QCD induced production of two vector bosons in association with two jets is available in VBFNLO at NLO QCD accuracy for the processes listed in Table 17. All spin correlations and finite width effects are included. These processes are not included

ProcId	Process	BSM
$1600 \\ 1601 \\ 1602 \\ 1603 \\ 1604 \\ 1605 \\ 1606 \\ 1607$	$\begin{split} p_{p}^{(-)} &\to W^{+}H j \to \ell^{+}\nu_{\ell}H j \\ p_{p}^{(-)} \to W^{+}H j \to \ell^{+}\nu_{\ell}\gamma\gamma j \\ p_{p}^{(-)} \to W^{+}H j \to \ell^{+}\nu_{\ell}\mu^{+}\mu^{-} j \\ p_{p}^{(-)} \to W^{+}H j \to \ell^{+}\nu_{\ell}b\bar{b} j \\ p_{p}^{(-)} \to W^{+}H j \to \ell^{+}\nu_{\ell}b\bar{b} j \\ p_{p}^{(-)} \to W^{+}H j \to W^{+}W^{+}W^{-} j \to \ell_{1}^{+}\nu_{\ell_{1}}\ell_{2}^{+}\nu_{\ell_{2}}\ell_{3}^{-}\bar{\nu}_{\ell_{3}} j \\ p_{p}^{(-)} \to W^{+}H j \to W^{+}ZZ j \to \ell_{1}^{+}\nu_{\ell_{1}}\ell_{2}^{+}\ell_{2}^{-}\ell_{3}^{+}\ell_{3}^{-} j \\ p_{p}^{(-)} \to W^{+}H j \to W^{+}ZZ j \to \ell_{1}^{+}\nu_{\ell_{1}}\ell_{2}^{+}\ell_{2}^{-}\nu_{\ell_{3}}\bar{\nu}_{\ell_{3}} j \end{split}$	<pre>anomalous couplings</pre>
$1610 \\ 1611 \\ 1612 \\ 1613 \\ 1614 \\ 1615 \\ 1616 \\ 1617 \\$	$\begin{split} p_{p}^{(-)} &\to W^{-}H j \to \ell^{-}\bar{\nu}_{\ell}H j \\ p_{p}^{(-)} \to W^{-}H j \to \ell^{-}\bar{\nu}_{\ell}\gamma\gamma j \\ p_{p}^{(-)} \to W^{-}H j \to \ell^{-}\bar{\nu}_{\ell}\mu^{+}\mu^{-} j \\ p_{p}^{(-)} \to W^{-}H j \to \ell^{-}\bar{\nu}_{\ell}\nu^{+}\tau^{-} j \\ p_{p}^{(-)} \to W^{-}H j \to \ell^{-}\bar{\nu}_{\ell}b\bar{b} j \\ p_{p}^{(-)} \to W^{-}H j \to W^{-}W^{+}W^{-} j \to \ell_{1}^{-}\bar{\nu}_{\ell_{1}}\ell_{2}^{+}\nu_{\ell_{2}}\ell_{3}^{-}\bar{\nu}_{\ell_{3}} j \\ p_{p}^{(-)} \to W^{-}H j \to W^{-}ZZ j \to \ell_{1}^{-}\bar{\nu}_{\ell_{1}}\ell_{2}^{+}\ell_{2}^{-}\ell_{3}^{+}\ell_{3}^{-} j \\ p_{p}^{(-)} \to W^{-}H j \to W^{-}ZZ j \to \ell_{1}^{-}\bar{\nu}_{\ell_{1}}\ell_{2}^{+}\ell_{2}^{-}\nu_{\ell_{3}}\bar{\nu}_{\ell_{3}} j \end{split}$	<pre>anomalous couplings</pre>

Table 15: Process IDs for the WH plus jet production processes at NLO QCD accuracy.

ProcId	Process
3120 3121 3130 3140	$\begin{split} p_{p}^{(-)} &\to Z jj \to \ell^{+}\ell^{-} jj \\ p_{p}^{(-)} &\to Z jj \to \nu_{\ell} \bar{\nu}_{\ell} jj \\ p_{p}^{(-)} &\to W^{+} jj \to \ell^{+} \nu_{\ell} jj \\ p_{p}^{(-)} &\to W^{-} jj \to \ell^{-} \bar{\nu}_{\ell} jj \end{split}$

Table 16: Process IDs for QCD induced vector boson + 2 jet production at NLO QCD accuracy.

by default and they have to be enabled at compilation, using the configure option --enable-processes=qcdvvjj or --enable-processes=all. These processes use quadruple precision to handle instabilities in the virtual amplitudes. If quadruple precision is not supported by the compiler it can be disabled by adding the configure option

ProcId	Process
3210	$p^{(-)}_{p} \rightarrow ZZ jj \rightarrow \ell_1^+ \ell_1^- \ell_2^+ \ell_2^- jj$
3211	$p_{p}^{(-)} ightarrow ZZ jj ightarrow \ell_{1}^{+} \ell_{1}^{-} \nu_{\ell_{2}} \bar{\nu}_{\ell_{2}} jj$
3220	$p_{p}^{(-)} \to W^{+}Z jj \to \ell_{1}^{+}\nu_{\ell_{1}}\ell_{2}^{+}\ell_{2}^{-} jj$
3230	$p_{p}^{(-)} \rightarrow W^{-}Z jj \rightarrow \ell_{1}^{-} \bar{\nu}_{\ell_{1}} \ell_{2}^{+} \ell_{2}^{-} jj$
3250	$p_{p}^{(-)} \to W^{+}W^{+}jj \to \ell_{1}^{+}\nu_{\ell_{1}}\ell_{2}^{+}\nu_{\ell_{2}}jj$
3260	$p_{p}^{(-)} \rightarrow W^{-}W^{-}jj \rightarrow \ell_{1}^{-}\bar{\nu}_{\ell_{1}}\ell_{2}^{-}\bar{\nu}_{\ell_{2}}jj$
3270	$p^{(-)}_{p} ightarrow W^+ \gamma jj ightarrow \ell^+ u_\ell \gamma jj$
3280	$p_{p}^{(-)} ightarrow W^{-} \gamma jj ightarrow \ell^{-} ar{ u}_{\ell} \gamma jj$
3290	$p^{(-)}_{p} ightarrow Z\gamma jj ightarrow \ell^+\ell^-\gamma jj$
3291	$p \stackrel{(-)}{p} ightarrow Z \gamma j j ightarrow u_\ell ar u_\ell \gamma j j$

Table 17: Process IDs for QCD induced diboson + 2 jet production at NLO QCD accuracy.

--disable-quad. An estimate of the error due to unstable points is printed at the end of program execution. Details of the calculation can be found in Refs. [64–69].

3.17 Higgs boson production in gluon fusion with two jets

 $C\mathcal{P}$ -even and $C\mathcal{P}$ -odd Higgs boson production in gluon fusion, associated with two additional jets, are processes that first appear at the one-loop level which, therefore, are counted as leading order in the strong coupling constant. These processes are simulated (via the ggflo executable) with the full mass dependence of the top- and bottom-quark¹⁴ running in the loop in the Standard Model, in the (complex) MSSM and in a generic two-Higgs-doublet model. Anomalous HVV couplings (for decays into W or Z bosons) can be input via anom_HVV.dat and the input file ggflo.dat can be used to define additional settings for these processes. The relevant process IDs are given in Table 18. Details of the calculations can be found in Refs. [70–75].

3.18 Gluon-induced diboson production

Gluon-induced diboson production can be studied separately in VBFNLO at LO with the ggflo executable, using the process IDs in Table 19¹⁵. Continuum production via box diagrams as well as production via an *s*-channel Higgs boson resonance are included, with interference effects fully taken into account. Anomalous HVV couplings can be included, using anom_HVV.dat. In the loop diagrams, first and second generation quarks are taken to be massless and third generation quark masses¹⁶ are included.

¹⁴The value $m_b(M_H)$ in the \overline{MS} scheme is used for both the mass and the Yukawa coupling of the bottom quark, while for the top quark we use its on-shell value.

¹⁵These are also included by default as higher order corrections to diboson production.

¹⁶Again, $m_b(M_H)$ in the \overline{MS} scheme is used.

ProcId	Process	Вѕм
4100 4101 4102 4103 4104 4105 4106 4107	$\begin{split} p_{p}^{(-)} &\to H jj \\ p_{p}^{(-)} &\to H jj \to \gamma\gamma jj \\ p_{p}^{(-)} &\to H jj \to \mu^{+}\mu^{-} jj \\ p_{p}^{(-)} &\to H jj \to \tau^{+}\tau^{-} jj \\ p_{p}^{(-)} &\to H jj \to b\bar{b} jj \\ p_{p}^{(-)} &\to H jj \to W^{+}W^{-} jj \to \ell_{1}^{+}\nu_{\ell_{1}}\ell_{2}^{-}\bar{\nu}_{\ell_{2}} jj \\ p_{p}^{(-)} &\to H jj \to ZZ jj \to \ell_{1}^{+}\ell_{1}^{-}\ell_{2}^{+}\ell_{2}^{-} jj \\ p_{p}^{(-)} &\to H jj \to ZZ jj \to \ell_{1}^{+}\ell_{1}^{-}\nu_{\ell_{2}}\bar{\nu}_{\ell_{2}} jj \\ p_{p}^{(-)} &\to H jj \to ZZ jj \to \ell_{1}^{+}\ell_{1}^{-}\nu_{\ell_{2}}\bar{\nu}_{\ell_{2}} jj \end{split}$	MSSM, general 2HDM

Table 18: Process IDs for LO Higgs boson plus 2 jet production via gluon fusion. Note that these processes are accessed via the ggflo executable.

ProcId	Process	BSM
4300 4330 4360 4370	$ \begin{array}{c} p \stackrel{(-)}{p} \rightarrow W^+ W^- \rightarrow \ell_1^+ \nu_{\ell_1} \ell_2^- \bar{\nu}_{\ell_2} \\ p \stackrel{(-)}{p} \rightarrow ZZ \rightarrow \ell_1^- \ell_1^+ \ell_2^- \ell_2^+ \\ p \stackrel{(-)}{p} \rightarrow Z\gamma \rightarrow \ell_1^- \ell_1^+ \gamma \\ p \stackrel{(-)}{p} \rightarrow \gamma\gamma \end{array} $	<pre>anomalous HVV couplings</pre>
4301 4302 4331	$p_{p}^{(-)} \rightarrow W^{+}W^{-} \rightarrow q\bar{q}\ell^{-}\bar{\nu}_{\ell}$ $p_{p}^{(-)} \rightarrow W^{+}W^{-} \rightarrow \ell^{+}\nu_{\ell}q\bar{q}$ $p_{p}^{(-)} \rightarrow ZZ \rightarrow q\bar{q}\ell^{-}\ell^{+}$	} anomalous <i>HVV</i> couplings

Table 19: Process IDs for the gluon-induced diboson production at LO (one-loop) QCD. Note that these processes are accessed via the ggflo executable.

Furthermore, semileptonic decay modes of the vector bosons are implemented for the WW and ZZ production processes [35]. Anomalous HVV couplings are available.

4 INPUT FILES AND PARAMETERS

VBFNLO is steered through the following input files:

- vbfnlo.dat: General parameters for a run.
- cuts.dat: Values for kinematic cuts.
- ggflo.dat: Additional parameters for the ggflo program.
- susy.dat: Parameters describing the MSSM scenario.
- anom_HVV.dat: Parameters for anomalous Higgs boson couplings.
- anomV.dat: Parameters for anomalous gauge boson couplings.
- kk_input.dat: Settings for the Warped Higgsless and Three-Site Higgsless Models.
- kk_coupl_inp.dat: Numerical values if externally calculated Kaluza-Klein couplings and masses should be used.
- spin2coupl.dat: Settings for the spin-two models.
- histograms.dat: Histogram options.
- random.dat: Seed for the random number generator.

The following subsections give a detailed description of all available parameters.

4.1 vbfnlo.dat

vbfnlo.dat is the main input file for VBFNLO.

4.1.1 vbfnlo.dat – general parameters

- **PROCESS**: Process ID as described in Sec. 3. Default is 100: Higgs boson production via VBF.
- LOPROCESS_PLUS_JET: If set to true, the leading order process with one additional jet is generated, i.e. only the real radiation contribution is generated. This option is available for all but gluon induced processes. Default is false.
- LEPTONS: Choice of the final state leptons (decay products of W and Z bosons) according to the MC particle numbering scheme [76]:
 - 11 : e^- 12 : ν_e 13 : μ^- 14 : ν_{μ} 15 : τ^- 16 : ν_{τ} 98 : leptons are either generation 1 or generation 2 99 : any lepton

If the selected configuration is not available, the appropriate first-generation leptons are used as default values. If 99(98) is set, results are output summed over all possible lepton combinations (all possible lepton combinations of generation 1 or 2) – for individual events (in the cuts, histograms and Les Houches event output) the specific leptons for that particular event are generated randomly.

- DECAY_QUARKS: Choice of the final state quarks from hadronic vector boson decays (decay products of W and Z bosons) according to the MC particle numbering scheme [76]:

If 93 is set, results are output summed over all possible quark / anti-quark combinations of the first and second generation. For DECAY_QUARKS = 94 additionally band \bar{b} are considered. For individual events in the Les Houches event output, the specific quarks for that particular event are generated randomly, weighted by the contribution of that specific quark combination. If the selected configuration is not available, all possible combinations of first and second generation quarks are used as default values (DECAY_QUARKS = 93).

- LO_ITERATIONS: Sets the number of iterations for the integration of LO cross sections. Usually more than one iteration is used in order to adapt the integration grid and thus improve the efficiency of the MC integration algorithm¹⁷. For an adapted grid file (see LO_GRID) this parameter can be set to 1. Default is 4.
- NLO_ITERATIONS: Analogous to LO_ITERATIONS, but for the real emission part of an NLO calculation. Since the corresponding phase-space is different from the LO configuration, a second independent MC integration has to be performed. Default is 4.
- LO_POINTS: Determines the number of phase-space points that are generated in each iteration. In the last iteration there are 2^N points, where $N = \text{LO}_POINTS$. In each previous iteration, the number of points is half the value of the following one. Example: For 4 iterations (LO_ITERATIONS = 4) and LO_POINTS = 20, there are 2^{17} generated points in the first, 2^{18} in the second, 2^{19} in the third and $2^{20} \approx 10^6$ in the last iteration¹⁸. Default is N = 20.
- NLO_POINTS: Similar to LO_POINTS, but for the real emission part of an NLO calculation. Default is 20.

¹⁷For all NLO calculations the virtual contributions are calculated using the already optimized leading order grid.

 $^{^{18}\}mathrm{The}$ virtual contributions are calculated for 2^N points only.

- LO_GRID: Sets the name of the grid files that are generated at the end of each iteration. Choosing name as the input parameter, in each iteration X a grid file name.out.X will be produced in the working directory. If a grid file name is already present in the input directory (specified by --input=INPUT), the program reads in this file when executed. Note that optimised grids for all processes (using the standard cuts given in the regress files) are provided on the VBFNLO webpage.
- FLOOP_GRID: Similar to LO_GRID, but for the gluon induced fermion loop contributions (the kinematics of which can differ significantly from the LO kinematics). The number of iterations used is given by LO_ITERATIONS and the number of points used is LO_POINTS-8.
- NLO_GRID: Similar to LO_GRID, but for the real emission part of an NLO calculation.
- PHTN_GRID: Similar to NLO_GRID, but for the real photon emission part of an NLO electroweak calculation.
- NLO_SWITCH: Switch for the NLO part of a process, if available. If set to true, cross sections and histograms are calculated to NLO QCD accuracy. Default is set to false.
- EWCOR_SWITCH: Switch for the electroweak corrections (note that this is only available for VBF Higgs boson production). If set to true, cross sections and histograms are calculated to NLO electroweak accuracy. This option can only be used if LOOPTOOLS was enabled at compilation. Default is set to false.
- FERMIONLOOP: Flag for the gluon-induced fermionic loop processes, such as $gg \rightarrow WW$ (currently only available for neutral diboson processes in the ranges 300-370 and 4300-4370). The options are:
 - 0 switches off these processes
 - -1 includes only the box contribution
 - 2 includes only diagrams via an *s*-channel Higgs resonance
 - 3 includes both contributions including interference effects.

The default value is 3 (all contributions included).

- NLO_SEMILEP_DECAY: This flag defines how the hadronic decay in processes with semileptonic vector boson decay should be calculated:
 - 0 the hadronic decay $V \rightarrow q\bar{q}$ is calculated at leading order QCD
 - 1 the hadronic decay $V \rightarrow q\bar{q}$ is calculated including approximate next-to leading order QCD effects: A factor of [77]

$$1 + \frac{\alpha_s(Q^2)}{\pi}$$

is applied onto the full matrix element (includes off-shell and singly / nonresonant contributions), which resembles the NLO corrections for the on-shell $V \rightarrow q\bar{q}$ decay. The real emission of a gluon is not resolved.

The default value is 0 (leading order calculation for the decay).

- ECM: The center-of-mass energy, \sqrt{s} , of the collider, measured in GeV. Default is 8000 GeV.
- BEAM1, BEAM2: Define the type of particle of each beam. Possible options are +1 for proton beams and -1 for anti-proton beams. Default is proton-proton collisions, (+1, +1).
- ID_MUF: Choice of the factorization scale. See Table 20 for a list of available options. Default is 0.

For the QCD induced processes, the following definitions are used:

$$H_T = \sum_{i \in \text{partons}} p_{T,i} + E_T(V_1) + E_T(V_2) \tag{2}$$

$$H'_{T} = \sum_{i \in jets} p_{T,i} e^{|y_{i} - y_{12}|} + E_{T}(V_{1}) + E_{T}(V_{2})$$
(3)

with

$$E_T = \sqrt{p_T^2 + m^2}$$
, and $y_{12} = \frac{1}{2}(y_1 + y_2)$

- ID_MUR: Choice of the renormalization scale. See Table 21 for a list of available options. Default is 0. For the QCD induced processes the definitions of Eqs. (2) and (3) are used.
- MUF_USER: If ID_MUF is set to 0, this parameter sets the user defined constant factorization scale measured in GeV. Default is 100 GeV.
- MUR_USER: If ID_MUR is set to 0, this parameter sets the user defined constant renormalization scale measured in GeV. Default is 100 GeV.
- XIF: Factor by which the factorization scale is multiplied. May be used to analyze the scale dependence of differential cross sections. Default is 1.
- XIR: Factor by which the renormalization scale is multiplied. May be used to analyze the scale dependence of differential cross sections. Default is 1.

Note that alternative scale choices can be implemented in the file utilities/scales.F.

4.1.2 vbfnlo.dat - physics parameters

- HMASS: Standard Model Higgs boson mass in GeV. Default value is 126 GeV.
- HTYPE: Type of Higgs boson produced:
 - HTYPE = 0 : SM Higgs boson, with mass HMASS
 - HTYPE = 1 : Light CP-even MSSM Higgs boson
 - HTYPE = 2 : Heavy CP-even MSSM Higgs boson
 - HTYPE = 3 : CP-odd MSSM Higgs boson (Note: this is not produced at LO unless we are working in the MSSM with complex parameters and include Higgs-propagator effects at LO.)

ID_MUF	FACTORIZATION SCALE	PROCESS CLASS
0	user defined constant scale set by MUF_USER momentum transfer of exchanged	all vbf (except Hjjj)
2	gauge boson $\min(p_{\mathrm{T}}(j_i))$	vbf, tribosonjet
3 or 4	invariant mass of the electroweak system $(V \ / \ VV \ / \ VH \ / \ VVV)$	diboson, dibosonjet, triboson, tribosonjet
5	$\sqrt{p_{\rm T}(j_1) \times p_{\rm T}(j_2)}$	ggf
6	constant scale = Higgs boson mass	all
7	Minimum transverse energy of the "primary" bosons	diboson (except W), dibosonjet, triboson, tribosonjet
8	$\frac{1}{2}H_T$ as defined in Eq. (2)	qcdvjj,qcdvvjj
9	$\frac{1}{2}H'_T$ as defined in Eq. (3)	qcdvjj,qcdvvjj
10	$\frac{1}{2} \left(E_T(j_1 j_2) + E_T(V_1 V_2) \right)$	qcdvjj,qcdvvjj

Table 20: Factorization scale options. The definition of the process classes can be found in Section 2.2.

Note that for HTYPE = 1-3, the input HMASS is not used. Default value is 0 (SM Higgs boson).

- HWIDTH: Although VBFNLO can calculate the Higgs total and partial widths, it is also possible to set the Higgs boson width with this input parameter. Default is -999 GeV, which means that the internally calculated value of the width is used. If a SLHA file is being used, the SLHA value will be taken rather than the input HWIDTH.
- MODEL: This flag determines whether we are working in the SM (1), the MSSM (2) or the Two-Higgs model (3). Default is SM (1). Note that if HTYPE = 1-3 is chosen with MODEL = 1, the code will run in the Standard Model, but with a Higgs boson mass equal to that given by the specified MSSM parameters.
- H2MASS: Mass of the second Higgs boson for MODEL = 3. Default value is 126 GeV.
- H2WIDTH: Width of the second Higgs boson for MODEL = 3. Default is -999 GeV, which means that an internally calculated value of the width is used.

ID_MUR	RENORMALIZATION SCALE	PROCESS CLASS
0	user defined constant scale set by MUR_USER	all
1	momentum transfer of exchanged gauge boson	vbf (except Hjjj)
2	$\min(p_{\mathrm{T}}(j_i))$	vbf, tribosonjet
3 or 4	invariant mass of the electroweak system $(V \ / \ VV \ / \ VH \ / \ VVV)$	diboson, dibosonjet, triboson, tribosonjet
5	$\alpha_s^4 = \alpha_s(p_{\mathrm{T}}(j_1)) \times \alpha_s(p_{\mathrm{T}}(j_2)) \times \alpha_s^2(m_H)$	ggf
6	constant scale = Higgs boson mass	all
7	Minimum transverse energy of the "primary" bosons	diboson (except W), dibosonjet, triboson, tribosonjet
8	$\frac{1}{2}H_T$ as defined in Eq. (2)	qcdvjj,qcdvvjj
9	$\frac{1}{2}H'_T$ as defined in Eq. (3)	qcdvjj,qcdvvjj
10	$\frac{1}{2} \left(E_T(j_1 j_2) + E_T(V_1 V_2) \right)$	qcdvjj,qcdvvjj

Table 21: Renormalization scale options. The definition of the process classes can be found in Section 2.2.

- SIN2BA: Multiplicative factor for the squared *HVV*-coupling of the first Higgs boson for MODEL = 3. Default value is 1.
- COS2BA: Multiplicative factor for the squared HVV-coupling of the second Higgs boson for MODEL = 3. Note that unitarity requires that SIN2BA + COS2BA = 1. Default value is -999, which means that the value which fulfills the unitarity relation is chosen.
- TOPMASS: Top-quark mass in GeV. Default value is 172.4 GeV. If a SLHA file is being used, the SLHA value will be taken rather than the input TOPMASS.
- BOTTOMMASS: Bottom-quark pole mass in GeV, used in the calculation of the Higgs boson width and branching ratios. In the gluon fusion processes and gluon-induced contributions to diboson production, $m_b(M_H)$ in the \overline{MS} scheme is used (which is calculated internally from the input pole mass). Default value is 4.855 GeV, which corresponds to $m_b^{\overline{MS}}(m_b) = 4.204$ GeV. The explicit formula used is given on the VBFNLO webpage. If a SLHA file is being used, the SLHA value will be taken rather than the input BOTTOMMASS.

- CHARMMASS: Charm-quark pole mass in GeV used in the calculation of the Higgs boson width and branching ratios. Default value is 1.65 GeV, corresponding to $m_c^{\overline{MS}}(m_c) = 1.273$ GeV. If a SLHA file is being used, the SLHA value will be taken rather than the input CHARMMASS.
- TAU_MASS: Tau mass in GeV used in the calculation of the Higgs boson width and branching ratios. Default value is 1.77684 GeV. If a SLHA file is being used, the SLHA value will be taken rather than the input TAU_MASS.
- EWSCHEME: Sets the scheme for the calculation of electroweak parameters. A summary of the six available options is given in Table 22. Note that if EWSCHEME = 4 is chosen, all variables in Table 22 are taken as inputs. As the parameters are not independent, this can lead to problems if the input values are not consistent. In this scheme, all photon couplings are set according to the input variable INVALFA and all other couplings are set according to FERMI_CONST. Note also that the choice of EWSCHEME can have a large effect on the relative size of the electroweak corrections, as the charge renormalization depends on the way in which the electromagnetic coupling in the LO cross section is parametrized. Full details of all changes and their effects, together with the explicit formulae used, are available on the VBFNLO webpage. Default value is 3.
- FERMI_CONST: Fermi constant, used as input for the calculation of electroweak parameters in EWSCHEME = 1-4. Default value is $1.16637 \times 10^{-5} \text{ GeV}^{-2}$. If a SLHA file is being used, the SLHA value will be taken rather than the input FERMI_CONST.
- INVALFA: One over the fine structure constant, used as input for EWSCHEME = 1, 4, 5 and 6. Within the other schemes this parameter is calculated. The default value depends on the choice of EWSCHEME, as given in Table 22. If EWSCHEME = 5 is chosen, the value of α should be $\alpha(M_Z)$, whereas if EWSCHEME = 6 is chosen, the value of α should be $\alpha(0)$. In order to ensure backwards compatibility with previous versions of VBFNLO, as an alternative ALFA, the fine structure constant, can be used as an input in vbfnlo.dat, which is read and used only if INVALFA is not present. If a SLHA file is being used, the SLHA value will be taken rather than the input INVALFA or ALFA.
- DEL_ALFA: Value of $\Delta \alpha$, where

$$\alpha(M_Z) = \frac{\alpha(0)}{1 - \Delta\alpha} \tag{4}$$

This is used as input for EWSCHEME = 6. Default value is 0.059047686. Note that this is only used for the electroweak corrections during the calculation of the charge renormalization constant.

- SIN2W: Sinus squared of the weak mixing angle. Used as input for EWSCHEME = 2 and 4. Within the other schemes this parameter is calculated. Default input value is 0.222646. If a SLHA file is being used, the SLHA value will be taken rather than the input SIN2W.
- WMASS: W boson mass in GeV. This parameter is calculated in EWSCHEME = 1 and 2. Default input value is 80.398 GeV. If a SLHA file is being used, the SLHA value will be taken rather than the input WMASS.

EWSCHEME	Parameter	Default Value	INPUT/CALCULATE
1	FERMI_CONST	$1.16637 \times 10^{-5} \text{ GeV}^{-2}$	Input
	INVALFA	128.944341122	Input
	SIN2W	0.230990	CALCULATED
	WMASS	$79.9654 \mathrm{GeV}$	Calculated
	ZMASS	$91.1876 {\rm GeV}$	Input
2	FERMI_CONST	$1.16637 \times 10^{-5} \text{ GeV}^{-2}$	Input
	INVALFA	132.340643024	CALCULATED
	SIN2W	0.222646	INPUT
	WMASS	80.3980 GeV	CALCULATED
	ZMASS	$91.1876 { m ~GeV}$	Input
3	FERMI_CONST	$1.16637 \times 10^{-5} \text{ GeV}^{-2}$	Input
	INVALFA	132.340705199	CALCULATED
	SIN2W	0.222646	CALCULATED
	WMASS	80.3980 GeV	INPUT
	ZMASS	91.1876 GeV	INPUT
4	FERMI_CONST	$1.16637 \times 10^{-5} \text{ GeV}^{-2}$	Input
	INVALFA	137.035999679	INPUT
	SIN2W	0.222646	INPUT
	WMASS	80.3980 GeV	INPUT
	ZMASS	91.1876 GeV	INPUT
5	INVALFA(ZMASS)	128.944341122	Input
	SIN2W	0.222646	CALCULATED
	WMASS	80.3980 GeV	INPUT
	ZMASS	91.1876 GeV	INPUT
6	INVALFA(0)	137.035999679	Input
	SIN2W	0.222646	CALCULATED
	WMASS	80.398 GeV	INPUT
	ZMASS	91.1876 GeV	INPUT

 Table 22: Electroweak input parameter schemes.

- ZMASS: Z boson mass in GeV. Default value is 91.1876 GeV. If a SLHA file is being used, the SLHA value will be taken rather than the input ZMASS.
- ANOM_CPL: If set to true, anomalous Higgs boson or gauge boson couplings are used if available for the selected process. Anomalous coupling parameters are set via the files anom_HVV.dat and anomV.dat. These are available for
 - Hjj, single and double vector production processes in VBF
 - diboson production processes, including WH
 - diboson + jet production processes, including WHj
 - triple vector boson production processes
 - triboson + jet production processes
 - $-Hjj \rightarrow VVjj$ production via gluon fusion
 - gluon-induced (contributions to) diboson production

Default is set to false.

- KK_MOD: Option for the Warped Higgsless Model and Three-Site Higgsless Model. This is available for all VVjj production modes in VBF except $W\gamma$ and same sign $W^{\pm}W^{\pm}$ production and for the triboson processes $W^{\pm}W^{+}W^{-}$, $W^{+}W^{-}Z$ and $W^{\pm}ZZ$. Default is set to false. Note that this needs to be enabled at compilation, using the configure option --enable-kk. Kaluza-Klein parameters are specified via the files kk_input.dat or kk_coupl_inp.dat.
- SPIN2: Option for the spin-2 models. This is available for the VVjj production modes in VBF except same sign W[±]W[±] production. Default is set to false. Note that this needs to be enabled at compilation, using the configure option --enable-spin2. Spin-2 parameters are set via the file spin2coupl.dat.
- EW_APPROX: Option controlling the electroweak corrections in Hjj production via VBF.
 - $EW_APPROX = 0$: No approximations involved. This option is not available when working in the MSSM.
 - EW_APPROX = 1 : Only top/bottom (and stop/sbottom in the MSSM) loops are calculated.
 - $EW_APPROX = 2$: All fermion (and sfermion in the MSSM) loops are calculated.
 - EW_APPROX = 3 : MSSM option all SM-type (i.e. fermions, gauge and Higgs bosons) and sfermion loops are calculated.
 - EW_APPROX = 4 : MSSM option all MSSM corrections to the Higgs boson vertex are calculated, together with all SM-type and sfermion corrections elsewhere.
 - EW_APPROX = 5: MSSM option all MSSM corrections to the Higgs boson vertex, the quark vertex and the vector boson self energies are calculated, together with all SM-type boxes and pentagons (i.e. only chargino and neutralino box and pentagon diagrams are neglected).

When working in the SM, EW_APPROX options 3-5 are equivalent to $EW_APPROX = 0$. Default is 5: full corrections in the SM, and the most complete available corrections in the MSSM.

4.1.3 vbfnlo.dat - parameters for event output

VBFNLO generates parton level events according to the most recent Les Houches Accord (LHA) format [78] and in the HEPMC format [79] for all processes at leading order, except for $W\gamma j$, WZj and $W\gamma\gamma j$ production. For WH(j) production the event output is only available in the case of a non-decaying Higgs boson.

- LHA_SWITCH: Switch on or off output of LHA event files. Default is set to false. Note that LHA event file output is not yet available for diboson plus jet or triboson plus jet processes.
- LHA_FILE: Name of output LHA event file. Default is "event.lhe".
- HEPMC_SWITCH: Switch on or off output of HEPMC event files. Default is set to false. Note that HEPMC event file output is not yet available for diboson plus jet or triboson plus jet processes.
- HEPMC_FILE: Name of output HEPMC event file. Default is "event.hepmc".
- UNWEIGHTING_SWITCH: Option for event weights. If set to true, events are unweighted (event weight = +1). If set to false, events are weighted. Default is set to true.
- DESIRED_EVENT_COUNT: With UNWEIGHTING_SWITCH = true, the number of unweighted events written out to disk can be specified. For multi-channel processes (for example diboson / triboson production with a final-state photon) this can be time-consuming.
 DESIRED_EVENT_COUNT = 0 stands for collecting all events generated during the

DESIRED_EVENT_COUNT = 0 stands for collecting all events generated during the normal integration (behaviour of VBFNLO up to version 2.7 beta 2). Default is DESIRED_EVENT_COUNT = 0.

• PARTIAL_UNWEIGHTING: For some processes or parameter settings it may not be possible to get the desired number of unweighted events: Single events with large weights in some problematic phase space regions can spoil the unweighting efficiency. For this case PARTIAL_UNWEIGHTING = true will give the desired number of events with weight 1 and additionally a few events with weight > 1 which occured during the event generation.

Default is PARTIAL_UNWEIGHTING = false.

• TAUMASS: Option to include the mass of τ leptons in the event files. Default is set to false.

All calculations (except for branching ratios) are done with massless τ leptons. However, as subsequent programs need the non-zero mass for the τ decay, VBFNLO can include the τ mass in the output and rescale the momentum consistently. The τ leptons in the events have to fulfill $m_{\tau\tau} > 2 \cdot m_{\tau}$ and $m_{\tau\nu_{\tau}} > m_{\tau}$, otherwise the inclusion of m_{τ} is not possible. All events where this requirement is not fulfilled will be dismissed. Usually this criterium should be always met when using reasonable cuts. To ensure that no events are thrown away please use a cut on the invariant lepton pair mass of at least $m_{\ell\ell} > 2 m_{\tau}$.

Important note for processes with more than one phase space (usually processes involving a final state photon):

VBFNLO writes the events of different phase spaces block-wise into the event file. Therefore the event file should always be used completely, otherwise some parts of phase space are underrepresented. Using only parts of the event file gives only correct results if the events are taken randomly from the whole file. This note is put out at the end of the VBFNLO run for the relevant processes if event output is requested.

4.1.4 vbfnlo.dat - PDF parameters

VBFNLO can use either built-in parton distribution functions (PDFs) or the LHAPDF [4] library, either in version 5 or 6.

- PDF_SWITCH: Flag to choose which PDFs are used. The options are
 - 0 : built-in PDFs CTEQ6L1 [13] for LO and CT10 [14] for NLO calculations
 - 1 : an interface to LHAPDF is provided
 - 2 : built-in PDFs MRST2004qed [15] are used at LO and NLO (if this option is chosen, photon-induced processes can be included when calculating the electroweak corrections to Hjj production via VBF)
 - 3 : the built-in PDFs MSTW2008 [16] are used

Default is 0.

The following options are used only if LHAPDF has been selected (i.e. PDF_SWITCH = 1).

- LO_PDFNAME: Name of the LO PDF set. Default is "cteq611.LHpdf" (cteq611).
- NLO_PDFNAME: Name of the NLO PDF set. Default is "CT10.LHgrid" (CT10).
- LO_PDFMEMBER: Member PDF of the LO PDF set. Default is 0.
- NLO_PDFMEMBER: Member PDF of the NLO PDF set. Default is 0.

The names of the PDF sets can be found on the LHAPDF website¹⁹. In case of LHAPDF 6 the file ending (.LHgrid/.LHpdf) is no longer needed, but using the LHAPDF 5 naming scheme is still supported. The list of PDF sets which are already available in LHAPDF 6 can be obtained from the LHAPDF website as well²⁰. The PDF name can also be obtained from the file PDFsets.index, which is located in the LHAPDF 5 subfolder share/lhapdf²¹.

For compatibility with earlier versions of VBFNLO, the following two variables are also supported for setting the PDF sets when using LHAPDF. If both are present, LO_PDFNAME and NLO_PDFNAME take precedence over LO_PDFSET and NLO_PDFSET, respectively.

- LO_PDFSET: LHAGLUE number for the LO PDF set.
- NLO_PDFSET: LHAGLUE number for the NLO PDF set.

The LHAGLUE numbers can be found on the LHAPDF website¹⁹ or in the file PDFsets.index, which is located in the LHAPDF 5 subfolder share/lhapdf²¹.

 $^{^{19} \}tt http://lhapdf.hepforge.org/pdfsets$

 $^{^{20}}$ http://www.hepforge.org/archive/lhapdf/pdfsets/6.0/

 $^{^{21}}When \ using \ LhapDF \ 6 \ this file is located at <LhapDF-PATH>/share/LhapDF/pdfsets.index .$

4.1.5 vbfnlo.dat - parameters for output and histograms

VBFNLO provides output for histograms in the following formats: $GNUPLOT^{22}$, $ROOT^{23}$ and $TOPDRAWER^{24}$, as well as raw data tables. Options controlling the histogram ranges and smearing are defined in histograms.dat. Additional histograms can be defined by the user in the file utilities/histograms.F.

- XSECFILE: Name of output file containing LO and NLO cross sections with the associated errors. Default is xsection.
- ROOT: Enable output of histograms in ROOT format. Default is set to false. Additionally, custom ROOT histograms can be defined by the user with the file utilities/rootuserhists.cpp, which are filled with the weighted events from Monte Carlo integration. This option needs to be enabled when building VBFNLO using the option --with-root.
- TOP: Enable output of histograms in TOPDRAWER format. Default is set to false.
- GNU: Enable output of histograms in GNUPLOT format. Default is set to true.
- DATA: Enable output of raw data in a directory hierarchy. Additionally, a GNUPLOT command file is written into the data output directory. Default is set to true.
- REPLACE: Switch to overwrite existing histogram output files. Default is set to true.
- ROOTFILE: Name of the ROOT output file. Default is histograms.
- TOPFILE: Name of the TOPDRAWER output file. Default is histograms.
- GNUFILE: Name of the GNUPLOT output file. Default is histograms.
- DATAFILE: Name of the data output directory. Default is histograms.

4.2 cuts.dat – parameters for kinematic cuts

The following general set of cuts has been implemented in VBFNLO. Alternative cuts can be added in the file utilities/cuts.F.

A brief documentation on how to implement additional cuts into the file <code>cuts.F</code> can be found on the VBFNLO webpage, http://www.itp.kit.edu/vbfnlo/.

4.2.1 cuts.dat - jet-specific cuts

- RJJ_MIN: Minimum separation of two identified jets, $\Delta R_{jj} = \sqrt{\Delta y_{jj}^2 + \Delta \phi_{jj}^2}$, used by the generalised k_{\perp} jet finding algorithm [80] that combines all partons. Default is 0.8.
- Y_P_MAX: Maximum allowed (pseudo)rapidity²⁵ for observation of final state partons (detector edge). Default is 5.0.

²²http://www.gnuplot.info/

 $^{^{23}}$ http://root.cern.ch/

²⁴http://www.pa.msu.edu/reference/topdrawer-docs/

 $^{^{25}}$ As all quarks and leptons are considered massless in VBFNLO, pseudorapidity and rapidity coincide for almost all final state particles, with one exception: Jets which consist of more than one parton have a non-vanishing mass and therefore rapidity \neq pseudorapidity.

- PGENKTJET: Exponent of the generalised k_{\perp} algorithm. This yields the k_{\perp} algorithm when setting the variable to 1, the Cambridge/Aachen algorithm [81] for 0 and the anti- k_{\perp} algorithm [82] when setting it to -1. Default value of the floating-point number is 1.0.
- PT_JET_MIN: List of minimum transverse momenta for identified jets in descending order. The later values can be omitted if they are the same as previous values. Default is 20 GeV.
- Y_JET_MAX: Maximum allowed rapidity for identified jets. Default is 4.5.

4.2.2 cuts.dat - lepton specific cuts

- Y_L_MAX: Maximum (pseudo)rapidity for charged leptons. Default is 2.5.
- PT_L_MIN: List of minimum transverse momenta for charged leptons in descending order. The later values can be omitted if they are the same as previous values. Default is 10 GeV.
- MLL_MIN: Minimum invariant mass for pairs of charged leptons. Whether this applies only to opposite-sign leptons or to all pairs is chosen by the variable MLL_OSONLY. Default is 15 GeV.
- MLL_MAX: Maximum invariant mass for pairs of charged leptons. Whether this applies only to opposite-sign leptons or to all pairs is chosen by the variable MLL_OSONLY. Default is 10²⁰ GeV.
- MLL_OSONLY: If set to true, the variables MLL_MIN and MLL_MAX only apply to pairs of oppositely signed leptons, otherwise to all pairs of charged leptons. Default is true.
- RLL_MIN: Minimum separation of charged lepton pairs, $\Delta R_{\ell\ell}$. Default is 0.4.
- RLL_MAX: Maximum separation of charged lepton pairs, $\Delta R_{\ell\ell}$. Default is 50.

4.2.3 cuts.dat – photon specific cuts

- Y_G_MAX: Maximum (pseudo)rapidity for photons. Default is 1.5.
- PT_G_MIN: List of minimum transverse momenta for photons in descending order. The later values can be omitted if they are the same as previous values. Default is 20 GeV.
- RGG_MIN: Minimum separation of photon pairs, $\Delta R_{\gamma\gamma}$. Default is 0.6.
- RGG_MAX: Maximum separation of photon pairs, $\Delta R_{\gamma\gamma}$. Default is 50.

VBFNLO has a photon isolation cut implemented as defined in Ref. [31],

$$\sum_{i} E_{T_{i}} \theta(\delta - R_{i\gamma}) \le \epsilon \ p_{T_{\gamma}} \frac{1 - \cos \delta}{1 - \cos \delta_{0}} \text{ for all } \delta < \delta_{0} , \qquad (5)$$

where *i* is a parton with transverse energy E_{T_i} and a separation $R_{i\gamma}$ with a photon of transverse momentum $p_{T\gamma}$. The parameters δ_0 and ϵ can be adjusted:

- PHISOLCUT: Photon isolation δ_0 . Default is 0.7.
- EFISOLCUT: Efficiency ϵ of photon isolation cut. Default is 1.

4.2.4cuts.dat - additional cuts

- RJL_MIN: Minimum separation of an identified jet and a charged lepton, $\Delta R_{i\ell}$. Default is 0.6.
- RJG_MIN: Minimum separation of an identified jet and a photon, $\Delta R_{i\gamma}$. Default is 0.6.
- RLG_MIN: Minimum separation of a charged lepton and a photon, $\Delta R_{\ell\gamma}$. Default is 0.6.
- MLG_MIN: Minimum invariant mass for any combination of a charged lepton and a photon. Default is 0 GeV.
- MLG_MAX: Maximum invariant mass for any combination of a charged lepton and a photon. Default is 10^{20} GeV.
- PTMISS_MIN: Minimum missing transverse momentum of the event

$$p_T^{miss} = -\sum_i p_{T,i}$$

summing over all visible jets, leptons and photons. Default is 0 GeV.

4.2.5cuts.dat - jet veto

- JVETO: If set to true, a jet veto is applied. For processes with fully leptonic decays of the vector bosons the following criteria apply:
 - For vbf and ggf processes it is applied to central jets beyond the two tagging jets, where the central region is bounded by the rapidities of the two tagging jets.
 - For all other processes the jet veto is applied to additional jets beyond the leading-order number, ordered by decreasing transverse momentum.

For processes with one hadronically decaying vector boson, one or two additional jets are allowed, depending on the value of SINGLE_DECAYJET (one jet for SINGLE_DECAYJET = 2, else two jets).

Default is false.

- YMAX_VETO: Maximum rapidity of the additional jet. Default is 4.5.
- PTMIN_VETO: Minimum transverse momentum of the additional jet. Default is 50 GeV.
- DELY_JVETO: Minimum rapidity separation of a central jet from the two tagging jets for vbf and ggf processes. Default is 0.

$4.2.6 \quad \texttt{cuts.dat} - VBF \ \text{specific cuts}$

These cuts apply only to vbf, qcdv(v)jj and ggf processes. Furthermore, they apply to the processes with semileptonic decays if VBFCUTS_ALWAYS = true.

- ETAJJ_MIN: Minimum required rapidity gap, $\Delta \eta_{jj}$, between two tagging jets, which are the two leading jets in a $p_{\rm T}$ ordering for fully leptonically decaying vector bosons. For tagging jet definition in semileptonic decay processes see DEF_TAGJET. Default is 0.
- YSIGN: If set to true, the two tagging jets are required to be found in opposite detector hemispheres. Default is false.
- LRAPIDGAP: If set to true all charged leptons are required to lie between the two tagging jets in rapidity. Default is false.
- DELY_JL: Minimum rapidity distance of the charged leptons from the tagging jets, if LRAPIDGAP is set to true. Default is 0.
- GRAPIDGAP: If set to true all photons are required to lie between the two tagging jets in rapidity. Default is false.
- DELY_JG: Minimum rapidity distance of photons from tagging jets, if GRAPIDGAP is set to true. Default is 0.
- MDIJ_MIN: Minimum dijet invariant mass of two tagging jets. Default is 0 GeV.
- MDIJ_MAX: Maximum dijet invariant mass of two tagging jets. Default is 10²⁰ GeV.

4.2.7 cuts.dat - special cuts for semileptonic decays

These cuts apply only to processes with one hadronically decaying vector boson.

- DEF_TAGJET: Switch for different tagging jet definitions.
 - DEF_TAGJET = 1: two jets with largest p_T
 - DEF_TAGJET = 2: two jets with largest p_T and $|y| > \text{ETA}_CENTRAL$. Furthermore both jets have to lie in opposite detector hemispheres.
 - DEF_TAGJET = 3: two jets with largest separation in rapidity
 - DEF_TAGJET = 4: two jets with largest p_T , except for the two jets (or one jet if SINGLE_DECAYJET > 0 and the mass of a single jet is closer to m_V than any two-jet combination) with an invariant mass closest to m_V .

Default is 1.

- ETA_CENTRAL: Defines the outer limit of the "central region" if DEF_TAGJET = 2. For other values of DEF_TAGJET the "central region" is defined by the rapidity values of the two tagging jets. Default is 2.
- PTMIN_TAG_1: Minimum transverse momentum for the harder tagging jet. Default is 20 GeV.

- PTMIN_TAG_2: Minimum transverse momentum for the softer tagging jet. Default is 20 GeV.
- HARD_CENTRAL: If set to true an additional jet is required within the central region. Default is false.
- PTMIN_CENTRAL: Minimum transverse momentum for the additional hard jet in the central region if PTMIN_CENTRAL = true. Default is 20 GeV.
- VBFCUTS_ALWAYS: Usually the VBF cuts are only applied for VBF processes. With VBFCUTS_ALWAYS = true, the VBF cuts are applied to the semileptonic diboson and triboson production processes as well, as they supplement the *s*-channel part of the electroweak V(V) jj production to the VBF processes. Default is false.
- RECONST_HAD_V: Choose between different options for a cut on the reconstructed invariant mass of the hadronically decaying vector boson. All possible jet combinations are taken into account, the one which gives an invariant mass closest to the vector boson mass is used to apply the cut.
 - RECONST_HAD_V = 0: No cut on the reconstructed invariant vector boson mass.
 - RECONST_HAD_V = 1: Use two-jet invariant mass, tagging jets are not considered.
 - RECONST_HAD_V = 2: Use invariant mass of a single jet, tagging jets are not considered ("subjet-analysis", only needed when SINGLE_DECAYJET > 0).
 - RECONST_HAD_V = 3: Use one- or two-jet invariant mass, tagging jets are not considered.

Default is 0.

- V_MASS_RANGE: Mass range for the cut on the reconstructed invariant vector boson mass: $|m_V m_reconst| < V_MASS_RANGE$. Default is 20 GeV.
- SINGLE_DECAYJET: This switch controls the number of additional jets which is required for processes with semileptonic decay of the vector bosons with respect to the fully leptonic process:
 - SINGLE_DECAYJET = 0: two jets are required from the hadronic decay (plus two tagging jets for the VBF processes).
 - SINGLE_DECAYJET = 1: a single jet is allowed if both quarks from the hadronic decay are collimated into one jet.
 - SINGLE_DECAYJET = 2: a single jet is allowed for all phase space points.

SINGLE_DECAYJET = 2 can only be used with LOPROCESS_PLUS_JET set to false in vbfnlo.dat.

Default is 0.

• QSQAMIN_ZDEC: Minimal photon virtuality of hadronically decaying Z/γ^* . Default is 0 GeV². However, any values below the Q^2 threshold (see Section 4.2.8) for u/d-quarks of $(0.373 \text{ GeV})^2$ have no effect. As the Higgs boson does not couple directly to photons, no special treatment or cut is needed for process 1010. Therefore QSQAMIN_ZDEC is not evaluated there.

4.2.8 Treatment of hadronic decays of low-virtuality photons

As the hadronic decay of a Z boson also includes the hadronic decay of photons, a divergence in $\gamma^* \rightarrow q\bar{q}$ occurs, when the final state quarks are treated massless and no cuts are applied. In the case of the semileptonic decays within VBFNLO, this can lead to problems in two cases:

- In the real emission case with one additional visible jet from QCD radiation both decay quarks are allowed to form a single jet.
- This can also happen already at leading order, when SINGLE_DECAYJET is set to true.

Therefore we apply a cut on the minimal photon virtuality, which is estimated from $e^+e^- \rightarrow$ hadrons individually for each final state quark flavour. The threshold for each quark is chosen such that the NLO approximation for $\sigma(e^+e^- \rightarrow \text{hadrons})$ gives the same contribution as the experimental continuum data plus the contribution from the sharp resonances of the respective quark flavours [83].

This procedure approximates the correct rates from low- q^2 photons. The kinematics of the quarks in this region are not modeled correctly, but this is of minor importance as the low- q^2 region is only relevant for semileptonic decays when the decay products form a single jet.

Unfortunately, this procedure can cause problems when interfacing VBFNLO with a parton shower Monte Carlo program by using the Les Houches event output without jet cuts or with SINGLE_DECAYJET = true. Events which involve $q\bar{q}$ pairs with an invariant mass below 1 GeV or below $2 \cdot m_q$ may be dismissed by the parton shower Monte Carlo. This can be avoided by using the option QSQAMIN_ZDEC.

4.3 ggflo.dat – general parameters for gluon fusion processes

In VBFNLO the double real-emission corrections to $gg \rightarrow \phi$, which lead to $\phi + 2$ jet events at order α_s^4 , are included [75]. Here, ϕ can be set to be a Standard Model Higgs boson or any of the three neutral MSSM Higgs bosons (including mixing between h, H and Ain the real or complex MSSM) by using the variables HTYPE and MODEL in vbfnlo.dat, or a mixture of scalar and pseudoscalar Higgs bosons as in a generic two-Higgs-doublet model (2HDM) of type II. Contributions contain top- and bottom-quark triangles, boxes and pentagon diagrams, i.e. the full mass dependence of the loop induced production²⁶. Interference effects between loops with bottom- and top-quarks, as well as between $C\mathcal{P}$ -even and $C\mathcal{P}$ -odd couplings of the heavy quarks, are fully taken into account. An option to use the large top mass approximation, which works well for intermediate Higgs boson masses (provided that the transverse momenta of the final state partons are smaller than the top-quark mass), is also implemented.

Note that these gluon fusion processes require the use of the ggflo executable rather than the vbfnlo one.

²⁶The bottom quark mass is taken as $m_b(M_H)$ in the \overline{MS} scheme.

If Higgs boson plus two jet production via gluon fusion is selected in vbfnlo.dat, i.e. PROCESS = 4100-4107, the following additional parameters can be adjusted in the ggflo.dat file:

- Q_LOOP: Input that sets how the Higgs boson coupling is determined.
 - Q_LOOP = 0: Effective theory in the large top-quark mass limit $(m_t \to \infty)$.
 - $Q_LOOP = 1$: Coupling derived from top-quark loop.
 - $Q_LOOP = 2$: Coupling derived from bottom-quark loop.
 - $Q_LOOP = 3$: Coupling derived from both top- and bottom-quark loops.

Default is set to 3.

- SUBPRQQ: Switch that determines whether the subprocesses with a quark-quark initial state are included. Default is set to true.
- SUBPRQG: Switch that determines whether the subprocesses with a quark-gluon initial state are included. Default is set to true.
- SUBPRGG: Switch that determines whether the subprocesses with a gluon-gluon initial state are included. Default is set to true.
- HIGGS_MIX: Switch for Higgs mixing. If set to 0, there is no Higgs mixing, which is the default. If set to 1, the mixing is determined via the user-input variables:
 - CP_EVEN_MOD: Changes the strength of the CP-even coupling. Default is set to 1d0.
 - CP_ODD_MOD: Changes the strength of the \mathcal{CP} -odd coupling. Default is set to 1d0.

using the Lagrangian

$$\mathcal{L}_{\text{Yukawa}} = \overline{q} \left(C_{\text{even}} \, y_q + \mathrm{i} \, C_{\text{odd}} \, \gamma_5 \, \tilde{y}_q \right) q \, \Phi \tag{6}$$

with $C_{\text{even}} = \text{CP}_{\text{EVEN}_{\text{MOD}}}$ and $C_{\text{odd}} = \text{CP}_{\text{ODD}_{\text{MOD}}}$ and

$$y_b = \tilde{y}_b = \frac{1}{v} m_b \tan \beta$$

$$y_t = \tilde{y}_t = \frac{1}{v} m_t \cot \beta.$$
(7)

When working in the Standard Model, $\tan \beta$ is set to 1. Note that this option is not yet available when decays of the Higgs boson to fermions or photons are included. The option HIGGS_MIX = 2 is only used when working in the MSSM, and incorporates mixing between all three neutral Higgs bosons according to the Z propagator matrix, as follows

$$h_i = Z_{ih} h_{\text{MSSM}} + Z_{iH} H_{\text{MSSM}} + Z_{iA} A_{\text{MSSM}} , \qquad (8)$$

where i = HTYPE.

4.4 susy.dat – parameters in the MSSM

The file susy.dat is used to specify the supersymmetric parameters when working in the MSSM. This file is used either if MODEL = 2 in vbfnlo.dat, or if HTYPE = 1-3 in vbfnlo.dat. As described earlier, if MODEL = 2 the code will run in the MSSM, which means that the Higgs boson masses, widths and couplings will all be set to the MSSM values. If MODEL = 1 but HTYPE = 1-3, the code will run in the Standard Model, and only the Higgs boson mass will be affected. Consequently, this file affects processes 100-107 (Higgs boson plus 2 jet production via VBF), processes 110-117 (Higgs boson plus 3 jet production via VBF), processes 2100-2107 (production of a Higgs boson in association with a photon and 2 jets via VBF) and gluon fusion processes 4100-4107. In particular, the electroweak corrections to Higgs boson production via VBF are affected by the inputs of susy.dat. As stated earlier, the Higgs boson contributions to the production of massive gauge bosons will be affected by susy.dat by fixing the Higgs boson mass and couplings, but the code will only provide a reasonable approximation to the full MSSM result in the decoupling region (i.e. when the Higgs is SM-like).

- FEYNH_SWITCH: Determines whether FEYNHIGGS is used to calculate the MSSM Higgs boson sector. Default is false. When working in the MSSM, especially when including electroweak corrections, it is recommended that FEYNHIGGS is used, as the Higgs boson mixing and the renormalization scheme used in VBFNLO are consistent with those used by FEYNHIGGS. If a SLHA file is used instead of FEYNHIGGS, inconsistencies may occur in the calculation of parameters.
- SLHA_SWITCH: Determines whether the MSSM parameters are taken from a SLHA file. Default is true. If set to true the values in the SLHA input file are used instead of internal settings or calculations²⁷.
- SLHA_FILE: Name of the SLHA input file. An example file sps1a.slha is provided, which is the default.
- BENCH: Various benchmark scenarios are pre-programmed in the code, as an alternative to using a SLHA file. These are:
 - 0: User-input scenario (see below for further inputs)
 - $-1: M_h^{\max}$ scenario [84]
 - 2: No-mixing scenario [84]
 - 3: Gluophobic scenario [84]
 - 4: Small α_{eff} scenario [84]
 - -5: CPX scenario [85]
 - $-10: SPS1a^{28}$ [86]
 - 11: SPS1b
 - 12-19: SPS 2-9

 $^{^{27}}Note$ that a SLHA file can also be used as the input for FeynHiggs by setting both FeynH_SWITCH and SLHA_SWITCH to true.

 $^{^{28}{\}rm The}~{\rm SPS}$ points are defined with low-energy parameters, as given at http://www.ippp.dur.ac.uk/~georg/sps/).

Default is $1 - \text{the } M_h^{\text{max}}$ scenario.

- **PROPLEVEL**: Level at which Higgs propagator corrections are included:
 - 0: Effective Higgs-mixing angle used.
 - -1: Propagator factors included at leading order.
 - 2: Propagator factors included at leading order and loop level.
 - 3: Propagator factors included as an additional loop correction.

Default is 1. These options are discussed in more detail on the VBFNLO webpage, as well as in [34].

- DELMB_SWITCH: Switch determining whether or not to correct the bottom-quark Yukawa coupling. Default is false.
- MH_LOOPS: Flag determining the value of the internal Higgs masses used in the electroweak loops:
 - 0: Tree level Higgs masses used in loops.
 - 1: Corrected Higgs masses used in loops.
- LOOPSQR_SWITCH: Flag determining whether the squared contributions of the electroweak corrections from the (s)fermion sector will be included i.e. if set to true the amplitude is given by:

$$|\mathcal{M}_{\text{Born}}|^2 + 2\Re \left[\mathcal{M}_{\text{Born}}^* \mathcal{M}_{loop}\right] + |\mathcal{M}_{(\text{s)fermion loop}}|^2 \tag{9}$$

Note that the loop squared component is only added if $|\mathcal{M}_{(s)\text{fermion loop}}|$ is greater than 10% of $|\mathcal{M}_{Born}|$. Default is set to true.

If a SLHA file is not being used, and BENCH = 0-5, the following inputs are also needed.

- TANB: Value of tan β. Default value is 10. Note that for the SPS benchmarks (BENCH = 10-19), this value of tan β is not used.
- MASSA0: Mass of $C\mathcal{P}$ -odd Higgs boson M_A . This should be used when working in the MSSM with real parameters. Default value is 400 GeV. Note that for the SPS benchmarks (BENCH=10-19), this value of M_A is not used.
- MASSHP: Mass of charged Higgs boson $M_{H^{\pm}}$. This should be used when working in the MSSM with complex parameters. Default value is -1 GeV.

Note that it is standard to use as input the mass of the $C\mathcal{P}$ -odd Higgs boson, M_A , when working in the MSSM with real parameters and the mass of the charged Higgs boson, $M_{H^{\pm}}$, when working in the MSSM with complex parameters²⁹. The mass that is not being used as input should be set to -1 GeV.

If desired, the SUSY breaking parameters that define the scenario can be input by the user, by selecting BENCH = 0. Default values are those for SPS1a. These parameters are (in the notation used by FEYNHIGGS):

²⁹This is because, when working with complex parameters, there is mixing between all three neutral Higgs bosons, and thus all neutral Higgs boson masses receive loop corrections.

- M3SQ etc.: The soft SUSY breaking parameters for the sfermion section.
- AT etc.: Trilinear coupling parameters.
- MUE: Higgs boson mixing parameter.
- M_1 etc.: Gaugino mass parameters.

By default, lower generation parameters are set to the corresponding higher generation parameters - e.g. Ac = At.

4.5 Parameters for anomalous couplings

VBFNLO supports anomalous HVV couplings, where $V = W, Z, \gamma$, in both the production and the decay of a Higgs boson in VBF-type reactions, i.e. for process IDs 100-107. Anomalous HVV couplings are also included in gluon induced diboson production (processes 430x, 433x, 4360, 4370, and processes 30x, 33x, 360 and 370), as well as in gluon fusion processes $Hjj \rightarrow VVjj$ (IDs 4105-7). The anomalous HVV couplings can be specified in the anom_HVV.dat input file.

Anomalous triple and quartic gauge boson couplings are available for single and double vector boson production via VBF (process IDs 120-150, 200-280) [87,88], all triple vector boson production processes (process IDs 400-530, 800, 810) [88,89], diboson production $WW, W^{\pm}\gamma, W^{\pm}Z$ and WH (process IDs 300-323, 340-350, 1300-1317) [51,52] and for diboson plus jet processes $W^{\pm}\gamma j$ [60], $W^{\pm}Z j$ [59] and WH j [51] (IDs 610-640, 1600-1617). The respective parameters are set in the input file anomV.dat. Note, however, that not all parameters in anomV.dat affect all processes and no neutral triple gauge boson couplings are included. By altering the triple gauge boson couplings (in anomV.dat), the couplings between a Higgs and a pair of gauge bosons are also affected – these changes are taken into account automatically for internal and external Higgs bosons occurring in these processes (and during the Higgs width calculations).

4.5.1 anom_HVV.dat - anomalous HVV couplings

The file anom_HVV.dat controls the anomalous Higgs boson coupling parameters. It is used if the input ANOM_CPL in vbfnlo.dat is set to true. Among the anomalous coupling input parameters, the user can choose between three different parametrizations.

The anomalous HVV couplings can be described by the following effective Lagrangian involving the dimension five operators

$$\mathcal{L} = \frac{g_{5e}^{HZZ}}{2\Lambda_5} H Z_{\mu\nu} Z^{\mu\nu} + \frac{g_{5o}^{HZZ}}{2\Lambda_5} H \widetilde{Z}_{\mu\nu} Z^{\mu\nu} + \frac{g_{5e}^{HWW}}{\Lambda_5} H W^+_{\mu\nu} W^+_{-} + \frac{g_{5o}^{HWW}}{\Lambda_5} H \widetilde{W}^+_{\mu\nu} W^{\mu\nu}_{-} + \frac{g_{5e}^{HZ\gamma}}{\Lambda_5} H Z_{\mu\nu} A^{\mu\nu} + \frac{g_{5o}^{HZ\gamma}}{\Lambda_5} H \widetilde{Z}_{\mu\nu} A^{\mu\nu} + \frac{g_{5e}^{H\gamma\gamma}}{2\Lambda_5} H A_{\mu\nu} A^{\mu\nu} + \frac{g_{5o}^{H\gamma\gamma}}{2\Lambda_5} H \widetilde{A}_{\mu\nu} A^{\mu\nu}$$
(10)

where the subscript e or o refers to the $C\mathcal{P}$ -even or $C\mathcal{P}$ -odd nature of the individual operators [90], $V^{\mu\nu}$ is the field strength tensor of the gauge boson V and $\tilde{V}^{\mu\nu}$ is the dual field strength.

An alternative approach is to write the effective Lagrangian in terms of the dimension-6 operators \mathcal{O}_{WW} , \mathcal{O}_{BB} , \mathcal{O}_W and \mathcal{O}_B and their corresponding \mathcal{CP} -odd operators according to Refs. [91,92]:

$$\mathcal{L}_{\text{eff}} = \frac{f_W}{\Lambda^2} \mathcal{O}_W + \frac{f_B}{\Lambda^2} \mathcal{O}_B + \frac{f_{WW}}{\Lambda^2} \mathcal{O}_{WW} + \frac{f_{BB}}{\Lambda^2} \mathcal{O}_{BB} + \text{ CP-odd part}$$
(11)

The explicit form of the operators is

$$\mathcal{O}_{W} = (D_{\mu}\phi^{\dagger})\widehat{W}^{\mu\nu}(D_{\nu}\phi)$$

$$\mathcal{O}_{B} = (D_{\mu}\phi^{\dagger})\widehat{B}^{\mu\nu}(D_{\nu}\phi)$$

$$\mathcal{O}_{WW} = \phi^{\dagger}\widehat{W}_{\mu\nu}\widehat{W}^{\mu\nu}\phi$$

$$\mathcal{O}_{BB} = \phi^{\dagger}\widehat{B}_{\mu\nu}\widehat{B}^{\mu\nu}\phi, \qquad (12)$$

with

$$\widehat{W}_{\mu\nu} = igT^a W^a_{\mu\nu}
\widehat{B}_{\mu\nu} = ig'Y B_{\mu\nu},$$
(13)

where g and g' are the SU(2) and U(1) gauge couplings, and T^a are the SU(2) generators. The \mathcal{CP} -odd part of the Lagrangian has the same form, although only three parameters (they are denoted with a tilde, see Appendix A.1) are needed.

The different parametrizations, and the relationships between them, are discussed in more detail on the VBFNLO webpage, where the explicit forms of the HVV couplings are given.

- 1. A parametrization in terms of couplings in the effective Lagrangian approach given by Eq. (10).
 - PARAMETR1: Parameter that switches on the effective Lagrangian parameterization of Eq. (10). The default value is true.
 - LAMBDA5: Mass scale Λ_5 in units of GeV with 480 GeV chosen as default.
 - G5E_HWW, G5E_HZZ, G5E_HGG, G5E_HGZ: Parameters that determine the couplings g_{5e}^{HVV} of the \mathcal{CP} -even dimension five operators. Their default values are set to 0.
 - G50_HWW, G50_HZZ, G50_HGG, G50_HGZ: Parameters that determine the couplings g_{5o}^{HVV} of the \mathcal{CP} -odd dimension five operators. Their default values are set to 0.
- 2. The parameterization of the anomalous couplings by the L3 Collaboration as given in Ref. [93]. The parameters are d, d_B , Δg_1^Z and $\Delta \kappa_{\gamma}$, which are related to the coefficients f_i/Λ^2 of the effective Lagrangian of Eq. (11) in the following manner [94]:

- PARAMETR2: Parameter that switches on the above mentioned parameterization of Eqs. (14). The default value is false.
- D_EVEN, DB_EVEN, DKGAM_EVEN, DG1Z_EVEN: Parameters that are the CP-even couplings in this parameterization. Default values are set to zero.
- D_ODD, DB_ODD, KGAM_ODD: Parameters that are the CP-odd couplings in this parameterization with default values equal to 0.
- HVV1: Parameter that determines which anomalous HVV couplings are used for the run. For HVV1 = 0, only the $HZ\gamma$ coupling, for HVV1 = 1, only the $H\gamma\gamma$ coupling, for HVV1 = 2, only the HZZ coupling and for HVV1 = 3, only the HWW coupling is used. If HVV1 is set to 4, all possible anomalous couplings are used. This is also the default value.
- 3. The parametrization of the anomalous couplings in terms of coefficients f_i/Λ^2 of the effective Lagrangian in Eq. (11).
 - PARAMETR3: Parameter that switches on the parametrization stated above. The default value is false.
 - FWW_EVEN, FBB_EVEN, FW_EVEN, FB_EVEN: Parameters that represent the coefficients of the CP-even operators – i.e. f_i/Λ^2 – with default values set to zero.
 - FWW_ODD, FBB_ODD, FB_ODD: Parameters that are the coefficients of the CP-odd operators i.e. f_i/Λ^2 with default values 0 GeV⁻².
 - HVV2: Parameter that allows the user to choose which anomalous HVV couplings are used. For HVV2 = 0, only the $HZ\gamma$ coupling, for HVV2 = 1, only the $H\gamma\gamma$ coupling, for HVV2 = 2, only the HZZ coupling and for HVV2 = 3, only the HWW coupling is used. If set to 4 all possible anomalous couplings are used. The default value is 4.

Moreover, for all parametrizations, two different form factors can be chosen as described in Refs. [90,94]. They model effective, momentum dependent HVV vertices, motivated by new physics entering with a large scale Λ at the loop level.

$$F_1 = \frac{\Lambda^2}{q_1^2 - \Lambda^2} \frac{\Lambda^2}{q_2^2 - \Lambda^2},$$
(15)

$$F_2 = -2\Lambda^2 C_0(q_1^2, q_2^2, (q_1 + q_2)^2, \Lambda^2).$$
(16)

Here the q_i are the momenta of the vector bosons and C_0 is the scalar one-loop three point function in the notation of Ref. [95].

- FORMFACTOR: Flag that switches on the above form factor. The default value is set to false.
- MASS_SCALE: Characteristic mass scale, Λ , of new physics in units of GeV. The default value is 200 GeV.
- FFAC: Parameter that is used to select one particular form factor out of Eqs. (15) and (16). If FFAC = 1, the form factor F_1 is used for the parametrization. FFAC = 2 selects F_2 , which is also the default value.

Finally, the following parameters can be used to rescale the SM HVV couplings.

- TREEFACW: Parameter that multiplies the *HWW* tensor present in the SM Lagrangian. Default is 1.
- TREEFACZ: Parameter that multiplies the HZZ tensor present in the SM Lagrangian. Default is 1.
- LOOPFAC: Parameter that multiplies the $HZ\gamma$ and $H\gamma\gamma$ vertices induced by SM loops. The default is chosen to be 1.

In order to comply with previous versions of VBFNLO, an input TREEFAC can be used, and both TREEFACW and TREEFACZ are set to this input.

Note that, when working in the SM, the loop-induced couplings $HZ\gamma$ and $H\gamma\gamma$ are used only in the calculation of the Higgs width and decays, not in the production amplitude. For the case of anomalous Higgs couplings (ANOM_CPL = .true. and one of the processes 10x, (4)300, (4)330, (4)360, (4)370 has been selected), these contributions are included in the production as well as in the decay of the Higgs boson.

4.5.2 anomV.dat – anomalous triple and quartic gauge boson couplings

The anomalous triple and quartic gauge boson couplings can be set in the file anomV.dat. They are parameterized using an effective Lagrangian, as described in Refs. [92,96–98]

$$\mathcal{L}_{\text{eff}} = \frac{f_i}{\Lambda^n} \mathcal{O}_i^{n+4},\tag{17}$$

where n + 4 signifies the dimension of the operator \mathcal{O}_i . VBFNLO defines the anomalous gauge couplings in terms of the coefficients f_i/Λ^n of the dimension-6 and dimension-8 operators. The full list of implemented operators can be found in Appendix A.1.

A common alternative parameterization (which VBFNLO can also use as input) of the trilinear couplings $WW\gamma$ and WWZ uses the following effective Lagrangians:

$$\mathcal{L}_{WW\gamma} = -ie \left[W^{\dagger}_{\mu\nu} W^{\mu} A^{\nu} - W^{\dagger}_{\mu} A_{\nu} W^{\mu\nu} + \kappa_{\gamma} W^{\dagger}_{\mu} W_{\nu} F^{\mu\nu} + \frac{\lambda_{\gamma}}{m_W^2} W^{\dagger}_{\sigma\mu} W^{\mu}_{\nu} F^{\nu\sigma} \right]$$
(18)

for the anomalous $WW\gamma$ vertex, and

$$\mathcal{L}_{WWZ} = -ie\cot\theta_w \left[g_1^Z \left(W^{\dagger}_{\mu\nu} W^{\mu} Z^{\nu} - W^{\dagger}_{\mu} Z_{\nu} W^{\mu\nu} \right) + \kappa_Z W^{\dagger}_{\mu} W_{\nu} Z^{\mu\nu} + \frac{\lambda_Z}{m_W^2} W^{\dagger}_{\sigma\mu} W^{\mu}_{\nu} Z^{\nu\sigma} \right]$$
(19)

for the anomalous WWZ vertex. It is customary to rephrase the electroweak modifications around the SM Lagrangian in terms of new quantities,

$$(\Delta g_1^Z, \Delta \kappa_Z, \Delta \kappa_\gamma) = (g_1^Z, \kappa_Z, \kappa_\gamma) - 1.$$
(20)

These quantities are related to the coefficients of the dimension-6 operators \mathcal{O}_W , \mathcal{O}_B and \mathcal{O}_{WWW} as shown in Eqs. (14) for $\Delta \kappa_{\gamma}$ and Δg_1^Z . The corresponding relations for $\Delta \kappa_Z$ and $\Delta \lambda_{\gamma}$, $\Delta \lambda_Z$ are

$$\Delta \kappa_Z = \frac{m_Z^2}{2\Lambda^2} \left(f_W \cos^2 \theta_W - f_B \sin^2 \theta_W \right),$$

$$\Delta \lambda_\gamma = \Delta \lambda_Z = \frac{3g^2 m_W^2}{2\Lambda^2} f_{WWW}.$$
(21)

In order to include anomalous vector boson couplings, the parameter ANOM_CPL must be switched to true in vbfnlo.dat. The parameters described above are input via the file anomV.dat:

- TRIANOM: Switches between parameterizations of the anomalous $WW\gamma$ and WWZ couplings. TRIANOM = 1 uses the coefficients of the dimension-6 operators as input:
 - FWWW: Coefficient of the operator \mathcal{O}_{WWW} , i.e. f_{WWW}/Λ^2 . Default is set to 0 GeV⁻².
 - FW: Coefficient of the operator \mathcal{O}_W , i.e. f_W/Λ^2 . Default is set to 0 GeV⁻².
 - FB: Coefficient of the operator \mathcal{O}_B , i.e. f_B/Λ^2 . Default is set to 0 GeV⁻².

TRIANOM = 2 uses the alternative parameterization of Eqs. (18) and (19) as input:

- LAMBDA0: The quantity $\lambda_{\gamma}(=\lambda_Z)$. Default is set to 0.0.
- ZDELTAKAPPAO: The quantity $\Delta \kappa_Z$. Default is set to 0.0.
- ZDELTAGO: The quantity Δg_1^Z . Default is set to 0.0.
- ADELTAKAPPAO: The quantity $\Delta \kappa_{\gamma}$. Default is set to 0.0.
- Note that, as can be seen from Eqs. (14) and (21), the quantities $\Delta \kappa_Z$, $\Delta \kappa_\gamma$ and Δg_1^Z are not independent, but obey the relation

$$\Delta \kappa_Z = \Delta g_1^Z - \frac{\sin^2 \theta_W}{\cos^2 \theta_W} \Delta \kappa_\gamma.$$
(22)

If one of these quantities is zero, it will be set by VBFNLO to be consistent with the other values. If the input values are inconsistent, $\Delta \kappa_{\gamma}$ will be reset to give the correct relation.

Default is TRIANOM = 1. The LEP limits on those couplings can be found in [99]. Note that Vjj and VVj processes (process IDs 120-150 and 610-640) only take account of the above anomalous coupling parameters and not the following parameters.

- FWW, FBB: The coefficients of the remaining $C\mathcal{P}$ -even dimension-6 operators, i.e. f_i/Λ^2 . Note that these are not implemented for Vjj production via VBF (process IDs 120-150) and VVj processes (IDs 610-640). Default value is 0 GeV⁻².
- FWWWt, FWt, FBt, FBWt, FDWt, FWWt, FBBt: The coefficients of the CP-odd dimension-6 operators, i.e. f_i/Λ^2 . Note that these are not implemented for Vjj production via VBF (process IDs 120-150) and VVj processes (IDs 610-640). Default value is 0 GeV⁻².
- FS0, FS1, FM0 FM7, FT0 FT2, FT5 FT9: Parameters that give the values of the coefficients of the dimension-8 operators, i.e. f_i/Λ^4 . The default values for these parameters are 0 GeV⁻⁴. Note that these are only relevant for triboson production and VVjj production via VBF.

In addition, a form factor can be applied, which takes the form

$$F = \left(1 + \frac{s}{\Lambda^2}\right)^{-p},\tag{23}$$

for all processes except $\gamma j j$ production in VBF (process ID 150), where Λ is the characteristic scale where the form factor effect becomes relevant. s is a universal scale (the invariant mass squared of the produced bosons) for each phase-space point.

- FORMFAC: Switch determining whether the above form factor F is included. Default is set to false.
- FFMASSSCALE: Mass scale Λ . Default is set to 2000 GeV.
- FFEXP: The exponent p. Default is set to 2.

Individual form factor mass scales and exponents can be set for the trilinear WWZ and $WW\gamma$ couplings, using either of the parametrizations above. If chosen, these values overwrite the "universal" mass scale and exponent (FFMASSSCALE and FFEXP) set above for the selected parameters.

• FORMFAC_IND: Switch determining whether individual or universal form factors are used. Default is set to false – universal form factors are used.

If TRIANOM = 1 then

- MASS_SCALE_FWWW: Mass scale Λ for coefficient f_{WWW} . Default is 2000 GeV.
- FFEXP_FWWW: Exponent p for coefficient f_{WWW} . Default is 2.
- MASS_SCALE_FW: Mass scale Λ for coefficient f_W . Default is 2000 GeV.
- FFEXP_FW: Exponent p for coefficient f_W . Default is 2.
- MASS_SCALE_FB: Mass scale Λ for coefficient f_B . Default is 2000 GeV.
- FFEXP_FB: Exponent p for coefficient f_B . Default is 2.

If TRIANOM = 2 then

- MASS_SCALE_AKAPPA: Mass scale Λ for parameter $\Delta \kappa_{\gamma}$. Default is 2000 GeV.
- FFEXP_AKAPPA: Exponent p for parameter $\Delta \kappa_{\gamma}$. Default is 2.
- MASS_SCALE_ZKAPPA: Mass scale Λ for parameter $\Delta \kappa_Z$. Default is 2000 GeV.
- FFEXP_ZKAPPA: Exponent p for parameter $\Delta \kappa_Z$. Default is 2.
- MASS_SCALE_LAMBDA: Mass scale Λ for parameter λ . Default is 2000 GeV.
- FFEXP_LAMBDA: Exponent p for parameter λ . Default is 2.
- MASS_SCALE_G: Mass scale Λ for parameter Δg_1^Z . Default is 2000 GeV.
- FFEXP_G: Exponent p for parameter Δg_1^Z . Default is 2.
- As with the anomalous parameters themselves, the formfactors in the parameterization of TRIANOM = 2 are not independent (see Eq. (22)). If one mass scale is set to zero, it will be set by VBFNLO to be consistent with the other values. If the input values are inconsistent, they will be reset to give the correct relation.

For $\gamma j j$ production in VBF (process ID 150), the form factor takes the form

$$F = \left(1 + \frac{q_1^2}{\Lambda^2} + \frac{q_2^2}{\Lambda^2} + \frac{q_3^2}{\Lambda^2}\right)^{-p},$$
(24)

with Λ and p set by FFMASSSCALE and FFEXP, respectively. q_1^2 , q_2^2 and q_3^2 are the invariant masses squared of the three vector bosons involved in the VVV vertex. For this process only the universal form factor can be applied.

4.5.3 Using anom_HVV.dat and anomV.dat simultaneously

Some of the anomalous coupling parameters affect both the VVV and HVV couplings. These parameters (f_W and f_B or, equivalently, Δg_1^Z and $\Delta \kappa_{\gamma}$) are consequently inputs in both anom_HVV.dat and anomV.dat. As stated previously, when working with anomalous VVV couplings with a process that contains internal Higgs bosons (e.g. WWZ triboson production), the anomalous HVV couplings resulting from f_W and f_B (input via anomV.dat) are calculated and used.

In diboson WW production (process ID 300), however, anomV.dat and anom_HVV.dat can be used simultaneously. The anomalous VVV couplings are taken directly from anomV.dat. The values of f_W and f_B for the HVV couplings are also taken from anomV.dat, but the additional parameters (f_{BB} , f_{WW} etc.) are taken from anom_HVV.dat using the appropriate parametrisation³⁰. Alternatively, the HVV couplings can be specified directly via g_5^{HXY} by setting PARAMETR1=true in anom_HVV.dat. In this case, the values g_5^{HXY} are used if they are consistent with the anomV.dat inputs – if they are inconsistent, a warning message is printed and HVV parametrisation 2 or 3 is used instead.

4.6 kk_input.dat - parameters for Higgsless models

VBFNLO allows the calculation of the vector boson fusion processes WWjj, WZjj and ZZjj in the Warped Higgsless scenario [100, 101] at LO and NLO QCD level (see, for example, Ref. [102] for a phenomenological application). This feature is used if the switch KK_MOD in vbfnlo.dat is switched to true and must be enabled at compilation using the configure option --enable-kk.

The triple vector-boson processes WWW, WWZ and WZZ can be calculated in both this model and a Three-Site Higgsless Model [103]. The model parameters (masses and couplings) can be generated by VBFNLO via the input file kk_input.dat for a choice of the relevant five dimensional gauge parameters. The input parameters are:

- VBFCALC_SWITCH: Switch that determines whether VBFNLO should calculate the parameters needed by the model. Default is **true**. Alternatively, the user can input their own model parameters (masses and couplings) as described below.
- MHLM_SWITCH: Switch that determines whether the Three-Site Higgsless Model [103] (true) or the Warped Higgsless Model [100] (false) should be used. Default is false (Warped Higgsless Model).
- The following parameters are used only when working in the Warped Higgsless Model (MHLM_SWITCH = false):
 - RDWN: Location of the UV brane for the generation of the model parameters in the Warped Higgsless Model. Default is $R = 9.75 \times 10^{-9}$, which amounts to the Kaluza-Klein excitations having masses of $m_{W_1} = 700$ GeV, $m_{Z_1} = 695$ GeV, and $m_{Z'_1} = 718$ GeV. Smaller values of R result in a heavier Kaluza-Klein spectrum.
 - KKMAXW: The maximum number of Kaluza-Klein W_k^{\pm} states to be included on top of the Standard Model W^{\pm} bosons, which correspond to $W_{k=0}^{\pm}$. All states $k \geq 3$ are phenomenologically irrelevant. Default is 1.

³⁰TRIANOM=1 in anomV.dat corresponds to PARAMETR3=true in anom_HVV.dat, and TRIANOM=2 corresponds to PARAMETR2=true.

- KKMAXZ: The maximum number of Kaluza-Klein Z_k states to be included on top of the Standard Model Z boson, which corresponds to $Z_{k=0}$. All states $k \geq 3$ are phenomenologically irrelevant. Default is 1.
- KKMAXG: The maximum number of Kaluza-Klein Z'_k bosons that are excitations of the Standard Model photon $Z'_{k=0}$. States $k \geq 2$ are phenomenologically irrelevant. Default is 1.
- WPMASS: $W_{k=1}$ mass in the Three-Site Higgsless Model (MHLM_SWITCH = true). Default is 500 GeV.

The explicit breaking of higher dimensional gauge invariance is balanced according to the description of Ref. [104], where more details regarding the model and its implementation can be found. Information on the widths and the sum rules relating the various gauge boson couplings [105] are written to the file kkcheck.dat.

VBFNLO generates the text file kk_coupl_inp.dat, which documents the calculated model parameters, i.e. Kaluza-Klein gauge boson masses and couplings of the specified input parameters. This file can also be used as an input file for advanced users who want to run the code with their own set of parameters – e.g. for simulation of more general technicolor-type scenarios. To that end, select VBFCALC_SWITCH = false in the file kk_input.dat. VBFNLO will then calculate the gauge boson widths on the basis of these parameters by the decay to the lower lying states. The inputs in kk_coupl_inp.dat are as follows:

- KKMAXW: The maximum number of Kaluza-Klein W_k^{\pm} states included on top of the Standard Model W^{\pm} bosons.
- KKMAXZ: The maximum number of Kaluza-Klein Z_k states included on top of the Standard Model Z boson.
- KKMAXG: The maximum number of Kaluza-Klein Z'_k bosons that are excitations of the Standard Model photon $Z'_{k=0}$.
- Kaluza-Klein masses:
 - KKMASSW: List of masses of the Kaluza-Klein W_k^{\pm} states.
 - KKMASSZ: List of masses of the Kaluza-Klein Z_k states.
 - KKMASSG: List of masses of the Kaluza-Klein Z'_k states.
- Couplings
 - CPL_Wx-Wy-ZX: List of couplings between Kaluza-Klein states: $W_x^{\pm} W_y^{\pm} Z_0$ to $W_x^{\pm} W_y^{\pm} Z_{\text{KKMAXZ}}$.
 - CPL_Wx-Wy-GX: List of couplings between Kaluza-Klein states: $W_x^{\pm} W_y^{\pm} Z_0'$ to $W_x^{\pm} W_y^{\pm} Z_{\text{KKMAXG}}'$.
 - CPL_W*x*-W*y*-W*z*-WX: List of couplings between Kaluza-Klein states: $W_x^{\pm} W_y^{\pm} W_z^{\pm} W_0^{\pm}$ to $W_x^{\pm} W_y^{\pm} W_z^{\pm} W_z^{\pm}$.
 - CPL_Wx-Wy-Zz-ZX: List of couplings between Kaluza-Klein states: $W_x^{\pm} W_y^{\pm} Z_z Z_0$ to $W_x^{\pm} W_y^{\pm} Z_z Z_{\text{KKMAXZ}}$.
 - CPL_W*x*-W*y*-G*z*-GX: List of couplings between Kaluza-Klein states: $W_x^{\pm} W_y^{\pm} Z'_z Z'_0$ to $W_x^{\pm} W_y^{\pm} Z'_z Z'_{\text{KKMAXG}}$.

- CPL_Wx-Wy-Gz-ZX: List of couplings between Kaluza-Klein states:
$$W_x^{\pm} - W_y^{\pm} - Z'_z - Z_0$$
 to $W_x^{\pm} - W_y^{\pm} - Z'_z - Z_{\text{KKMAXZ}}$.

The default values in kk_coupl_inp.dat are those produced when VBFNLO is used to calculate the couplings and masses using the default values of kk_input.dat as described above.

4.7 spin2coupl.dat – parameters for spin-2 models

The file spin2coupl.dat is used to set the parameters for the spin-2 models. It is read if the switch SPIN2 in vbfnlo.dat is set to true, and will only run if the spin-2 models were enabled at compilation using the configure option --enable-spin2.

VBFNLO uses an effective model to describe the interactions of spin-2 particles with electroweak gauge bosons for two cases: an isospin singlet spin-2 state and a spin-2 triplet in the adjoint representation, as described in Refs. [40–42]. For the singlet spin-2 field, $T^{\mu\nu}$, the effective Lagrangian is

$$\mathcal{L}_{\text{singlet}} = \frac{1}{\Lambda} T_{\mu\nu} \left(f_1 B^{\alpha\nu} B^{\mu}_{\alpha} + f_2 W^{\alpha\nu}_i W^{i,\mu}_{\alpha} + f_3 \widetilde{B}^{\alpha\nu} B^{\mu}_{\alpha} + f_4 \widetilde{W}^{\alpha\nu}_i W^{i,\mu}_{\alpha} + 2f_5 (D^{\mu} \Phi)^{\dagger} (D^{\nu} \Phi) + f_9 G^{\alpha\nu}_a G^{a,\mu}_{\alpha} \right),$$
(25)

and for the spin-2 triplet field, $T_i^{\mu\nu}$, the effective Lagrangian is given by

$$\mathcal{L}_{\text{triplet}} = \frac{1}{\Lambda} T_{\mu\nu j} \left(f_6 (D^{\mu} \Phi)^{\dagger} \sigma^j (D^{\nu} \Phi) + f_7 W^{j,\mu}_{\alpha} B^{\alpha\nu} \right), \qquad (26)$$

where W, B and G are the usual field strength tensors of the SM gauge fields, \widetilde{W} and \widetilde{B} the dual field strength tensors, Φ is the Higgs field and D^{μ} is the covariant derivative. f_i are variable coupling parameters and Λ is the characteristic energy scale of the new physics.

In order to preserve unitarity, a formfactor is introduced to multiply the amplitudes. The formfactor has the form:

$$f(q_1^2, q_2^2, p_{\text{sp2}}^2) = \left(\frac{\Lambda_{ff}^2}{|q_1^2| + \Lambda_{ff}^2} \cdot \frac{\Lambda_{ff}^2}{|q_2^2| + \Lambda_{ff}^2} \cdot \frac{\Lambda_{ff}^2}{|p_{\text{sp2}}^2| + \Lambda_{ff}^2}\right)^{n_{ff}}.$$
 (27)

Here p_{sp2}^2 is the invariant mass of a virtual s-channel spin-2 particle and $q_{1,2}^2$ are the invariant masses of the electroweak bosons. The energy scale Λ_{ff} and the exponent n_{ff} describe the scale of the cutoff and the suppression power.

The input parameters used by VBFNLO are:

- F1,F2,F3,F4,F5,F9: Coupling parameters for the spin-2 singlet field.
- F6, F7: Coupling parameters for the spin-2 triplet field.
- LAMBDA: Energy scale of the couplings in GeV.
- LAMBDAFF: Energy scale of the formfactor in GeV.
- NFF: Exponent of the formfactor.

The gluon coupling F9 only affects the implemented VBF processes via the total width of the spin-2 particle. Note that the electroweak part of the graviton scenario corresponds to F1=F2=F5=1 and F3=F4=F6=F7=F9=0.

VBFNLO also needs the masses and branching ratios of the spin-2 particles into SM gauge bosons.

- SP2MASS: Mass of the spin-2 singlet particle in GeV.
- MSP2TRIPPM: Mass of charged spin-2 triplet particles in GeV.
- MSP2TRIPN: Mass of neutral spin-2 triplet particle in GeV.
- BRRAT: Branching ratio for spin-2 singlet particle into SM gauge bosons. Default value is 1.
- BRRATTRIPPM: Branching ratio for charged spin-2 triplet particles into SM gauge bosons. Default value is 1.
- BRRATTRIPN: Branching ratio for neutral spin-2 triplet particle into SM gauge bosons. Default value is 1.

Default values for different processes and scenarios can be found in Refs. $[40-42]^{31}$.

4.8 histograms.dat – parameters for histogram options

VBFNLO can output histogram data in a variety of different formats (ROOT, GNUPLOT, TOPDRAWER, raw data tables), as described in Sec.4.1.5.

The file histograms.dat allows the user to set the x-axis range, enable a bin smearing, and enable the calculation of the Monte Carlo error per bin^{32} .

VBFNLO can calculate the Monte Carlo error for each bin and output this to the root and the raw histogram data output for 1D and 2D histograms. For the gnuplot histogram output only the 1D histograms can display the error bars.

- CALC_ERROR_GNUPLOT: Enable or disable *y*-error bars in 1D GNUPLOT histograms. Default is false.
- CALC_ERROR_ROOT: Enable or disable y/z-error bars in 1D/2D ROOT histograms. Please note: only the histograms defined in the FORTRAN file histograms.F can be generated with error bars. Default is false.
- CALC_ERROR_1D: Enable or disable *y*-error bars in raw 1D histogram output. Default is true.
- CALC_ERROR_2D: Enable or disable z-error bars in raw 2D histogram output. Default is false.

Furthermore, VBFNLO uses a smearing between adjacent bins to avoid artefacts at NLO when the real emission kinematics and the corresponding subtraction term fall into different bins. As this can lead to remnants at the sharp edges caused by cuts the smearing can be switched off.

³¹Note that in Ref. [40], process 191 ($pp \rightarrow \text{spin-}2\,jj \rightarrow \gamma\gamma\,jj$) is referred to as process 240.

 $^{^{32}\}mathrm{By}$ default 100 bins are used. This number can be altered in utilities/histograms.F.

- SMEARING: Enable or disable smearing. Default is true.
- SMEAR_VALUE: Set the bin fraction where the bin smearing is active. The part that is put to the next bin becomes larger when the x-value is closer to a bin border. Default is 0.2.

The range of the *x*-axis of the produced histograms is input in the format: xmin xmax. The following describes those histograms which are already implemented in VBFNLO. By altering the file utilities/histograms.F, however, it should be easy for the user to add new histograms – VBFNLO will automatically read in the range of each created histogram.

- HIST_ID1: Range for p_T of tagging jets. Default range is 0 to 250 GeV.
- HIST_ID2: Range for p_T of tagging jet with higher p_T . Default range is 0 to 500 GeV.
- HIST_ID3: Range for p_T of tagging jet with lower p_T . Default range is 0 to 200 GeV.
- HIST_ID4: Range for rapidity of tagging jets. Default range is -5 to 5.
- HIST_ID5: Range for rapidity of tagging jet with higher p_T . Default range is -5 to 5.
- HIST_ID6: Range for rapidity of tagging jet with lower p_T . Default range is -5 to 5.
- HIST_ID7: Range for p_T^{max} of leptons. Default range is 0 to 500 GeV.
- HIST_ID8: Range for p_T^{\min} of leptons. Default range is 0 to 500 GeV.
- HIST_ID9: Range for η_{max} of leptons. Default range is 0 to 5.
- HIST_ID10: Range for η_{\min} of leptons. Default range is 0 to 5.
- HIST_ID11: Range for azimuthal angle (in degrees) of tagging jets. Default range is -180 to 180.

VBFNLO can also produce 2D histograms. In this case, both the x and y ranges can be set using histograms.dat in the format xmin xmax ymin ymax.

• 2DHIST_ID1: Range for 2D histogram of $d^2\sigma/(d\eta_{jj}dm_{jj})$. Default ranges are 0 to 6 for the η (x) axis and 0 to 800 GeV for the m_{jj} (y) axis.

If the x-axis and y-axis ranges are not provided in the file histograms.dat the default values, which are set in utilities/histograms.F, are used.

A brief documentation on how to implement additional histograms into the file histograms.F can be found on the VBFNLO webpage, http://www.itp.kit.edu/vbfnlo/.

4.9 random.dat - parameters for seeds

To run with different seeds, simply set the variable SEED in the file random.dat to a different integer value.

4.10 Calculating the *s*-channel vector boson exchange contributions for the VBF processes

The VVV processes with semileptonic decays can be used to calculate the *s*-channel vector boson exchange contributions which are neglected in the VVjj processes with fully leptonic decays in VBF. The same holds for semileptonic VV production and Vjj production in VBF.

Using the available processes with semileptonic decays it is possible to calculate the *s*-channel contributions to the processes Zjj, $W^{\pm}jj$, $W^{+}W^{-}jj$, $W^{\pm}Zjj$, $W^{\pm}\gamma jj$, $Z\gamma jj$ and ZZjj in VBF with fully leptonic decays. In order to achieve this, the corresponding processes with semileptonic decay should be run with the same settings as the VBF process, except for the scale choice in case a dynamical scale has been used in the VBF processes. Additionally, the following settings should be made in cuts.dat:

- DEF_TAGJET = 1
- PTMIN_TAG_1 = 0 and PTMIN_TAG_2 = 0
- HARD_CENTRAL = false
- VBFCUTS_ALWAYS = true
- RECONST_HAD_V = 0
- SINGLE_DECAYJET = 0
- RECONST_HAD_V = 0

The option DECAY_QUARKS in the file vbfnlo.dat has to be set to the value 93 (or 94 if initial and final-state *b*-quarks should be included). The list of corresponding *s*- and *t*-channel contributions in VBFNLO can be found in Table 23.

With this prescription a few simplifications are in place: interferences between *s*- and *t*-channel contributions are still neglected. Additionally, the NLO QCD corrections of the hadronic vector boson decay can be included only in an approximation (see Section 4.1).

Process	PROCID of <i>t</i> -channel	PROCIDs of <i>s</i> -channel
$\begin{array}{c} p \stackrel{(-)}{p} \rightarrow Z jj \rightarrow \ell^+ \ell^- jj \\ p \stackrel{(-)}{p} \rightarrow W^+ jj \rightarrow \ell^+ \nu_\ell jj \\ p \stackrel{(-)}{p} \rightarrow W^- jj \rightarrow \ell^- \bar{\nu}_\ell jj \end{array}$	120 130 140	312, 331 302, 313 301, 323
$\begin{split} p \stackrel{(-)}{p} &\to W^+ W^- jj \to \ell_1^+ \nu_{\ell_1} \ell_2^- \bar{\nu}_{\ell_2} jj \\ p \stackrel{(-)}{p} &\to W^+ Z jj \to \ell_1^+ \nu_{\ell_1} \ell_2^+ \ell_2^- jj \\ p \stackrel{(-)}{p} &\to W^- Z jj \to \ell_1^- \bar{\nu}_{\ell_1} \ell_2^+ \ell_2^- jj \\ p \stackrel{(-)}{p} &\to Z Z jj \to \ell_1^+ \ell_1^- \ell_2^+ \ell_2^- jj \\ p \stackrel{(-)}{p} &\to W^+ \gamma jj \to \ell^+ \nu_{\ell} \gamma jj \\ p \stackrel{(-)}{p} &\to W^- \gamma jj \to \ell^- \bar{\nu}_{\ell} \gamma jj \\ p \stackrel{(-)}{p} &\to Z \gamma jj \to \ell^+ \ell^- \gamma jj \end{split}$	200 220 230 210 270 280 290	$\begin{array}{c} 403,431,442\\ 402,412\\ 401,422\\ 411,421,451\\ 462,482\\ 461,492\\ 471,481,491 \end{array}$

Table 23: Corresponding s- and t-channel vector boson exchange contributions of electroweak V(V)jj production in VBFNLO.

5 CHANGES

The release VERSION 2.7.0 includes some changes that alter previous results:

5.1 Running scales in NLO calculations

In release 2.7.0 a problem with certain dynamical renormalization and factorization scales has been fixed, which lead to wrong results at NLO QCD in the subtraction part of the real emission calculation. In particular, the scale choices " $\min(p_T(j_i))$ " (ID=2) and "minimal transverse energy of the bosons" (ID=7) did not give correct results in previous releases.

5.2 Jet cuts in VBF/gluon fusion Higgs boson production with $H \rightarrow b\bar{b}$

Starting with VBFNLO 2.7.0 the jet cuts will be applied to the b-quarks from Higgs boson decay.

5.3 NLO calculation of W^+W^-Z production

A bug in the calculation of the virtual contributions for WWZ production has been fixed while comparing with the results of Ref. [106]. The new results are roughly one per cent smaller, and agree between both codes for squared amplitudes at the level of the machine precision and for integrated cross sections at the per mill level.

5.4 LO and NLO calculation of W^+jj / Zjj production in VBF

The particle–anti-particle–assignment in W^+jj , Zjj has been fixed. In case of W^+jj production this leads to an increase in cross section of roughly one per cent with basic cuts.

5.5 Event output

Several bugs have been fixed concerning the event output to Les Houches or HepMC files:

- The color information in the event output for W^-W^-jj in VBF has been fixed.
- The momenta assignment in the event output for $W^-W^+W^-$ has been corrected.

5.6 Previous changes – version 2.6.3

The release VERSION 2.6.3 includes some changes that alter previous results:

5.6.1 Event output

Several bugs have been fixed concerning the event output to Les Houches or HepMC files:

- Fixed bugs in output of particle IDs for processes 191 and 43xx: In previous versions some particles had the particle ID 0.
- Parton and beam particle IDs have been fixed for process 260.
- The tau mass can now be included in the event output of all processes. Furthermore, several bugs have been fixed in the existing implementation of tau mass inclusion.
- Several bugs have been fixed in the helicity output.

5.6.2 Calculation of the $H \rightarrow gg$ partial width

Higher-order corrections to the $H \rightarrow gg$ partial width have been included which lead to slightly smaller branching ratios for all other decay channels. Therefore cross sections of processes involving Higgs bosons can be up to a few per cent smaller.

5.6.3 Electroweak corrections in the VBF *Hjj* processes

Some bugs have been fixed in the calculation of electroweak corrections for the processes 10x.

5.7 Previous changes – version 2.6.2

The release VERSION 2.6.2 included some changes that altered previous results:

5.7.1 Distributions and cross section for $H \rightarrow WW$ in VBF and gluon fusion

Due to a bug which has been fixed in the lepton assignment for $H \to WW/ZZ \to 4\ell$ distributions (and cross sections after the $m_{\ell\ell}$ cut) were off for the 1x5 and 4105 processes in the previous versions. This bug has been fixed in v.2.6.2.

5.7.2 Les Houches event output for processes with more than one phase space

The fraction of events coming from the different phase spaces was not sampled correctly in previous versions. Processes affected are $W\gamma$, $Z\gamma$, $W\gamma j$, $Z\gamma j$, ZZZ, $WW\gamma$, $WZ\gamma$, $W\gamma\gamma$, $Z\gamma\gamma$, $\gamma\gamma\gamma$ and $W\gamma\gamma j$.

5.7.3 ZZZ production

The QCD real emission part of the NLO computation gave no reliable result in previous versions due to a bug in the dipole subtraction. This bug has been fixed in v.2.6.2.

5.7.4 Form factor in $\gamma j j$ production with anomalous couplings

For the $\gamma j j$ production in VBF (procID 150) a different form factor is used.

5.8 Previous changes – version 2.6.1

The release VERSION 2.6.1 included some changes that altered previous results:

5.8.1 Anomalous Higgs couplings

A bug was found and fixed in the implementation of the TREEFACZ and TREEFACW, the factors which multiply the SM HZZ and HWW couplings. Note that this bug was only present in VERSION 2.6.0, not in earlier versions. Additionally, a small bug was found and fixed in the coefficient of the input FB_ODD in the a_3^{HZZ} coupling.

5.8.2 Symmetry factor $ZZ \rightarrow \ell^+ \ell^- \ell^+ \ell^-$

In the processes $pp \to H\gamma jj \to ZZ\gamma jj \to \ell^+\ell^-\ell^+\ell^-\gamma jj$ (ID 2106) and gluon fusion $pp \to Hjj \to ZZjj \to \ell^+\ell^-\ell^+\ell^- jj$ (ID 4106) a symmetry factor was missing when identical final-state leptons were chosen.

5.9 Previous changes – version 2.6.0

The release VERSION 2.6.0 included some changes that alter results (events, cross sections and distributions) from earlier versions.

5.9.1 Allowed width of virtuality

In the phase-space generators, the allowed range of the virtuality of a resonance of intermediate vector bosons has been increased. This mainly affects processes where an intermediate Z boson decays into a pair of neutrinos – i.e.

- $pp \to Hjj \to ZZjj \to \ell^+ \ell^- \nu \overline{\nu} jj$ via vector boson fusion (process ID 107) and gluon fusion (process ID 4107)
- $pp \to Hjjj \to ZZjjj \to \ell^+ \ell^- \nu \overline{\nu} jjj$ (process ID 117)
- $pp \to H\gamma jj \to ZZ\gamma jj \to \ell^+ \ell^- \nu \overline{\nu} \gamma jj$ (process ID 2107)
- $pp \to ZZjj \to \ell^+ \ell^- \nu \overline{\nu} jj$ (process ID 211)

This not only affects the cross sections for these processes, but also means that the events produced by VBFNLO-2.6.0 will differ from those produced by VBFNLO-2.5, even if the same random numbers are used.

5.9.2 Matrix element $H \rightarrow ZZ \rightarrow 4\ell$

A bug was found and fixed in the implementation of the matrix element calculating the decay $H \rightarrow ZZ \rightarrow 4\ell$.

5.9.3 Anomalous couplings

Several changes have been made to the implementation of the anomalous couplings. For Higgs production via vector boson fusion (process IDs 100-107) the variable TREEFAC, which multiplies the Standard Model contribution to the tree-level HVV couplings, has been corrected and altered – now, separate factors for HZZ and HWW are input (TREEFACZ and TREEFACW respectively).

When working with anomalous HVV couplings two types of formfactor can be applied which model effective, momentum dependent HVV vertices, motivated by new physics entering with a large scale Λ at loop level. Corrections to the HVV formfactor F_2 (see Eq. 16) have been made. The implementation of the parameterization described by **PARAMETR3** – where the input determining the anomalous couplings is in terms of the dimension-6 operators (\mathcal{O}_W , \mathcal{O}_B , \mathcal{O}_{WW} and \mathcal{O}_{BB}) have also been altered.

If anomalous triple (and quartic) gauge boson couplings are being studied, a formfactor given by

$$F = \left(1 + \frac{s}{\Lambda^2}\right)^{-p},\tag{28}$$

can be applied in order to preserve unitarity, where Λ is the scale of new physics. The momentum dependence of the applied formfactor (i.e. s) is now universal for each phase-space point, with the invariant mass of the produced bosons as the scale. This ensures the proper cancellations for anomalous contributions. The values of the formfactor scales Λ and p can be set to different values for each input describing the triboson couplings. In the parameterization TRIANOM = 2, the formfactor scales for $\Delta \kappa_{\gamma}$ and $\Delta \kappa_{Z}$ are now separately set, and the consistency of related parameters (i.e. Δg_1^Z , $\Delta \kappa_{\gamma}$ and $\Delta \kappa_Z$) is enforced when formfactors are applied.

When processes involving resonant Higgs diagrams (e.g. WWW production) are studied with anomalous couplings, the Higgs width is now calculated with the appropriate anomalous HVV couplings (the anomalous HVV couplings in the production amplitudes were taken into account in previous versions of VBFNLO). Various corrections have also been made to the anomalous triboson couplings in diboson plus jet processes (these were incorporated into the intermediate release VBFNLO 2.5.3).

5.9.4 VBF Higgs boson production in association with three jets

A small bug was found and fixed in the calculation of the processes $pp \rightarrow Hjjj$, with process IDs 110-117.

5.10 Previous changes – version 2.5.0

The previous version of VBFNLO -2.5.0 – was altered in such a way that some results differ from VBFNLO-2.0 and below. These changes are described briefly here, and in more

detail on the VBFNLO website, http://www.itp.kit.edu/vbfnlo/.

5.10.1 EWSCHEME

The implementation of options EWSCHEME = 1 and 4, which are described in Section 4.1.2, was altered. The new implementation is hopefully more transparent, and is described in this manual.

5.10.2 Gluon fusion

Since version 2.5.0, in gluon fusion processes the bottom-quark mass $M_b(M_H)$ is used throughout the calculation. New, more stable, tensor routines for the boxes and pentagons were implemented, reducing the number of omitted points with bad numerical accuracy.

6 CHECKS

Extensive checks for the LO and the real emission amplitudes, as well as for the total LO cross sections, have been performed for all processes implemented in VBFNLO. Born amplitudes and real emission diagrams have been compared with the fully automatically generated results provided by MADGRAPH [17]. Complete agreement has been found in each case. Moreover, total LO cross sections with a minimal set of cuts agree with the respective results obtained by MADEVENT³³ [18, 107], SHERPA³⁴ [108] and/or HELAC-PHEGAS³⁵ [109–111].

LHA event files for the LO processes have been tested with $\text{HERWIG}++^{36}$ [112], a general purpose Monte Carlo event generator for the simulation of hard lepton-lepton and hadron-hadron collisions.

As a final and very important test, comparisons with already published results have been made. The NLO results for Higgs boson production via VBF agree with those produced by the code HAWK³⁷. In Ref. [113], a tuned comparison of LO and NLO QCD results for Higgs boson production via vector boson fusion at the LHC has been performed. Three different calculations have been cross checked: VBFNLO, the results of Refs. [114,115], and the VV2H program³⁸. For the dominant t- and u-channel contributions which are implemented in VBFNLO, good agreement has been found. Diboson processes, including WH, as well as W and Wj production have been checked against MCFM³⁹ [116–118]. The results for WH+jet production have been compared with Ref. [119]. For the triboson processes a comparison for the production of on-shell gauge bosons without leptonic decays has been performed with the results presented in Ref. [120]. Additionally, the tree-level results for $W^{\pm}\gamma\gamma$ have been compared to the results with an on-shell W boson of Ref. [121]. Again, in all cases good agreement has been found. Triple photon production has been tested against FEYNARTS, FORMCALC and HADCALC [5,6,122]. Processes with anomalous quartic gauge couplings have been compared with MADGRAPH/MADEVENT and WHIZARD⁴⁰ [123] in Ref. [98]. Results for the \mathcal{CP} -odd and \mathcal{CP} -even Higgs boson production via gluon fusion have been tested against FEYNARTS and FORMCALC [22,23].

All fermion loops have been checked against results obtained with FEYNARTS, FORM-CALC and LOOPTOOLS. and the gluon-gluon loops have also been checked against $GG2VV^{41}$ [124, 125].

³³http://madgraph.hep.uiuc.edu/

³⁴http://sherpa.hepforge.org/

³⁵http://helac-phegas.web.cern.ch/helac-phegas/

³⁶http://herwig.hepforge.org/

³⁷ http://omnibus.uni-freiburg.de/~sd565/programs/hawk/hawk.html

³⁸http://tiger.web.psi.ch/vv2h/

³⁹http://mcfm.fnal.gov/

⁴⁰https://whizard.hepforge.org/

⁴¹http://gg2VV.hepforge.org/

7 OUTLOOK

Additional processes and features will become available in the near future and will be included in the code version on the VBFNLO website.

Acknowledgments

We are very grateful to Ken Arnold, Manuel Bähr, Nicolas Greiner, Nicolas Kaiser, Gunnar Klämke and Stefan Prestel who, as earlier members of the VBFNLO collaboration, made important contributions to the original release. We also gratefully acknowledge the collaboration of Stefan Kallweit and Georg Weiglein in calculating corrections for specific processes. TF would like to thank the North American Foundation for The University of Manchester and George Rigg for their financial support.

A OPERATORS FOR ANOMALOUS GAUGE BOSON COUPLINGS

A.1 List of operators implemented in VBFNLO

This is a list of the full set of operators included the effective Lagrangian which is used for calculations with anomalous gauge boson couplings. The full set can be used in the diboson, triboson and VVjj in VBF production processes. The dimension-6 operators are constructed according to Refs. [91,92] and the dimension-8 operators are taken from [97]. More details on the implementation of these operators can be found in Refs. [87–89].

With the building blocks (following the notation of [91, 92])

$$\widehat{W}_{\mu\nu} = igT^{a}W^{a}_{\mu\nu}$$

$$\widehat{B}_{\mu\nu} = ig'YB_{\mu\nu}$$

$$D_{\mu} = \partial_{\mu} + igT^{a}W^{a}_{\mu} + ig'YB_{\mu},$$
(29)

we can construct the following operators, where g and g' are the SU(2) and U(1) gauge couplings, and T^a are the SU(2) generators. We obtain slightly different expressions for the dimension-8 operators compared to [97], as they use different field strength tensor expressions ($\widehat{W}_{\mu\nu} = T^a W^a_{\mu\nu}$ and $\widehat{B}_{\mu\nu} = B_{\mu\nu}$). The conversion factors for the coupling strengths f_i between [97] and our implementation can be found in Appendix A.2.

The explicit form of the \mathcal{CP} -even operators is

$$\mathcal{O}_{W} = (D_{\mu}\Phi)^{\dagger}\widehat{W}^{\mu\nu}(D_{\nu}\Phi)$$

$$\mathcal{O}_{B} = (D_{\mu}\Phi)^{\dagger}\widehat{B}^{\mu\nu}(D_{\nu}\Phi)$$

$$\mathcal{O}_{WWW} = Tr\left[\widehat{W}_{\mu\nu}\widehat{W}^{\nu\rho}\widehat{W}_{\rho}^{\mu}\right]$$

$$\mathcal{O}_{WW} = \Phi^{\dagger}\widehat{W}_{\mu\nu}\widehat{W}^{\mu\nu}\Phi$$

$$\mathcal{O}_{BB} = \Phi^{\dagger}\widehat{B}_{\mu\nu}\widehat{B}^{\mu\nu}\Phi.$$
(30)

If we replace one field strength tensor with the corresponding dual field strength tensor, we obtain the \mathcal{CP} -odd part of the Lagrangian

$$\begin{aligned}
\mathcal{O}_{\widetilde{W}} &= (D_{\mu}\Phi)^{\dagger} \widehat{\widetilde{W}}^{\mu\nu} (D_{\nu}\Phi) \\
\mathcal{O}_{\widetilde{B}} &= (D_{\mu}\Phi)^{\dagger} \widehat{\widetilde{B}}^{\mu\nu} (D_{\nu}\Phi) \\
\mathcal{O}_{\widetilde{W}WW} &= Tr \left[\widehat{\widetilde{W}}_{\mu\nu} \widehat{W}^{\nu\rho} \widehat{W}_{\rho}^{\mu} \right] \\
\mathcal{O}_{\widetilde{W}W} &= \Phi^{\dagger} \widehat{\widetilde{W}}_{\mu\nu} \widehat{W}^{\mu\nu}\Phi \\
\mathcal{O}_{\widetilde{B}B} &= \Phi^{\dagger} \widehat{\widetilde{B}}_{\mu\nu} \widehat{B}^{\mu\nu}\Phi \\
\mathcal{O}_{D\widetilde{W}} &= Tr \left([D_{\mu}, \widehat{\widetilde{W}}_{\nu\rho}] [D^{\mu}, \widehat{W}^{\nu\rho}] \right) \\
\mathcal{O}_{B\widetilde{W}} &= \Phi^{\dagger} \widehat{B}_{\mu\nu} \widehat{\widetilde{W}}^{\mu\nu}\Phi.
\end{aligned}$$
(31)

The operators $\mathcal{O}_{B\widetilde{W}}$ and $\mathcal{O}_{D\widetilde{W}}$ are included only in their \mathcal{CP} -odd version, as their \mathcal{CP} even counterparts affect the gauge boson two-point functions and are already extremely

constrained by electroweak precision tests. Furthermore, only 4 of these 7 operators are linearly independent. For example $\mathcal{O}_{\widetilde{W}}$, $\mathcal{O}_{B\widetilde{W}}$ and $\mathcal{O}_{D\widetilde{W}}$ can be written as

$$\mathcal{O}_{\widetilde{W}} = \mathcal{O}_{\widetilde{B}} - \frac{1}{2}\mathcal{O}_{\widetilde{W}W} + \frac{1}{2}\mathcal{O}_{\widetilde{B}B}$$
$$\mathcal{O}_{B\widetilde{W}} = -2\mathcal{O}_{\widetilde{B}} - \mathcal{O}_{\widetilde{B}B}$$
$$\mathcal{O}_{D\widetilde{W}} = -4\mathcal{O}_{\widetilde{W}WW}.$$
(32)

The dimension-8 operators can be split into three categories:

1. Operators using $D_{\mu}\Phi$:

$$\mathcal{L}_{S,0} = \left[(D_{\mu} \Phi)^{\dagger} D_{\nu} \Phi \right] \times \left[(D^{\mu} \Phi)^{\dagger} D^{\nu} \Phi \right]$$

$$\mathcal{L}_{S,1} = \left[(D_{\mu} \Phi)^{\dagger} D^{\mu} \Phi \right] \times \left[(D_{\nu} \Phi)^{\dagger} D^{\nu} \Phi \right]$$
(33)

2. Operators using $D_{\mu}\Phi$, $\hat{W}_{\mu\nu}$ and $\hat{B}_{\mu\nu}$:

$$\mathcal{L}_{M,0} = \operatorname{Tr} \left[\hat{W}_{\mu\nu} \hat{W}^{\mu\nu} \right] \times \left[(D_{\beta} \Phi)^{\dagger} D^{\beta} \Phi \right]$$

$$\mathcal{L}_{M,1} = \operatorname{Tr} \left[\hat{W}_{\mu\nu} \hat{W}^{\nu\beta} \right] \times \left[(D_{\beta} \Phi)^{\dagger} D^{\mu} \Phi \right]$$

$$\mathcal{L}_{M,2} = \left[\hat{B}_{\mu\nu} \hat{B}^{\mu\nu} \right] \times \left[(D_{\beta} \Phi)^{\dagger} D^{\beta} \Phi \right]$$

$$\mathcal{L}_{M,3} = \left[\hat{B}_{\mu\nu} \hat{B}^{\nu\beta} \right] \times \left[(D_{\beta} \Phi)^{\dagger} D^{\mu} \Phi \right]$$

$$\mathcal{L}_{M,4} = \left[(D_{\mu} \Phi)^{\dagger} \hat{W}_{\beta\nu} D^{\mu} \Phi \right] \times \hat{B}^{\beta\nu}$$

$$\mathcal{L}_{M,5} = \left[(D_{\mu} \Phi)^{\dagger} \hat{W}_{\beta\nu} D^{\nu} \Phi \right] \times \hat{B}^{\beta\mu}$$

$$\mathcal{L}_{M,6} = \left[(D_{\mu} \Phi)^{\dagger} \hat{W}_{\beta\nu} \hat{W}^{\beta\mu} D^{\mu} \Phi \right]$$

$$\mathcal{L}_{M,7} = \left[(D_{\mu} \Phi)^{\dagger} \hat{W}_{\beta\nu} \hat{W}^{\beta\mu} D^{\nu} \Phi \right]$$
(34)

3. Operators using $\hat{W}_{\mu\nu}$ and $\hat{B}_{\mu\nu}$:

$$\mathcal{L}_{T,0} = \operatorname{Tr} \left[\hat{W}_{\mu\nu} \hat{W}^{\mu\nu} \right] \times \operatorname{Tr} \left[\hat{W}_{\alpha\beta} \hat{W}^{\alpha\beta} \right]$$

$$\mathcal{L}_{T,1} = \operatorname{Tr} \left[\hat{W}_{\alpha\nu} \hat{W}^{\mu\beta} \right] \times \operatorname{Tr} \left[\hat{W}_{\mu\beta} \hat{W}^{\alpha\nu} \right]$$

$$\mathcal{L}_{T,2} = \operatorname{Tr} \left[\hat{W}_{\alpha\mu} \hat{W}^{\mu\beta} \right] \times \operatorname{Tr} \left[\hat{W}_{\beta\nu} \hat{W}^{\nu\alpha} \right]$$

$$\mathcal{L}_{T,5} = \operatorname{Tr} \left[\hat{W}_{\mu\nu} \hat{W}^{\mu\nu} \right] \times \hat{B}_{\alpha\beta} \hat{B}^{\alpha\beta}$$

$$\mathcal{L}_{T,6} = \operatorname{Tr} \left[\hat{W}_{\alpha\nu} \hat{W}^{\mu\beta} \right] \times \hat{B}_{\mu\beta} \hat{B}^{\alpha\nu}$$

$$\mathcal{L}_{T,7} = \operatorname{Tr} \left[\hat{W}_{\alpha\mu} \hat{W}^{\mu\beta} \right] \times \hat{B}_{\beta\nu} \hat{B}^{\nu\alpha}$$

$$\mathcal{L}_{T,8} = \hat{B}_{\mu\nu} \hat{B}^{\mu\nu} \hat{B}_{\alpha\beta} \hat{B}^{\alpha\beta}$$

$$\mathcal{L}_{T,9} = \hat{B}_{\alpha\mu} \hat{B}^{\mu\beta} \hat{B}_{\beta\nu} \hat{B}^{\nu\alpha} \qquad (35)$$

Each new operator introduces a new coupling strength f_i , so the complete effective Lagrangian containing effects from dimension six and eight operators is

$$\mathcal{L}_{eff} = \mathcal{L}_{SM} + \frac{f_W}{\Lambda^2} \mathcal{O}_W + \frac{f_B}{\Lambda^2} \mathcal{O}_B + \frac{f_{WWW}}{\Lambda^2} \mathcal{O}_{WWW} + \frac{f_{WW}}{\Lambda^2} \mathcal{O}_{WW} + \frac{f_{BB}}{\Lambda^2} \mathcal{O}_{BB} + \frac{f_{Wt}}{\Lambda^2} \mathcal{O}_{\widetilde{W}} + \frac{f_{BH}}{\Lambda^2} \mathcal{O}_{\widetilde{B}} + \frac{f_{WWt}}{\Lambda^2} \mathcal{O}_{\widetilde{W}W} + \frac{f_{WWt}}{\Lambda^2} \mathcal{O}_{\widetilde{W}W} + \frac{f_{BHt}}{\Lambda^2} \mathcal{O}_{\widetilde{B}B} + \frac{f_{DWt}}{\Lambda^2} \mathcal{O}_{D\widetilde{W}} + \frac{f_{BWt}}{\Lambda^2} \mathcal{O}_{B\widetilde{W}} + \frac{f_{S0}}{\Lambda^4} \mathcal{L}_{S,0} + \frac{f_{S1}}{\Lambda^4} \mathcal{L}_{S,1} + \frac{f_{M0}}{\Lambda^4} \mathcal{L}_{M,0} + \frac{f_{M1}}{\Lambda^4} \mathcal{L}_{M,1} + \frac{f_{M2}}{\Lambda^4} \mathcal{L}_{M,2} + \frac{f_{M3}}{\Lambda^4} \mathcal{L}_{M,3} + \frac{f_{M4}}{\Lambda^4} \mathcal{L}_{M,4} + \frac{f_{M5}}{\Lambda^4} \mathcal{L}_{M,5} + \frac{f_{M6}}{\Lambda^4} \mathcal{L}_{M,6} + \frac{f_{M7}}{\Lambda^4} \mathcal{L}_{M,7} + \frac{f_{T0}}{\Lambda^4} \mathcal{L}_{T,0} + \frac{f_{T1}}{\Lambda^4} \mathcal{L}_{T,1} + \frac{f_{T2}}{\Lambda^4} \mathcal{L}_{T,2} + \frac{f_{T5}}{\Lambda^4} \mathcal{L}_{T,5} + \frac{f_{T6}}{\Lambda^4} \mathcal{L}_{T,6} + \frac{f_{T7}}{\Lambda^4} \mathcal{L}_{T,7}. \quad (36)$$

A.2 Conventions for anomalous gauge boson coupling parameters in VBFNLO

As mentioned in Appendix A.1, our definition of the field strengths is slightly different than the one of [97]. For comparisons with programs that use the definition from [97] (for example MadGraph5 [126] with the UFO file written by Éboli et al.⁴²), you should rescale the coupling strengths by

$$f_{S,0,1} = f_{S,0,1}^{\text{Éboli}} \tag{37}$$

$$f_{M,0,1} = -\frac{1}{g^2} \cdot f_{M,0,1}^{\text{Éboli}}$$
(38)

$$f_{M,2,3} = -\frac{4}{g'^2} \cdot f_{M,2,3}^{\text{Éboli}}$$
(39)

$$f_{M,4,5} = -\frac{2}{gg'} \cdot f_{M,4,5}^{\text{Éboli}}$$
(40)

$$f_{M,6,7} = -\frac{1}{g^2} \cdot f_{M,6,7}^{\text{Éboli}}$$
(41)

$$f_{T,0,1,2} = \frac{1}{g^4} \cdot f_{T,0,1,2}^{\text{Éboli}}$$
(42)

$$f_{T,5,6,7} = \frac{4}{g^2 g'^2} \cdot f_{T,5,6,7}^{\text{Éboli}}$$
(43)

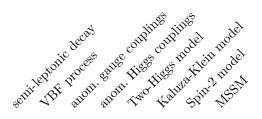
$$f_{T,8,9} = \frac{16}{g'^4} \cdot f_{T,8,9}^{\text{Éboli}} \tag{44}$$

where g and g' are the SU(2) and U(1) gauge couplings. The numerical values of g, g used in the calculation are printed out at the beginning of the VBFNLO run.

⁴²available from http://feynrules.irmp.ucl.ac.be/wiki/AnomalousGaugeCoupling

B Process list

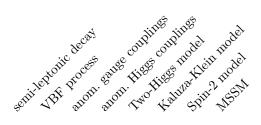
The following is a complete list of all processes available in VBFNLO, including any Beyond the Standard Model (BSM) effects that are implemented. Firstly, the processes that are accessed via the vbfnlo executable are given.



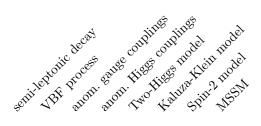
100	$p \stackrel{(-)}{p} ightarrow H j j$	_	\checkmark	_	\checkmark	—	—	_	\checkmark
101	$p \stackrel{(-)}{p} ightarrow H j j ightarrow \gamma \gamma j j$	_	\checkmark	—	\checkmark	—	—	—	\checkmark
102	$p \stackrel{(-)}{p} ightarrow H jj ightarrow \mu^+ \mu^- jj$	—	\checkmark	—	\checkmark	_	_	_	\checkmark
103	$p \stackrel{(-)}{p} \rightarrow H j j \rightarrow \tau^+ \tau^- j j$	_	\checkmark	_	\checkmark	_	_	_	\checkmark
104	$p \stackrel{(-)}{p} ightarrow H j j ightarrow b ar{b} j j$	_	\checkmark	_	\checkmark	_	_	_	\checkmark
105	$p \stackrel{(-)}{p} \rightarrow H j j \rightarrow W^+ W^- j j \rightarrow \ell_1^+ \nu_{\ell_1} \ell_2^- \bar{\nu}_{\ell_2} j j$	_	\checkmark	_	\checkmark	—	—	—	\checkmark
106	$p \stackrel{(-)}{p} \rightarrow H j j \rightarrow Z Z j j \rightarrow \ell_1^+ \ell_1^- \ell_2^+ \ell_2^- j j$	_	\checkmark	_	\checkmark	—	—	—	\checkmark
107	$p\stackrel{(-)}{p} ightarrow Hjj ightarrow ZZjj ightarrow \ell_1^+ \ell_1^- u_{\ell_2} ar{ u}_{\ell_2}jj$	_	\checkmark	_	\checkmark	—	_	—	\checkmark
108	$p \stackrel{(-)}{p} \rightarrow H j j \rightarrow W^+ W^- j j \rightarrow q \bar{q} \ell^- \bar{\nu}_\ell j j$	\checkmark	\checkmark	_	\checkmark	_	_	_	\checkmark
109	$p \stackrel{(-)}{p} ightarrow H jj ightarrow W^+ W^- jj ightarrow \ell^+ u_\ell q ar q jj$	\checkmark	\checkmark	_	\checkmark	—	—	_	\checkmark
1010	$p \stackrel{(-)}{p} ightarrow H jj ightarrow ZZ jj ightarrow q ar{q} \ell^+ \ell^- jj$	\checkmark	\checkmark	_	\checkmark	_	_	_	\checkmark
110	$p \stackrel{(-)}{p} ightarrow H j j j$	_	./	_	_	_	_	_	_
110	$p \stackrel{(-)}{p} \rightarrow H j j j \rightarrow \gamma \gamma j j j$	_	•	_	_	_	_	_	_
112	$p \stackrel{(-)}{p} \rightarrow H j j j \rightarrow \mu^+ \mu^- j j j$	_		_	_	_	_	_	_
113	$p \stackrel{(-)}{p} \rightarrow H j j j \rightarrow au^+ au^- j j j$	_	• √	_	_	_	_	_	_
114	$p \stackrel{(-)}{p} \rightarrow H j j j \rightarrow b \bar{b} j j j$	_	√	_	_	_	_	_	_
115	$p \stackrel{(-)}{p} \rightarrow H jjj \rightarrow W^+ W^- jjj \rightarrow \ell_1^+ \nu_{\ell_1} \ell_2^- \bar{\nu}_{\ell_2} jjj$	_	√	_	_	_	_	_	_
116	$p_{p}^{(-)} \to H jjj \to ZZ jjj \to \ell_{1}^{+} \ell_{1}^{-} \ell_{2}^{+} \ell_{2}^{-} jjj$	_	√	_	_	_	_	_	_
117	$p_{p}^{(-)} \rightarrow H jjj \rightarrow ZZ jjj \rightarrow \ell_{1}^{+} \ell_{1}^{-} \nu_{\ell_{2}} \bar{\nu}_{\ell_{2}} jjj$	_	√	_	_	_	_	_	_
	FF = -555 = -555 = -555 = -1 = 1 = 1 = 22 = 2255		·						
120	$p \stackrel{(-)}{p} ightarrow Z jj ightarrow \ell^+ \ell^- jj$	_	\checkmark	\checkmark	—	—	—	—	—
121	$p \stackrel{(-)}{p} ightarrow Z jj ightarrow u_\ell ar u_\ell jj$	_	\checkmark	\checkmark	_	_	_	_	_
130	$p \stackrel{(-)}{p} ightarrow W^+ j j ightarrow \ell^+ u_\ell j j$	_	\checkmark	\checkmark	_	_	_	_	_
140	$p \stackrel{(-)}{p} ightarrow W^- j j ightarrow \ell^- ar{ u}_\ell j j$	_	\checkmark	\checkmark	_	-	-	_	_
150	$p \stackrel{(-)}{p} ightarrow \gamma j j$	_	\checkmark	\checkmark	_	-	-	_	_

	Diocess		oupi	Hiess L	183 183	model
seni-leptoni	Process	58110 ⁶	1100	Hisson L	noe in in	NESN N
Some ABE	Suon.	910H	(TAIO	K all	ŞPIL	MSSN

191 195 196 197	$p \stackrel{(-)}{p} \rightarrow S_2 jj \rightarrow \gamma \gamma jj$ $p \stackrel{(-)}{p} \rightarrow S_2 jj \rightarrow W^+ W^- jj \rightarrow \ell_1^+ \nu_{\ell_1} \ell_2^- \bar{\nu}_{\ell_2} jj$ $p \stackrel{(-)}{p} \rightarrow S_2 jj \rightarrow ZZ jj \rightarrow \ell_1^+ \ell_1^- \ell_2^+ \ell_2^- jj$ $p \stackrel{(-)}{p} \rightarrow S_2 jj \rightarrow ZZ jj \rightarrow \ell_1^+ \ell_1^- \nu_{\ell_2} \bar{\nu}_{\ell_2} jj$	$ \begin{array}{cccccccccccccccccccccccccccccccccccc$
160 161 162	$p \stackrel{(-)}{p} ightarrow HH jj$ $p \stackrel{(-)}{p} ightarrow HH jj ightarrow bar{b} au^+ au^- jj$ $p \stackrel{(-)}{p} ightarrow HH jj ightarrow bar{b}\gamma\gamma jj$	$\begin{array}{cccccccccccccccccccccccccccccccccccc$
2100 2101 2102 2103 2104 2105 2106 2107	$\begin{split} p_{p}^{(-)} &\to H\gamma jj \\ p_{p}^{(-)} &\to H\gamma jj \to \gamma\gamma\gamma jj \\ p_{p}^{(-)} &\to H\gamma jj \to \mu^{+}\mu^{-}\gamma jj \\ p_{p}^{(-)} &\to H\gamma jj \to \tau^{+}\tau^{-}\gamma jj \\ p_{p}^{(-)} &\to H\gamma jj \to b\bar{b}\gamma jj \\ p_{p}^{(-)} &\to H\gamma jj \to W^{+}W^{-}\gamma jj \to \ell_{1}^{+}\nu_{\ell_{1}}\ell_{2}^{-}\bar{\nu}_{\ell_{2}}\gamma jj \\ p_{p}^{(-)} &\to H\gamma jj \to ZZ\gamma jj \to \ell_{1}^{+}\ell_{1}^{-}\ell_{2}^{+}\ell_{2}^{-}\gamma jj \\ p_{p}^{(-)} &\to H\gamma jj \to ZZ\gamma jj \to \ell_{1}^{+}\ell_{1}^{-}\nu_{\ell_{2}}\bar{\nu}_{\ell_{2}}\gamma jj \\ p_{p}^{(-)} &\to H\gamma jj \to ZZ\gamma jj \to \ell_{1}^{+}\ell_{1}^{-}\nu_{\ell_{2}}\bar{\nu}_{\ell_{2}}\gamma jj \end{split}$	$\begin{array}{cccccccccccccccccccccccccccccccccccc$



	(-)	
200	$p_{p}^{(-)} \to W^{+}W^{-} jj \to \ell_{1}^{+}\nu_{\ell_{1}}\ell_{2}^{-}\bar{\nu}_{\ell_{2}} jj$	$ \checkmark$ \checkmark $ \checkmark$ \checkmark $-$
201	$p^{(-)}_{I\!$	\checkmark \checkmark \checkmark $ \checkmark$ $ -$
202	$p^{(-)}_p ightarrow W^+ W^- jj ightarrow \ell^+ u_\ell q ar q jj$	\checkmark \checkmark \checkmark $ \checkmark$ $ -$
210	$p^{(-)}_{\ p} o ZZ jj o \ell_1^+ \ell_1^- \ell_2^+ \ell_2^- jj$	$ \checkmark$ \checkmark $ \checkmark$ \checkmark $-$
211	$p\stackrel{(-)}{p} ightarrow ZZjj ightarrow \ell_1^+ \ell_1^- u_{\ell_2} ar{ u}_{\ell_2}jj$	$ \checkmark$ \checkmark $ \checkmark$ \checkmark $-$
212	$p^{(-)}_{\ p} ightarrow ZZ jj ightarrow q ar{q} \ell^+ \ell^- jj$	\checkmark \checkmark \checkmark $ \checkmark$ $ -$
220	$p_{p}^{(-)} \to W^{+}Zjj \to \ell_{1}^{+}\nu_{\ell_{1}}\ell_{2}^{+}\ell_{2}^{-}jj$	$ \checkmark$ \checkmark $ \checkmark$ \checkmark \checkmark $-$
$\boldsymbol{221}$	$p^{(-)}_{\ p} ightarrow W^+ Z jj ightarrow q ar{q} \ell^+ \ell^- jj$	\checkmark \checkmark \checkmark $ \checkmark$ $ -$
222	$p^{(-)}_{\ p} ightarrow W^+ Z jj ightarrow \ell^+ u_\ell q ar q jj$	\checkmark \checkmark \checkmark $ \checkmark$ $ -$
230	$p_{p}^{(-)} \to W^{-}Zjj \to \ell_{1}^{-} \bar{\nu}_{\ell_{1}} \ell_{2}^{+} \ell_{2}^{-} jj$	$ \checkmark$ \checkmark $ \checkmark$ \checkmark \checkmark $-$
231	$p^{(-)}_p \rightarrow W^- Z jj \rightarrow q\bar{q} \ell^+ \ell^- jj$	\checkmark \checkmark \checkmark $ \checkmark$ $ -$
232	$p^{(-)}_p ightarrow W^- Z jj ightarrow \ell^- \bar{ u}_\ell q \bar{q} jj$	\checkmark \checkmark \checkmark $ \checkmark$ $ -$
250	$p_{p}^{(-)} \to W^{+}W^{+}jj \to \ell_{1}^{+}\nu_{\ell_{1}}\ell_{2}^{+}\nu_{\ell_{2}}jj$	$ \checkmark$ \checkmark $ \checkmark$ $ -$
251	$p^{(-)}_{\ p} ightarrow W^+ W^+ jj ightarrow q ar{q} \ell^+ u_\ell jj$	\checkmark \checkmark \checkmark $ \checkmark$ $ -$
260	$p^{(-)}_{\ p} o W^- W^- jj o \ell_1^- \bar{\nu}_{\ell_1} \ell_2^- \bar{\nu}_{\ell_2} jj$	$ \checkmark$ \checkmark $ \checkmark$ $ -$
261	$p^{(-)}_{\ p} ightarrow W^- W^- jj ightarrow q ar q \ell^- ar u_\ell jj$	\checkmark \checkmark \checkmark $ \checkmark$ $ -$
270	$p^{(-)}_{\ p} ightarrow W^+ \gamma jj ightarrow \ell^+ u_\ell \gamma jj$	$ \checkmark$ \checkmark $ -$
280	$p^{(-)}_{\ p} ightarrow W^- \gamma jj ightarrow \ell^- ar{ u}_\ell \gamma jj$	$ \checkmark$ \checkmark $ -$
290	$p\stackrel{(-)}{p} \to Z\gammajj \to \ell^+\ell^-\gammajj$	- ✓ ✓
291	$p \stackrel{(-)}{p} \rightarrow Z \gamma j j \rightarrow \nu_\ell \bar{\nu}_\ell \gamma j j$	- ✓ ✓
3120	$p \stackrel{(-)}{p} ightarrow Z jj ightarrow \ell^+ \ell^- jj$	
3121	$p \stackrel{(-)}{p} ightarrow Z jj ightarrow u_\ell ar u_\ell jj$	
3130	$p^{(-)}_p ightarrow W^+ jj ightarrow \ell^+ u_\ell jj$	
3140	$p^{(-)}_{\ p} ightarrow W^- jj ightarrow \ell^- ar{ u}_\ell jj$	

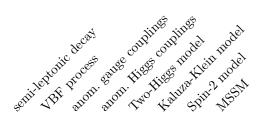


3210	$p^{(-)}_{\ p} \rightarrow ZZ jj \rightarrow \ell_1^+ \ell_1^- \ell_2^+ \ell_2^- jj$	
3211	$p \stackrel{(-)}{p} \rightarrow ZZ jj \rightarrow \ell_1^+ \ell_1^- \nu_{\ell_2} \bar{\nu}_{\ell_2} jj$	
3220	$p_{p}^{(-)} \rightarrow W^{+}Z jj \rightarrow \ell_{1}^{+}\nu_{\ell_{1}}\ell_{2}^{+}\ell_{2}^{-} jj$	
3230	$p^{(-)}_{\ p} \rightarrow W^- Z jj \rightarrow \ell_1^- \bar{\nu}_{\ell_1} \ell_2^+ \ell_2^- jj$	
3250	$p \stackrel{(-)}{p} \to W^+ W^+ j j \to \ell_1^+ \nu_{\ell_1} \ell_2^+ \nu_{\ell_2} j j$	
3260	$p \stackrel{(-)}{p} \to W^- W^- jj \to \ell_1^- \bar{\nu}_{\ell_1} \ell_2^- \bar{\nu}_{\ell_2} jj$	
3270	$p \stackrel{(-)}{p} ightarrow W^+ \gamma jj ightarrow \ell^+ u_\ell \gamma jj$	
3280	$p \stackrel{(-)}{p} ightarrow W^- \gamma jj ightarrow \ell^- ar{ u}_\ell \gamma jj$	
3290	$p \stackrel{(-)}{p} ightarrow Z \gamma jj ightarrow \ell^+ \ell^- \gamma jj$	
3291	$p \stackrel{(-)}{p} ightarrow Z \gamma jj ightarrow u_\ell ar u_\ell \gamma jj$	
1330	$p \stackrel{(-)}{p} \to W^+ \to \ell^+ \nu_\ell$	
1330 1340	$p \stackrel{p}{p} \xrightarrow{\rightarrow} W \xrightarrow{\rightarrow} \ell \stackrel{\nu}{\nu_{\ell}} p \stackrel{(-)}{p} \xrightarrow{\rightarrow} W^{-} \xrightarrow{\rightarrow} \ell^{-} \bar{\nu}_{\ell}$	
1630	$p \stackrel{p}{p} \rightarrow W^+ j \rightarrow \ell^+ \nu_\ell j$	
1640	$p \stackrel{p}{p} \rightarrow W^{-} j \rightarrow \ell^{-} \bar{ u}_{\ell} j$	
1010	pp , m j , \sim $\nu_{\ell}j$	
300	$p \stackrel{(-)}{p} \to W^+ W^- \to \ell_1^+ \nu_{\ell_1} \ell_2^- \bar{\nu}_{\ell_2}$	🗸 🗸
300 301	$p \stackrel{(-)}{p} \to W^+ W^- \to \ell_1^+ \nu_{\ell_1} \ell_2^- \bar{\nu}_{\ell_2}$ $p \stackrel{(-)}{p} \to W^+ W^- \to q \bar{q} \ell^- \bar{\nu}_{\ell}$	$ \checkmark \checkmark$ $\checkmark - \checkmark \checkmark$
	$p \stackrel{(-)}{p} \to W^+ W^- \to q \bar{q} \ell^- \bar{\nu}_\ell$ $p \stackrel{(-)}{p} \to W^+ W^- \to \ell^+ \nu_\ell q \bar{q}$	$\begin{array}{cccccccccccccccccccccccccccccccccccc$
301	$p \stackrel{(-)}{p} \to W^+ W^- \to q \bar{q} \ell^- \bar{\nu}_\ell$ $p \stackrel{(-)}{p} \to W^+ W^- \to \ell^+ \nu_\ell q \bar{q}$ $p \stackrel{(-)}{p} \to W^+ Z \to \ell_1^+ \nu_{\ell_1} \ell_2^+ \ell_2^-$	$\begin{array}{cccccccccccccccccccccccccccccccccccc$
301 302	$p \stackrel{(-)}{p} \to W^+ W^- \to q \bar{q} \ell^- \bar{\nu}_\ell$ $p \stackrel{(-)}{p} \to W^+ W^- \to \ell^+ \nu_\ell q \bar{q}$ $p \stackrel{(-)}{p} \to W^+ Z \to \ell_1^+ \nu_{\ell_1} \ell_2^+ \ell_2^-$ $p \stackrel{(-)}{p} \to W^+ Z \to q \bar{q} \ell^+ \ell^-$	$\begin{array}{cccccccccccccccccccccccccccccccccccc$
301 302 310	$p \stackrel{(-)}{p} \rightarrow W^+ W^- \rightarrow q\bar{q} \ell^- \bar{\nu}_\ell$ $p \stackrel{(-)}{p} \rightarrow W^+ W^- \rightarrow \ell^+ \nu_\ell q\bar{q}$ $p \stackrel{(-)}{p} \rightarrow W^+ Z \rightarrow \ell_1^+ \nu_{\ell_1} \ell_2^+ \ell_2^-$ $p \stackrel{(-)}{p} \rightarrow W^+ Z \rightarrow q\bar{q} \ell^+ \ell^-$ $p \stackrel{(-)}{p} \rightarrow W^+ Z \rightarrow \ell^+ \nu_\ell q\bar{q}$	$\begin{array}{cccccccccccccccccccccccccccccccccccc$
301 302 310 312	$p \stackrel{(-)}{p} \rightarrow W^+ W^- \rightarrow q \bar{q} \ell^- \bar{\nu}_\ell$ $p \stackrel{(-)}{p} \rightarrow W^+ W^- \rightarrow \ell^+ \nu_\ell q \bar{q}$ $p \stackrel{(-)}{p} \rightarrow W^+ Z \rightarrow \ell_1^+ \nu_{\ell_1} \ell_2^+ \ell_2^-$ $p \stackrel{(-)}{p} \rightarrow W^+ Z \rightarrow q \bar{q} \ell^+ \ell^-$ $p \stackrel{(-)}{p} \rightarrow W^+ Z \rightarrow \ell^+ \nu_\ell q \bar{q}$ $p \stackrel{(-)}{p} \rightarrow W^- Z \rightarrow \ell_1^- \bar{\nu}_{\ell_1} \ell_2^+ \ell_2^-$	$\begin{array}{cccccccccccccccccccccccccccccccccccc$
301 302 310 312 313	$p \stackrel{(-)}{p} \rightarrow W^+ W^- \rightarrow q\bar{q} \ell^- \bar{\nu}_\ell$ $p \stackrel{(-)}{p} \rightarrow W^+ W^- \rightarrow \ell^+ \nu_\ell q\bar{q}$ $p \stackrel{(-)}{p} \rightarrow W^+ Z \rightarrow \ell_1^+ \nu_{\ell_1} \ell_2^+ \ell_2^-$ $p \stackrel{(-)}{p} \rightarrow W^+ Z \rightarrow q\bar{q} \ell^+ \ell^-$ $p \stackrel{(-)}{p} \rightarrow W^+ Z \rightarrow \ell^+ \nu_\ell q\bar{q}$ $p \stackrel{(-)}{p} \rightarrow W^- Z \rightarrow \ell_1^- \bar{\nu}_{\ell_1} \ell_2^+ \ell_2^-$ $p \stackrel{(-)}{p} \rightarrow W^- Z \rightarrow q\bar{q} \ell^+ \ell^-$	$\begin{array}{cccccccccccccccccccccccccccccccccccc$
301 302 310 312 313 320	$\begin{split} p \stackrel{(-)}{p} &\rightarrow W^+ W^- \rightarrow q \bar{q} \ell^- \bar{\nu}_\ell \\ p \stackrel{(-)}{p} &\rightarrow W^+ W^- \rightarrow \ell^+ \nu_\ell q \bar{q} \\ p \stackrel{(-)}{p} &\rightarrow W^+ Z \rightarrow \ell_1^+ \nu_{\ell_1} \ell_2^+ \ell_2^- \\ p \stackrel{(-)}{p} &\rightarrow W^+ Z \rightarrow q \bar{q} \ell^+ \ell^- \\ p \stackrel{(-)}{p} &\rightarrow W^+ Z \rightarrow \ell^+ \nu_\ell q \bar{q} \\ p \stackrel{(-)}{p} &\rightarrow W^- Z \rightarrow \ell_1^- \bar{\nu}_{\ell_1} \ell_2^+ \ell_2^- \\ p \stackrel{(-)}{p} &\rightarrow W^- Z \rightarrow q \bar{q} \ell^+ \ell^- \\ p \stackrel{(-)}{p} &\rightarrow W^- Z \rightarrow \ell^- \bar{\nu}_\ell q \bar{q} \end{split}$	$\begin{array}{cccccccccccccccccccccccccccccccccccc$
301 302 310 312 313 320 322	$\begin{split} p \stackrel{(-)}{p} &\to W^+ W^- \to q \bar{q} \ell^- \bar{\nu}_\ell \\ p \stackrel{(-)}{p} &\to W^+ W^- \to \ell^+ \nu_\ell q \bar{q} \\ p \stackrel{(-)}{p} &\to W^+ Z \to \ell_1^+ \nu_{\ell_1} \ell_2^+ \ell_2^- \\ p \stackrel{(-)}{p} &\to W^+ Z \to q \bar{q} \ell^+ \ell^- \\ p \stackrel{(-)}{p} &\to W^+ Z \to \ell^+ \nu_\ell q \bar{q} \\ p \stackrel{(-)}{p} &\to W^- Z \to \ell_1^- \bar{\nu}_{\ell_1} \ell_2^+ \ell_2^- \\ p \stackrel{(-)}{p} &\to W^- Z \to \ell_1^- \bar{\nu}_\ell q \bar{q} \\ p \stackrel{(-)}{p} &\to W^- Z \to \ell^- \bar{\nu}_\ell q \bar{q} \\ p \stackrel{(-)}{p} &\to Z Z \to \ell_1^- \ell_1^+ \ell_2^- \ell_2^+ \end{split}$	$\begin{array}{cccccccccccccccccccccccccccccccccccc$
301 302 310 312 313 320 322 323	$\begin{split} p \stackrel{(-)}{p} &\to W^+ W^- \to q \bar{q} \ell^- \bar{\nu}_\ell \\ p \stackrel{(-)}{p} &\to W^+ W^- \to \ell^+ \nu_\ell q \bar{q} \\ p \stackrel{(-)}{p} &\to W^+ Z \to \ell_1^+ \nu_{\ell_1} \ell_2^+ \ell_2^- \\ p \stackrel{(-)}{p} &\to W^+ Z \to q \bar{q} \ell^+ \ell^- \\ p \stackrel{(-)}{p} &\to W^+ Z \to \ell^+ \nu_\ell q \bar{q} \\ p \stackrel{(-)}{p} &\to W^- Z \to \ell_1^- \bar{\nu}_{\ell_1} \ell_2^+ \ell_2^- \\ p \stackrel{(-)}{p} &\to W^- Z \to \ell^- \bar{\nu}_\ell q \bar{q} \\ p \stackrel{(-)}{p} &\to Z Z \to \ell_1^- \ell_1^+ \ell_2^- \ell_2^+ \\ p \stackrel{(-)}{p} &\to Z Z \to q \bar{q} \ell^- \ell^+ \end{split}$	$\begin{array}{cccccccccccccccccccccccccccccccccccc$
301 302 310 312 313 320 322 323 330	$\begin{split} p \stackrel{(-)}{p} &\rightarrow W^+ W^- \rightarrow q \bar{q} \ell^- \bar{\nu}_\ell \\ p \stackrel{(-)}{p} &\rightarrow W^+ W^- \rightarrow \ell^+ \nu_\ell q \bar{q} \\ p \stackrel{(-)}{p} &\rightarrow W^+ Z \rightarrow \ell_1^+ \nu_{\ell_1} \ell_2^+ \ell_2^- \\ p \stackrel{(-)}{p} &\rightarrow W^+ Z \rightarrow q \bar{q} \ell^+ \ell^- \\ p \stackrel{(-)}{p} &\rightarrow W^- Z \rightarrow \ell^- \bar{\nu}_\ell q \bar{q} \\ p \stackrel{(-)}{p} &\rightarrow W^- Z \rightarrow q \bar{q} \ell^+ \ell^- \\ p \stackrel{(-)}{p} &\rightarrow W^- Z \rightarrow q \bar{q} \ell^+ \ell^- \\ p \stackrel{(-)}{p} &\rightarrow W^- Z \rightarrow \ell^- \bar{\nu}_\ell q \bar{q} \\ p \stackrel{(-)}{p} &\rightarrow Z Z \rightarrow \ell^- \ell^- \ell_1^+ \ell_2^- \ell_2^+ \\ p \stackrel{(-)}{p} &\rightarrow Z Z \rightarrow q \bar{q} \ell^- \ell^+ \\ p \stackrel{(-)}{p} &\rightarrow W^+ \gamma \rightarrow \ell_1^+ \nu_{\ell_1} \gamma \end{split}$	$\begin{array}{cccccccccccccccccccccccccccccccccccc$
301 302 310 312 313 320 322 323 330 331	$\begin{split} p_{p}^{(-)} &\to W^{+}W^{-} \to q\bar{q}\ell^{-}\bar{\nu}_{\ell} \\ p_{p}^{(-)} &\to W^{+}W^{-} \to \ell^{+}\nu_{\ell}q\bar{q} \\ p_{p}^{(-)} &\to W^{+}Z \to \ell_{1}^{+}\nu_{\ell_{1}}\ell_{2}^{+}\ell_{2}^{-} \\ p_{p}^{(-)} &\to W^{+}Z \to q\bar{q}\ell^{+}\ell^{-} \\ p_{p}^{(-)} &\to W^{+}Z \to \ell^{+}\nu_{\ell}q\bar{q} \\ p_{p}^{(-)} &\to W^{-}Z \to \ell_{1}^{-}\bar{\nu}_{\ell_{1}}\ell_{2}^{+}\ell_{2}^{-} \\ p_{p}^{(-)} &\to W^{-}Z \to \ell^{-}\bar{\nu}_{\ell}q\bar{q} \\ p_{p}^{(-)} &\to W^{-}Z \to \ell^{-}\bar{\nu}_{\ell}q\bar{q} \\ p_{p}^{(-)} &\to ZZ \to \ell_{1}^{-}\ell_{1}^{+}\ell_{2}^{-}\ell_{2}^{+} \\ p_{p}^{(-)} &\to ZZ \to q\bar{q}\ell^{-}\ell^{+} \\ p_{p}^{(-)} &\to W^{+}\gamma \to \ell_{1}^{+}\nu_{\ell_{1}}\gamma \\ p_{p}^{(-)} &\to W^{-}\gamma \to \ell_{1}^{-}\bar{\nu}_{\ell_{1}}\gamma \end{split}$	$\begin{array}{cccccccccccccccccccccccccccccccccccc$
301 302 310 312 313 320 322 323 330 331 340	$\begin{split} p_{p}^{(-)} &\rightarrow W^{+}W^{-} \rightarrow q\bar{q} \ell^{-}\bar{\nu}_{\ell} \\ p_{p}^{(-)} &\rightarrow W^{+}W^{-} \rightarrow \ell^{+}\nu_{\ell} q\bar{q} \\ p_{p}^{(-)} &\rightarrow W^{+}Z \rightarrow \ell_{1}^{+}\nu_{\ell_{1}}\ell_{2}^{+}\ell_{2}^{-} \\ p_{p}^{(-)} &\rightarrow W^{+}Z \rightarrow q\bar{q} \ell^{+}\ell^{-} \\ p_{p}^{(-)} &\rightarrow W^{-}Z \rightarrow \ell_{1}^{-}\bar{\nu}_{\ell_{1}}\ell_{2}^{+}\ell_{2}^{-} \\ p_{p}^{(-)} &\rightarrow W^{-}Z \rightarrow \ell_{1}^{-}\bar{\nu}_{\ell_{1}}\ell_{2}^{+}\ell_{2}^{-} \\ p_{p}^{(-)} &\rightarrow W^{-}Z \rightarrow \ell^{-}\bar{\nu}_{\ell} q\bar{q} \\ p_{p}^{(-)} &\rightarrow ZZ \rightarrow \ell_{1}^{-}\ell_{1}^{+}\ell_{2}^{-}\ell_{2}^{+} \\ p_{p}^{(-)} &\rightarrow ZZ \rightarrow q\bar{q} \ell^{-}\ell^{+} \\ p_{p}^{(-)} &\rightarrow W^{-}\gamma \rightarrow \ell_{1}^{-}\bar{\nu}_{\ell_{1}}\gamma \\ p_{p}^{(-)} &\rightarrow W^{-}\gamma \rightarrow \ell_{1}^{-}\bar{\nu}_{\ell_{1}}\gamma \\ p_{p}^{(-)} &\rightarrow Z\gamma \rightarrow \ell_{1}^{-}\ell_{1}^{+}\gamma \end{split}$	$\begin{array}{cccccccccccccccccccccccccccccccccccc$
301 302 310 312 313 320 322 323 330 331 340 350	$\begin{split} p_{p}^{(-)} &\to W^{+}W^{-} \to q\bar{q}\ell^{-}\bar{\nu}_{\ell} \\ p_{p}^{(-)} &\to W^{+}W^{-} \to \ell^{+}\nu_{\ell}q\bar{q} \\ p_{p}^{(-)} &\to W^{+}Z \to \ell_{1}^{+}\nu_{\ell_{1}}\ell_{2}^{+}\ell_{2}^{-} \\ p_{p}^{(-)} &\to W^{+}Z \to q\bar{q}\ell^{+}\ell^{-} \\ p_{p}^{(-)} &\to W^{+}Z \to \ell^{+}\nu_{\ell}q\bar{q} \\ p_{p}^{(-)} &\to W^{-}Z \to \ell_{1}^{-}\bar{\nu}_{\ell_{1}}\ell_{2}^{+}\ell_{2}^{-} \\ p_{p}^{(-)} &\to W^{-}Z \to \ell^{-}\bar{\nu}_{\ell}q\bar{q} \\ p_{p}^{(-)} &\to W^{-}Z \to \ell^{-}\bar{\nu}_{\ell}q\bar{q} \\ p_{p}^{(-)} &\to ZZ \to \ell_{1}^{-}\ell_{1}^{+}\ell_{2}^{-}\ell_{2}^{+} \\ p_{p}^{(-)} &\to ZZ \to q\bar{q}\ell^{-}\ell^{+} \\ p_{p}^{(-)} &\to W^{+}\gamma \to \ell_{1}^{+}\nu_{\ell_{1}}\gamma \\ p_{p}^{(-)} &\to W^{-}\gamma \to \ell_{1}^{-}\bar{\nu}_{\ell_{1}}\gamma \end{split}$	$\begin{array}{cccccccccccccccccccccccccccccccccccc$



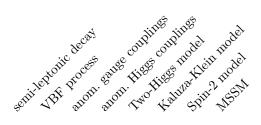
PROCID PROCESS

1300	$p \stackrel{(-)}{p} \to W^+ H \to \ell^+ \nu_\ell H$	—	—	\checkmark	—	—	—	—	—
1301	$p \stackrel{(-)}{p} \to W^+ H \to \ell^+ \nu_\ell \gamma \gamma$	_	_	\checkmark	_	_	_	_	_
1302	$p \stackrel{(-)}{p} \rightarrow W^+ H \rightarrow \ell^+ \nu_\ell \mu^+ \mu^-$	—	_	\checkmark	_	_	_	_	_
1303	$p^{(-)}_p \to W^+ H \to \ell^+ \nu_\ell \tau^+ \tau^-$	_	_	\checkmark	_	_	_	_	_
1304	$p \stackrel{(-)}{p} \rightarrow W^+ H \rightarrow \ell^+ \nu_\ell b \bar{b}$	_	_	\checkmark	_	_	_	_	_
1305	$p_{p}^{(-)} \to W^{+}H \to W^{+}W^{+}W^{-} \to \ell_{1}^{+}\nu_{\ell_{1}}\ell_{2}^{+}\nu_{\ell_{2}}\ell_{3}^{-}\bar{\nu}_{\ell_{3}}$	_	_	\checkmark	_	_	_	_	_
1306	$p_{p}^{(-)} \to W^{+}H \to W^{+}ZZ \to \ell_{1}^{+}\nu_{\ell_{1}}\ell_{2}^{+}\ell_{2}^{-}\ell_{3}^{+}\ell_{3}^{-}$	_	_	\checkmark	_	_	_	_	_
1307	$p_{p}^{(-)} \rightarrow W^{+}H \rightarrow W^{+}ZZ \rightarrow \ell_{1}^{+}\nu_{\ell_{1}}\ell_{2}^{+}\ell_{2}^{-}\nu_{\ell_{3}}\bar{\nu}_{\ell_{3}}$	_	_	\checkmark	_	_	_	_	_
	(-)								
1310	$p \stackrel{(-)}{p} \to W^- H \to \ell^- \bar{\nu}_\ell H$	—	—	\checkmark	—	_	—	—	_
1311	$p \stackrel{(-)}{p} \to W^- H \to \ell^- \bar{\nu}_\ell \gamma \gamma$	-	-	\checkmark	_	—	_	_	_
1312	$p \stackrel{(-)}{p} \rightarrow W^- H \rightarrow \ell^- \bar{\nu}_\ell \mu^+ \mu^-$	_	_	\checkmark	_	-	_	_	_
1313	$p \stackrel{(-)}{p} \to W^- H \to \ell^- \bar{\nu}_\ell \tau^+ \tau^-$	_	_	\checkmark	_	-	_	_	_
1314	$p \stackrel{(-)}{p} \to W^- H \to \ell^- \bar{\nu}_\ell b \bar{b}$	—	—	\checkmark	—	—	—	—	—
1315	$p_{p}^{(-)} \to W^{-}H \to W^{-}W^{+}W^{-} \to \ell_{1}^{-}\bar{\nu}_{\ell_{1}}\ell_{2}^{+}\nu_{\ell_{2}}\ell_{3}^{-}\bar{\nu}_{\ell_{3}}$	-	_	\checkmark	-	-	-	_	_
1316	$p \stackrel{(-)}{p} \to W^- H \to W^- Z Z \to \ell_1^- \bar{\nu}_{\ell_1} \ell_2^+ \ell_2^- \ell_3^+ \ell_3^-$	—	_	\checkmark	_	_	_	_	_
1317	$p \stackrel{(-)}{p} \to W^- H \to W^- Z Z \to \ell_1^- \bar{\nu}_{\ell_1} \ell_2^+ \ell_2^- \nu_{\ell_3} \bar{\nu}_{\ell_3}$	_	_	\checkmark	_	_	_	_	—
610	$p^{(-)}_p o W^- \gamma j o \ell^- \bar{\nu}_\ell \gamma j$			/					
610 620	$p p \to W \forall j \to \ell \nu_{\ell} \forall j$ $p p \to W^+ \gamma j \to \ell^+ \nu_{\ell} \gamma j$	_	_	v	_	_	_	_	_
		_	_	V	_	_	_	_	_
630	$p \stackrel{(-)}{p} \to W^{-} Z j \to \ell_{1}^{-} \bar{\nu}_{\ell_{1}} \ell_{2}^{-} \ell_{2}^{+} j$	_	_	V	_	_	_	_	_
640	$p p^{(-)} \to W^+ Z j \to \ell_1^+ \nu_{\ell_1} \ell_2^- \ell_2^+ j$	_	_	\checkmark	_	_	_	_	_
1600	$p \stackrel{(-)}{p} \to W^+ H j \to \ell^+ \nu_\ell H j$	_	_	\checkmark	_	_	_	_	_
1601	$p \stackrel{(-)}{p} \to W^+ H j \to \ell^+ \nu_\ell \gamma \gamma j$	_	_	\checkmark	_	_	_	_	_
1602	$p \stackrel{(-)}{p} \rightarrow W^+ H j \rightarrow \ell^+ \nu_\ell \mu^+ \mu^- j$	_	_	\checkmark	_	_	_	_	_
1603	$p \stackrel{(-)}{p} \rightarrow W^+ H j \rightarrow \ell^+ \nu_\ell \tau^+ \tau^- j$	_	_	\checkmark	_	_	_	_	_
1604	$p \stackrel{(-)}{p} \rightarrow W^+ H \ j \rightarrow \ell^+ \nu_\ell b \bar{b} \ j$	_	_	\checkmark	_	_	_	_	_
1605	$p_{p}^{(-)} \to W^{+}H j \to W^{+}W^{+}W^{-} j \to \ell_{1}^{+}\nu_{\ell_{1}}\ell_{2}^{+}\nu_{\ell_{2}}\ell_{3}^{-}\bar{\nu}_{\ell_{3}} j$	_	_	\checkmark	_	_	_	_	_
1606	$p_{p}^{(-)} \to W^{+}H j \to W^{+}ZZ j \to \ell_{1}^{+}\nu_{\ell_{1}}\ell_{2}^{+}\ell_{2}^{-}\ell_{3}^{+}\ell_{3}^{-} j$	_	_	√	_	_	_	_	_
1607	$p_{p}^{(-)} \rightarrow W^{+}H j \rightarrow W^{+}ZZ j \rightarrow \ell_{1}^{+}\nu_{\ell_{1}}\ell_{2}^{+}\ell_{2}^{-}\nu_{\ell_{3}}\bar{\nu}_{\ell_{3}} j$	_	_	√	_	_	_	_	_
2001	$r r \qquad \qquad$			•					



PROCID PROCESS

1610	$p \stackrel{(-)}{p} \to W^- H j \to \ell^- \bar{\nu}_\ell H j$	_	_	\checkmark	_	-	_	—	_
1611	$p \stackrel{(-)}{p} \rightarrow W^- H j \rightarrow \ell^- \bar{\nu}_\ell \gamma \gamma j$	—	—	\checkmark	—	_	—	_	_
1612	$p \stackrel{(-)}{p} \rightarrow W^- H j \rightarrow \ell^- \bar{\nu}_\ell \mu^+ \mu^- j$	—	_	\checkmark	_	_	_	—	_
1613	$p \stackrel{(-)}{p} \to W^- H j \to \ell^- \bar{\nu}_\ell \tau^+ \tau^- j$	_	_	\checkmark	_	_	_	_	_
1614	$p \stackrel{(-)}{p} \to W^- H j \to \ell^- \bar{\nu}_\ell b \bar{b} j$	_	_	\checkmark	_	_	_	_	_
1615	$p_{p}^{(-)} \to W^-Hj \to W^-W^+W^-j \to \ell_1^-\bar{\nu}_{\ell_1}\ell_2^+\nu_{\ell_2}\ell_3^-\bar{\nu}_{\ell_3}j$	—	—	\checkmark	_	_	_	_	_
1616	$p \stackrel{(-)}{p} \to W^- H j \to W^- Z Z j \to \ell_1^- \bar{\nu}_{\ell_1} \ell_2^+ \ell_2^- \ell_3^+ \ell_3^- j$	—	_	\checkmark	_	_	_	_	_
1617	$p^{(-)}_{\ p} \to W^- H j \to W^- Z Z j \to \ell_1^- \bar{\nu}_{\ell_1} \ell_2^+ \ell_2^- \nu_{\ell_3} \bar{\nu}_{\ell_3} j$	_	_	\checkmark	_	_	_	_	_
400	$p \stackrel{(-)}{p} \to W^+ W^- Z \to \ell_1^+ \nu_{\ell_1} \ell_2^- \bar{\nu}_{\ell_2} \ell_3^+ \ell_3^-$	_	_	\checkmark	_	_	\checkmark	_	_
401	$p \stackrel{(-)}{p} \to W^+ W^- Z \to q \bar{q} \ell_1^- \bar{\nu}_{\ell_1} \ell_2^+ \ell_2^-$	\checkmark	-	\checkmark	-	-	-	—	—
402	$p \stackrel{(-)}{p} \to W^+ W^- Z \to \ell_1^+ \nu_{\ell_1} q \bar{q} \ell_2^+ \ell_2^-$	\checkmark	—	\checkmark	—	—	_	_	_
403	$p \stackrel{(-)}{p} \to W^+ W^- Z \to \ell_1^+ \nu_{\ell_1} \ell_2^- \bar{\nu}_{\ell_2} q \bar{q}$	\checkmark	-	\checkmark	-	-	-	—	_
410	$p_{p}^{(-)} \to ZZW^{+} \to \ell_{1}^{+}\ell_{1}^{-}\ell_{2}^{+}\ell_{2}^{-}\ell_{3}^{+}\nu_{\ell_{3}}$	_	-	\checkmark	_	_	\checkmark	_	_
411	$p \stackrel{(-)}{p} \to ZZW^+ \to \ell_1^+ \ell_1^- \ell_2^+ \ell_2^- q \bar{q}$	\checkmark	—	\checkmark	—	—	—	—	—
412	$p \stackrel{(-)}{p} \to ZZW^+ \to q \bar{q} \ell_1^+ \ell_1^- \ell_2^+ \nu_{\ell_2}$	\checkmark	—	\checkmark	—	_	—	—	_
420	$p \stackrel{(-)}{p} \to ZZW^- \to \ell_1^+ \ell_1^- \ell_2^+ \ell_2^- \ell_3^- \bar{\nu}_{\ell_3}$	—	_	\checkmark	_	_	\checkmark	—	_
421	$p \stackrel{(-)}{p} \to Z Z W^- \to \ell_1^+ \ell_1^- \ell_2^+ \ell_2^- q \bar{q}$	\checkmark	—	\checkmark	—	—	—	—	—
422	$p \stackrel{(-)}{p} \to Z Z W^- \to q \bar{q} \ell_1^+ \ell_1^- \ell_2^- \bar{\nu}_{\ell_2}$	\checkmark	_	\checkmark	_	_	_	_	_
430	$p \stackrel{(-)}{p} \to W^+ W^- W^+ \to \ell_1^+ \nu_{\ell_1} \ell_2^- \bar{\nu}_{\ell_2} \ell_3^+ \nu_{\ell_3}$	_	_	\checkmark	_	_	\checkmark	_	_
431	$p \stackrel{(-)}{p} \to W^+ W^- W^+ \to q \bar{q} \ell_1^- \bar{\nu}_{\ell_1} \ell_2^+ \nu_{\ell_2}$	\checkmark	_	\checkmark	_	_	_	_	_
432	$p \stackrel{(-)}{p} \to W^+ W^- W^+ \to \ell_1^+ \nu_{\ell_1} q \bar{q} \ell_2^+ \nu_{\ell_2}$	\checkmark	_	\checkmark	_	_	_	_	_
440	$p \stackrel{(-)}{p} \to W^- W^+ W^- \to \ell_1^- \bar{\nu}_{\ell_1} \ell_2^+ \nu_{\ell_2} \ell_3^- \bar{\nu}_{\ell_3}$	—	_	\checkmark	_	_	\checkmark	_	_
441	$p \stackrel{(-)}{p} \to W^- W^+ W^- \to \ell_1^- \bar{\nu}_{\ell_1} q \bar{q} \ell_2^- \bar{\nu}_{\ell_2}$	\checkmark	_	\checkmark	_	_	_	_	_
$\boldsymbol{442}$	$p \stackrel{(-)}{p} \to W^- W^+ W^- \to q \bar{q} \ell_1^+ \nu_{\ell_1} \ell_2^- \bar{\nu}_{\ell_2}$	\checkmark	_	\checkmark	_	_	_	_	_
450	$p \stackrel{(-)}{p} \to ZZZ \to \ell_1^- \ell_1^+ \ell_2^- \ell_2^+ \ell_3^- \ell_3^+$	_	_	\checkmark	_	_	_	_	_
451	$p \stackrel{(-)}{p} \rightarrow ZZZ \rightarrow q \bar{q} \ell_1^- \ell_1^+ \ell_2^- \ell_2^+$	\checkmark	_	\checkmark	_	_	_	_	_
	~~ • •								



PROCID PROCESS

	(-)	
460	$p_{p}^{(-)} \rightarrow W^{-}W^{+}\gamma \rightarrow \ell_{1}^{-}\bar{\nu}_{\ell_{1}}\ell_{2}^{+}\nu_{\ell_{2}}\gamma$	$ \checkmark$ $ -$
461	$p \stackrel{(-)}{p} \to W^+ W^- \gamma \to q \bar{q} \ell^- \bar{\nu}_\ell \gamma$	\checkmark - \checkmark
462	$p \stackrel{(-)}{p} ightarrow W^+ W^- \gamma ightarrow \ell^+ u_\ell q \bar{q} \gamma$	\checkmark - \checkmark
470	$p^{(-)}_{p} \rightarrow ZZ\gamma \rightarrow \ell_{1}^{-}\ell_{1}^{+}\ell_{2}^{-}\ell_{2}^{+}\gamma$	🗸
471	$p^{(-)}_{\ p} ightarrow ZZ\gamma ightarrow \ell^- \ell^+ q \bar{q} \gamma$	\checkmark - \checkmark
472	$p \stackrel{(-)}{p} \rightarrow ZZ\gamma \rightarrow \ell_1^- \ell_1^+ \nu_{\ell_2} \bar{\nu}_{\ell_2} \gamma$	
480	$p \stackrel{(-)}{p} \to W^+ Z \gamma \to \ell_1^+ \nu_{\ell_1} \ell_2^- \ell_2^+ \gamma$	
481	$p^{(-)}_{\ p} ightarrow W^+ Z \gamma ightarrow q ar q \ell^- \ell^+ \gamma$	\checkmark - \checkmark
$\boldsymbol{482}$	$p^{(-)}_{p} ightarrow W^{+} Z \gamma ightarrow \ell^{+} \nu_{\ell} q \bar{q} \gamma$	\checkmark - \checkmark
490	$p^{(-)}_{\ p} \rightarrow W^- Z \gamma \rightarrow \ell_1^- \bar{\nu}_{\ell_1} \ell_2^- \ell_2^+ \gamma$	$ \checkmark$ $ -$
491	$p_{p}^{(-)} ightarrow W^- Z \gamma ightarrow q \bar{q} \ell^- \ell^+ \gamma$	\checkmark - \checkmark
$\boldsymbol{492}$	$p \stackrel{(-)}{p} \to W^- Z \gamma \to \ell^- \bar{\nu}_\ell q \bar{q} \gamma$	\checkmark - \checkmark
500	$p_{p}^{(-)} \rightarrow W^{+} \gamma \gamma \rightarrow \ell^{+} \nu_{\ell} \gamma \gamma$	
510	$p \stackrel{(-)}{p} \to W^- \gamma \gamma \to \ell^- \bar{\nu}_\ell \gamma \gamma$	
520	$p \stackrel{(-)}{p} \rightarrow Z \gamma \gamma \rightarrow \ell^- \ell^+ \gamma \gamma$	$ \checkmark$ $ -$
521	$p \stackrel{(-)}{p} ightarrow Z \gamma \gamma ightarrow u_\ell ar u_\ell \gamma \gamma$	
530	$p \stackrel{(-)}{p} ightarrow \gamma \gamma \gamma$	
	(-)	
800	$p_{P}^{(-)} \rightarrow W^{+}\gamma\gamma j \rightarrow \ell^{+}\nu_{\ell}\gamma\gamma j$	$ \checkmark$ $ -$
810	$p^{(-)}_{p} \to W^{-} \gamma \gamma j \to \ell^{-} \bar{\nu}_{\ell} \gamma \gamma j$	

The gluon-fusion processes accessed via the executable $\tt ggflo$ are given below.



-

4100	$p \stackrel{(-)}{p} ightarrow H j j$	\checkmark	_	_	\checkmark	\checkmark
4101	$p \stackrel{(-)}{p} ightarrow H jj ightarrow \gamma \gamma jj$	\checkmark	_	_	_	\checkmark
$\boldsymbol{4102}$	$p \stackrel{(-)}{p} \rightarrow H j j \rightarrow \mu^+ \mu^- j j$	\checkmark	_	_	_	\checkmark
4103	$p \stackrel{(-)}{p} \rightarrow H j j \rightarrow \tau^+ \tau^- j j$	\checkmark	_	_	_	\checkmark
4104	$p\stackrel{(-)}{p} ightarrow Hjj ightarrow bar{b}jj$	\checkmark	_	_	_	\checkmark
4105	$p \stackrel{(-)}{p} \rightarrow H jj \rightarrow W^+ W^- jj \rightarrow \ell_1^+ \nu_{\ell_1} \ell_2^- \bar{\nu}_{\ell_2} jj$	\checkmark	_	\checkmark	\checkmark	\checkmark
4106	$p_{p}^{(-)} \rightarrow H jj \rightarrow ZZ jj \rightarrow \ell_{1}^{+}\ell_{1}^{-}\ell_{2}^{+}\ell_{2}^{-} jj$	\checkmark	_	\checkmark	\checkmark	\checkmark
4107	$p \stackrel{(-)}{p} \rightarrow H jj \rightarrow ZZ jj \rightarrow \ell_1^+ \ell_1^- \nu_{\ell_2} \bar{\nu}_{\ell_2} jj$	\checkmark	_	\checkmark	\checkmark	\checkmark
4300	$p_{p}^{(-)} \to W^{+}W^{-} \to \ell_{1}^{+}\nu_{\ell_{1}}\ell_{2}^{-}\bar{\nu}_{\ell_{2}}$	\checkmark	_	\checkmark	_	_
1001	(-)					
4301	$p \stackrel{(-)}{p} \to W^+ W^- \to q \bar{q} \ell^- \bar{\nu}_\ell$	\checkmark	\checkmark	\checkmark	_	_
$\begin{array}{c} 4301\\ 4302 \end{array}$	$p \stackrel{'p'}{p} \rightarrow W^+ W^- \rightarrow q\bar{q} \ell^- \bar{\nu}_\ell \\ p \stackrel{(-)}{p} \rightarrow W^+ W^- \rightarrow \ell^+ \nu_\ell q\bar{q}$		√ √		_	_
	$p \stackrel{(-)}{p} \rightarrow W^+ W^- \rightarrow \ell^+ \nu_\ell q \bar{q}$				_	_
4302	$p \stackrel{(-)}{p} \rightarrow W^+ W^- \rightarrow \ell^+ \nu_\ell q \bar{q}$ $p \stackrel{(-)}{p} \rightarrow ZZ \rightarrow \ell_1^- \ell_1^+ \ell_2^- \ell_2^+$	√ √		√ √		
4302 4330	$p_{p}^{(-)} \rightarrow W^{+}W^{-} \rightarrow \ell^{+}\nu_{\ell} q\bar{q}$ $p_{p}^{(-)} \rightarrow ZZ \rightarrow \ell_{1}^{-}\ell_{1}^{+}\ell_{2}^{-}\ell_{2}^{+}$ $p_{p}^{(-)} \rightarrow ZZ \rightarrow q\bar{q} \ell^{-}\ell^{+}$	√ √	✓ _	√ √		
4302 4330 4331	$p \stackrel{(-)}{p} \rightarrow W^+ W^- \rightarrow \ell^+ \nu_\ell q \bar{q}$ $p \stackrel{(-)}{p} \rightarrow ZZ \rightarrow \ell_1^- \ell_1^+ \ell_2^- \ell_2^+$	√ √	✓ _	√ √		

References

- K. Arnold, M. Bahr, G. Bozzi *et al.*, "VBFNLO: A Parton level Monte Carlo for processes with electroweak bosons", *Comput. Phys. Commun.* 180 (2009) 1661-1670, arXiv:0811.4559.
- [2] K. Arnold, J. Bellm, G. Bozzi et al., "VBFNLO: A parton level Monte Carlo for processes with electroweak bosons – Manual for Version 2.5.0," arXiv:1107.4038v1.
- [3] K. Arnold, J. Bellm, G. Bozzi *et al.*, "VBFNLO: A parton level Monte Carlo for processes with electroweak bosons Manual for Version 2.6.0," arXiv:1107.4038v2.
- [4] M. R. Whalley, D. Bourilkov and R. C. Group, "The Les Houches accord PDFs (LHAPDF) and LHAGLUE", hep-ph/0508110.
- [5] T. Hahn and M. Perez-Victoria, "Automatized one-loop calculations in four and D dimensions", Comput. Phys. Commun. 118 (1999) 153, hep-ph/9807565.
- [6] T. Hahn and M. Rauch, "News from FormCalc and LoopTools", Nucl. Phys. Proc. Suppl. 157 (2006) 236-240, hep-ph/0601248.
- [7] M. Frank, T. Hahn, S. Heinemeyer *et al.*, "The Higgs boson masses and mixings of the complex MSSM in the Feynman-diagrammatic approach", *JHEP* 0702 (2007) 047, hep-ph/0611326.
- [8] G. Degrassi, S. Heinemeyer, W. Hollik *et al.*, "Towards high-precision predictions for the MSSM Higgs sector", *Eur. Phys. J.* C28 (2003) 133, hep-ph/0212020.
- [9] S. Heinemeyer, W. Hollik and G. Weiglein, "The masses of the neutral CP-even Higgs bosons in the MSSM: Accurate analysis at the two loop level", *Eur. Phys. J.* C9 (1999) 343-366, hep-ph/9812472.
- [10] S. Heinemeyer, W. Hollik and G. Weiglein, "FeynHiggs: A program for the calculation of the masses of the neutral CP even Higgs bosons in the MSSM", *Comput. Phys. Commun.* **124** (2000) 76-89, hep-ph/9812320.
- [11] H. Murayama, I. Watanabe and K. Hagiwara, "Helas: HELicity amplitude subroutines for Feynman diagram evaluations", KEK-91-11.
- [12] F. Campanario, "Towards $pp \rightarrow VVjj$ at NLO QCD: Bosonic contributions to triple vector boson production plus jet," *JHEP* **1110** (2011) 070, arXiv:1105.0920.
- [13] J. Pumplin, D.R. Stump, J. Huston et al., "New generation of parton distributions with uncertainties from global QCD analysis", JHEP 0207 (2002) 012, hep-ph/0201195.
- [14] H. -L. Lai, M. Guzzi, J. Huston et al., "New parton distributions for collider physics", Phys. Rev. D82 (2010) 074024, arXiv:1007.2241.
- [15] A. D. Martin, R. G. Roberts, W. J. Stirling and R. S. Thorne, "Parton distributions incorporating QED contributions", Eur. Phys. J. C39 (2005) 155, hep-ph/0411040.
- [16] A. D. Martin, W. J. Stirling, R. S. Thorne and G. Watt, "Parton distributions for the LHC", Eur. Phys. J. C63 (2009) 189-285, arXiv:0901.0002.

- [17] T. Stelzer and W. F. Long, "Automatic generation of tree level helicity amplitudes", Comput. Phys. Commun. 81 (1994) 357, hep-ph/9401258.
- [18] J. Alwall, P Demin, S. de Visscher et al., "MadGraph/MadEvent v4: The New Web Generation", JHEP 0709 (2007) 028, arXiv:0706.2334.
- [19] J. Kublbeck, M. Bohm, and A. Denner, Feyn Arts: Computer Algebraic Generation of Feynman Graphs and Amplitudes, Comput. Phys. Commun. 60 (1990) 165–180.
- [20] A. Denner, H. Eck, O. Hahn, and J. Kublbeck, Feynman rules for fermion number violating interactions, Nucl. Phys. B387 (1992) 467–484.
- [21] J. Kublbeck, H. Eck, and R. Mertig, Computeralgebraic generation and calculation of feynman graphs using feynarts and feyncalc, Nucl. Phys. Proc. Suppl. 29A (1992) 204–208.
- [22] T. Hahn, Generating Feynman diagrams and amplitudes with FeynArts 3, Comput. Phys. Commun. 140 (2001) 418–431, [hep-ph/0012260].
- [23] T. Hahn and C. Schappacher, The implementation of the minimal supersymmetric standard model in FeynArts and FormCalc, Comput. Phys. Commun. 143 (2002) 54-68, [hep-ph/0105349].
- [24] T. Hahn, A Mathematica interface for FormCalc-generated code, Comput. Phys. Commun. 178 (2008) 217–221, [hep-ph/0611273].
- [25] B. C. Allanach, C. Balazs, G. Belanger, M. Bernhardt, F. Boudjema, D. Choudhury, K. Desch and U. Ellwanger *et al.*, "SUSY Les Houches Accord 2," Comput. Phys. Commun. **180** (2009) 8 arXiv:0801.0045.
- [26] T. Hahn, "SUSY Les Houches Accord 2 I/O made easy," Comput. Phys. Commun. 180 (2009) 1681 hep-ph/0605049.
- [27] G. J. van Oldenborgh and J. A. M. Vermaseren, "New Algorithms for One Loop Integrals," Z. Phys. C 46 (1990) 425.
- [28] C. Georg, "Interferenzeffekte in Vektorboson-Fusion", Diploma Thesis, ITP Karlsruhe 2005, http://www.itp.kit.edu/diplomatheses.en.shtml.
- [29] J. R. Andersen, T. Binoth, G. Heinrich and J. M. Smillie, "Loop induced interference effects in Higgs Boson plus two jet production at the LHC", JHEP 0802 (2008) 057, arXiv:0709.3513.
- [30] A. Bredenstein, K. Hagiwara and B. Jäger, "Mixed QCD-electroweak contributions to Higgs-plus-dijet production at the LHC", *Phys. Rev.* D77 (2008) 073004, arXiv:0801.4231.
- [31] S. Frixione, "Isolated photons in perturbative QCD", Phys. Lett. B429 (1998) 369-374, hep-ph/9801442.
- [32] T. Figy, C. Oleari and D. Zeppenfeld, "Next-to-leading order jet distributions for Higgs boson production via weak boson fusion", *Phys. Rev.* D68 (2003) 073005, hep-ph/0306109.

- [33] W. Hollik, T. Plehn, M. Rauch and H. Rzehak, "Supersymmetric Higgs Bosons in Weak Boson Fusion", Phys. Rev. Lett. 102, 091802 (2009), arXiv:0804.2676.
- [34] T. Figy, S. Palmer and G. Weiglein, "Higgs Production via Weak Boson Fusion in the Standard Model and the MSSM," JHEP 1202 (2012) 105, arXiv:1012.4789.
- [35] B. Feigl, "Electroweak Processes in the Standard Model and Beyond: Backgrounds to Higgs Physics and Semileptonic Decay Modes", PhD Thesis, ITP Karlsruhe 2013, http://digbib.ubka.uni-karlsruhe.de/volltexte/1000037298.
- [36] T. Figy, V. Hankele and D. Zeppenfeld, "Next-to-leading order QCD corrections to Higgs plus three jet production in vector-boson fusion", *JHEP* 0802 (2008) 076, arXiv:0710.5621.
- [37] K. Arnold, T. Figy, B. Jager and D. Zeppenfeld, "Next-to-leading order QCD corrections to Higgs boson production in association with a photon via weak-boson fusion at the LHC", JHEP 1008 (2010) 088, arXiv:1006.4237.
- [38] C. Oleari and D. Zeppenfeld, "QCD corrections to electroweak $l\nu_l jj$ and $l^+l^- jj$ production", *Phys. Rev.* D69 (2004) 093004, hep-ph/0310156.
- [39] B. Jager, "Next-to-leading order QCD corrections to photon production via weak-boson fusion", Phys. Rev. D81 (2010) 114016, arXiv:1004.0825.
- [40] J. Frank, "Spin-2 Resonances in Vector Boson Fusion Processes at the LHC", Diploma Thesis, ITP Karlsruhe 2011, http://www.itp.kit.edu/diplomatheses.en.shtml.
- [41] J. Frank, M. Rauch and D. Zeppenfeld, "Spin-2 Resonances in Vector-Boson-Fusion Processes at NLO QCD", Phys. Rev. D87, 055020 (2013) arXiv:1211.3658.
- [42] J. Frank, M. Rauch and D. Zeppenfeld, "Higgs Spin Determination in the WW channel and beyond" arXiv:1305.3658.
- [43] B. Jager, C. Oleari and D. Zeppenfeld, "Next-to-leading order QCD corrections to W^+W^- production via vector-boson fusion", *JHEP* 0607 (2006) 015, hep-ph/0603177.
- [44] B. Jager, C. Oleari, and D. Zeppenfeld, "Next-to-leading order QCD corrections to Z boson pair production via vector-boson fusion", *Phys. Rev.* D73 (2006) 113006, hep-ph/0604200.
- [45] G. Bozzi, B. Jager, C. Oleari and D. Zeppenfeld, "Next-to-leading order QCD corrections to W⁺Z and W⁻Z production via vector-boson fusion", Phys. Rev. D75 (2007) 073004, hep-ph/0701105.
- [46] B. Jager, C. Oleari and D. Zeppenfeld, "Next-to-leading order QCD corrections to W⁺W⁺jj and W⁻W⁻jj production via weak-boson fusion," Phys. Rev. D80 (2009) 034022, arXiv:0907.0580.
- [47] F. Campanario, N. Kaiser and D. Zeppenfeld, " $W\gamma$ production in vector boson fusion at NLO in QCD," *Phys. Rev.* **D89** (2014) 014009, arXiv:1309.7259.
- [48] N. Kaiser, "NLO QCD corrections to $W\gamma$ production via vector boson fusion," Diploma Thesis, ITP Karlsruhe 2013, http://www.itp.kit.edu/diplomatheses.en.shtml.

- [49] T. Figy, "Next-to-leading order QCD corrections to light Higgs Pair production via vector boson fusion," Mod. Phys. Lett. A 23 (2008) 1961, arXiv:0806.2200.
- [50] J. Baglio, A. Djouadi, R. Groeber, M. M. Muehlleitner, J. Quevillon and M. Spira, "The measurement of the Higgs self-coupling at the LHC: theoretical status," *JHEP* 1304 (2013) 151, arXiv:1212.5581.
- [51] R. Roth, "NLO QCD corrections to WH + jet production at the LHC," Diploma Thesis, ITP Karlsruhe 2013, http://www.itp.kit.edu/diplomatheses.en.shtml.
- [52] J. Bellm, "NLO-QCD-Korrekturen zur WZ- und Wγ-Produktion am LHC", Diploma Thesis, ITP Karlsruhe 2012, http://www.itp.kit.edu/diplomatheses.en.shtml.
- [53] V. Hankele and D. Zeppenfeld, "QCD corrections to hadronic WWZ production with leptonic decays", Phys. Lett. B661 (2008) 103, arXiv:0712.3544.
- [54] F. Campanario, V. Hankele, C. Oleari *et al.*, "QCD corrections to charged triple vector boson production with leptonic decay," *Phys. Rev.* D78 (2008) 094012, arXiv:0809.0790.
- [55] G. Bozzi, F. Campanario, V. Hankele *et al.*, "NLO QCD corrections to $W^+W^-\gamma$ and $ZZ\gamma$ production with leptonic decays", *Phys. Rev.* **D81** (2010) 094030, arXiv:0911.0438.
- [56] G. Bozzi, F. Campanario, M. Rauch *et al.*, "NLO QCD corrections to $W^{\pm}Z\gamma$ production with leptonic decays", *Phys. Lett.* **B696** (2011) 380, arXiv:1011.2206.
- [57] G. Bozzi, F. Campanario, M. Rauch and D. Zeppenfeld, " $W^{\pm}\gamma\gamma$ production with leptonic decays at NLO QCD", *Phys. Rev.* D83 (2011) 114035, arXiv:1103.4613.
- [58] G. Bozzi, F. Campanario, M. Rauch and D. Zeppenfeld, " $Z\gamma\gamma$ production with leptonic decays and triple photon production at NLO QCD," *Phys. Rev.* D84 (2011) 074028, arXiv:1107.3149.
- [59] F. Campanario, C. Englert and M. Spannowsky, "Precise predictions for (non-standard) Wγ+jet production", Phys. Rev. D83 (2011) 074009, arXiv:1010.1291.
- [60] F. Campanario, C. Englert and M. Spannowsky, "QCD corrections to non-standard WZ+jet production with leptonic decays at the LHC", Phys. Rev. D82 (2010) 054015, arXiv:1006.3090.
- [61] F. Campanario, C. Englert, S. Kallweit *et al.*, "NLO QCD corrections to WZ+jet production with leptonic decays", JHEP 1007 (2010) 076, arXiv:1006.0390.
- [62] F. Campanario, C. Englert, M. Spannowsky and D. Zeppenfeld, "NLO-QCD corrections to Wγj production", Europhys. Lett. 88 (2009) 11001, arXiv:0908.1638.
- [63] F. Campanario, C. Englert, M. Rauch and D. Zeppenfeld, "Precise predictions for $W\gamma\gamma$ +jet production at hadron colliders," *Phys. Lett.* **B704** (2011) 515, arXiv:1106.4009.
- [64] F. Campanario, M. Kerner, L. D. Ninh and D. Zeppenfeld, "WZ production in association with two jets at NLO in QCD," *Phys. Rev. Lett.* **111** (2013) 052003, arXiv:1305.1623.

- [65] F. Campanario, M. Kerner, L. D. Ninh and D. Zeppenfeld, "Next-to-leading order QCD corrections to W⁺W⁺ and W⁻W⁻ production in association with two jets," *Phys. Rev.* D89 (2014) 054009, arXiv:1311.6738.
- [66] F. Campanario, M. Kerner, L. D. Ninh and D. Zeppenfeld, "Next-to-leading order QCD corrections to Wγ production in association with two jets", Eur. Phys. J. C74 (2014) 5, 2882 arXiv:1402.0505.
- [67] F. Campanario, M. Kerner, L. D. Ninh and D. Zeppenfeld, "Next-to-leading order QCD corrections to ZZ production in association with two jets", *JHEP* 1407 (2014) 148 arXiv:1405.3972.
- [68] F. Campanario, M. Kerner, L. D. Ninh and D. Zeppenfeld, " $Z\gamma$ production in association with two jets at next-to-leading order QCD", *Eur. Phys. J.* C74 (2014) 9, 3085 arXiv:1407.7857.
- [69] M. Kerner, "Next-to-Leading Order QCD Corrections to Vector Boson Pair Production in Association with two Jets at the LHC", PhD Thesis, ITP Karlsruhe 2014, http://digbib.ubka.uni-karlsruhe.de/volltexte/1000042285.
- [70] V. Del Duca, W. Kilgore, C. Oleari *et al.*, "H + 2 jets via gluon fusion", Phys. Rev. Lett. 87 (2001) 122001, hep-ph/0105129.
- [71] V. Del Duca, W. Kilgore, C. Oleari *et al.*, "Gluon-fusion contributions to H + 2 jet production", Nucl. Phys. B616 (2001) 367, hep-ph/0108030.
- [72] V. Del Duca, G. Klamke, M.L. Mangano *et al.*, "Monte Carlo studies of the jet activity in Higgs + 2 jet events", *JHEP* 0610 (2006) 016, hep-ph/0608158.
- [73] G. Klamke and D. Zeppenfeld, "Higgs plus two jet production via gluon fusion as a signal at the CERN LHC", JHEP 0704 (2007) 052, hep-ph/0703202.
- "Produktion [74] M. Kubocz, des **CP**-ungeraden Higgs-Bosons im $p_p^{(-)}$ Prozess \rightarrow $A^0 j j X$ ", Diploma ITP Karlsruhe Thesis, 2006,http://www.itp.kit.edu/diplomatheses.en.shtml.
- [75] F. Campanario, M. Kubocz and D. Zeppenfeld, "Gluon-fusion contributions to Phi + 2 Jet production," *Phys. Rev.* D84 (2011) 095025, arXiv:1011.3819.
- [76] Particle Data Group Collaboration, "Review of Particle Physics", Phys. Lett. B667 (2008) 1.
- [77] D. Albert, W. J. Marciano, D. Wyler and Z. Parsa, "Decays of Intermediate Vector Bosons, Radiative Corrections and QCD Jets," Nucl. Phys. B 166 (1980) 460.
- [78] J. Alwall, A. Ballestrero, P. Bartalini *et al.*, "A standard format for Les Houches event files", *Comput. Phys. Commun.* **176** (2007) 300, hep-ph/0609017.
- [79] M. Dobbs and J. B. Hansen, "The HepMC C++ Monte Carlo event record for High Energy Physics", Comput. Phys. Commun. 134, 41-46 (2001).
- [80] M. H. Seymour, "Jet shapes in hadron collisions: Higher orders, resummation and hadronization", Nucl. Phys. B513 (1998) 269, hep-ph/9707338.

- [81] Y. L. Dokshitzer, G. D. Leder, S. Moretti and B. R. Webber, "Better Jet Clustering Algorithms", JHEP 9708 (1997) 001, hep-ph/9707323.
- [82] M. Cacciari, G. P. Salam and G. Soyez, "The anti- k_T jet clustering algorithm", *JHEP* **0804** (2008) 063, arXiv:0802.1189.
- [83] J. Beringer et al. [Particle Data Group Collaboration], "Review of Particle Physics (RPP)," Phys. Rev. D86 (2012) 010001.
- [84] M. S. Carena, S. Heinemeyer, C. E. M. Wagner and G. Weiglein, "Suggestions for benchmark scenarios for MSSM Higgs boson searches at hadron colliders", *Eur. Phys. J.* C26 (2003) 601, hep-ph/0202167.
- [85] ALEPH Collaboration and DELPHI Collaboration and L3 Collaboration, "Search for neutral MSSM Higgs bosons at LEP", Eur. Phys. J. C47 (2006) 547, hep-ex/0602042.
- [86] B. C. Allanach, M. Battaglia, G. A. Blair et al., "The Snowmass points and slopes: Benchmarks for SUSY searches", Eur. Phys. J. C25 (2002) 113-123, hep-ph/0202233.
- [87] N. Greiner, "Anomale Kopplungen bei der W-Paar-Produktion in Vektor-Boson-Fusion", Diploma Thesis, ITP Karlsruhe 2006, http://www.itp.kit.edu/diplomatheses.en.shtml.
- [88] O. Schlimpert, "Anomale Kopplungen bei der Streuung schwacher Eichbosonen", Diploma Thesis, ITP Karlsruhe 2013, http://www.itp.kit.edu/diplomatheses.en.shtml.
- [89] B. Feigl, "Anomale Vier-Vektorboson-Kopplungen bei der Produktion von drei Vektorbosonen am LHC", Diploma Thesis, ITP Karlsruhe 2009, http://www.itp.kit.edu/diplomatheses.en.shtml.
- [90] T. Figy and D. Zeppenfeld, "QCD corrections to jet correlations in weak boson fusion", *Phys. Lett.* B591 (2004) 297, hep-ph/0403297.
- [91] K. Hagiwara, R. Szalapski and D. Zeppenfeld, "Anomalous Higgs boson production and decay", Phys. Lett. B318 (1993) 155, hep-ph/9308347.
- [92] K. Hagiwara, S. Ishihara, R. Szalapski and D. Zeppenfeld, "Low-energy effects of new interactions in the electroweak boson sector", *Phys. Rev.* D48 (1993) 2182.
- [93] L3 Collaboration, "Search for anomalous couplings in the Higgs sector at LEP", Phys. Lett. B589 (2004) 89, hep-ex/0403037.
- [94] V. Hankele, G. Klamke, D. Zeppenfeld and T. Figy, "Anomalous Higgs boson couplings in vector boson fusion at the CERN LHC", *Phys. Rev.* D74 (2006) 095001, hep-ph/0609075.
- [95] G. Passarino and M. J. G. Veltman, "One Loop Corrections for e^+e^- Annihilation into $\mu^+\mu^-$ in the Weinberg Model", Nucl. Phys. **B160** (1979) 151.
- [96] W. Buchmuller and D. Wyler, "Effective Lagrangian Analysis of New Interactions and Flavor Conservation", Nucl. Phys. B268 (1986) 621.

- [97] O. J. P. Eboli, M. C. Gonzalez-Garcia and J. K. Mizukoshi, " $pp \rightarrow jje^{\pm}\mu^{\pm}\nu\nu$ and $jje^{\pm}\mu^{\mp}\nu\nu$ at $O(\alpha_{\rm em}^6)$ and $O(\alpha_{\rm em}^4\alpha_S^2)$ for the study of the quartic electroweak gauge boson vertex at LHC", *Phys. Rev.* D74 (2006) 073005, hep-ph/0606118.
- [98] C. Degrande, O. Eboli, B. Feigl *et al.*, "Monte Carlo tools for studies of non-standard electroweak gauge boson interactions in multi-boson processes: A Snowmass White Paper," arXiv:1309.7890.
- [99] S. Schael *et al.* [ALEPH and DELPHI and L3 and OPAL and LEP Electroweak Working Group Collaborations], "Electroweak Measurements in Electron-Positron Collisions at W-Boson-Pair Energies at LEP," arXiv:1302.3415.
- [100] C. Csaki, C. Grojean, L. Pilo and J. Terning, "Towards a realistic model of Higgsless electroweak symmetry breaking", *Phys. Rev. Lett.* **92** (2004) 101802, hep-ph/0308038.
- [101] C. Englert, B. Jager and D. Zeppenfeld, "QCD Corrections to Vector-Boson Fusion Processes in Warped Higgsless Models", JHEP 0903 (2009) 060, arXiv:0812.2564.
- [102] C. Englert, B. Jager, M. Worek and D. Zeppenfeld, "Observing Strongly Interacting Vector Boson Systems at the CERN Large Hadron Collider", *Phys. Rev.* D80 (2009) 035027, arXiv:0810.4861.
- [103] R. S. Chivukula, B. Coleppa, S. Di Chiara *et al.*, "A three site higgsless model", *Phys. Rev.* D74 (2006) 075011, hep-ph/0607124.
- [104] C. Englert, "Spin Vector 1 Resonances inBoson Fusion in Warped Higgsless Models", Diploma Thesis. ITP Karlsruhe 2007.http://www.itp.kit.edu/diplomatheses.en.shtml.
- [105] C. Csaki, C. Grojean, H. Murayama et al., "Gauge theories on an interval: Unitarity without a Higgs", Phys. Rev. D69 (2004) 055006, hep-ph/0305237.
- [106] D. T. Nhung, L. D. Ninh and M. M. Weber, "NLO corrections to WWZ production at the LHC," JHEP 1312 (2013) 096, arXiv:1307.7403.
- [107] F. Maltoni and T. Stelzer, "MadEvent: Automatic event generation with MadGraph", JHEP 0302 (2003) 027, hep-ph/0208156.
- [108] T. Gleisberg, S. Hoeche, F. Krauss *et al.*, "Event generation with SHERPA 1.1", *JHEP* 0902 (2009) 007, arXiv:0811.4622.
- [109] A. Kanaki and C. G. Papadopoulos, "HELAC: A package to compute electroweak helicity amplitudes", Comput. Phys. Commun. 132 (2000) 306, hep-ph/0002082.
- [110] C. G. Papadopoulos and M. Worek, "Multi-parton cross sections at hadron colliders", Eur. Phys. J. C50 (2007) 843, hep-ph/0512150.
- [111] A. Cafarella, C. G. Papadopoulos and M. Worek, "Helac-Phegas: A Generator for all parton level processes", *Comput. Phys. Commun.* 180 (2009) 1941-1955, arXiv:0710.2427.
- [112] M. Bahr, S. Gieseke, M. A. Gigg *et al.*, "Herwig++ Physics and Manual", *Eur. Phys. J.* C58 (2008) 639, arXiv:0803.0883.

- [113] N. E. Adam, T. Aziz, J.R. Andersen et al., "Higgs Working Group Summary Report", arXiv:0803.1154.
- [114] M. Ciccolini, A. Denner, and S. Dittmaier, "Strong and electroweak corrections to the production of Higgs + 2 jets via weak interactions at the LHC", *Phys. Rev. Lett.* 99 (2007) 161803, arXiv:0707.0381.
- [115] M. Ciccolini, A. Denner and S. Dittmaier, "Electroweak and QCD corrections to Higgs production via vector-boson fusion at the LHC", *Phys. Rev.* D77 (2008) 013002, arXiv:0710.4749.
- [116] J. M. Campbell and R. K. Ellis, "An update on vector boson pair production at hadron colliders," *Phys. Rev.* D60 (1999) 113006, hep-ph/9905386.
- [117] J. M. Campbell, R. K. Ellis and C. Williams, "Vector boson pair production at the LHC," JHEP 1107 (2011) 018, arXiv:1105.0020.
- [118] J. M. Campbell, R. K. Ellis and C. Williams, "Gluon-Gluon Contributions to W^+W^- Production and Higgs Interference Effects," *JHEP* **1110** (2011) 005, arXiv:1107.5569.
- [119] S. Ji-Juan, M. Wen-Gan, Z. Ren-You and G. Lei, "Next-to-leading order QCD predictions for the hadronic WH+jet production", Phys. Rev. D81 (2010) 114037, arXiv:1006.0279.
- [120] T. Binoth, G. Ossola, C. G. Papadopoulos and R. Pittau, "NLO QCD corrections to tri-boson production", JHEP 0806 (2008) 082, arXiv:0804.0350.
- [121] U. Baur, D. Wackeroth and M. M. Weber, "Radiative corrections to $W\gamma\gamma$ production at the LHC", PoS **RADCOR2009**, 067 (2010), arXiv:1001.2688.
- [122] M. Rauch, "Quantum Effects in Higgs-Boson Production Processes at Hadron Colliders", arXiv:0804.2428.
- [123] W. Kilian, T. Ohl and J. Reuter, "WHIZARD: Simulating Multi-Particle Processes at LHC and ILC," Eur. Phys. J. C71 (2011) 1742, arXiv:0708.4233.
- [124] T. Binoth, N. Kauer and P. Mertsch, "Gluon-induced QCD corrections to $pp \rightarrow ZZ \rightarrow \ell \bar{\ell} \ell' \bar{\ell}$," arXiv:0807.0024.
- [125] N. Kauer, "Signal-background interference in $gg \to H \to VV$," arXiv:1201.1667.
- [126] J. Alwall, M. Herquet, F. Maltoni, O. Mattelaer and T. Stelzer, "MadGraph 5 : Going Beyond," JHEP 1106 (2011) 128 arXiv:1106.0522.